Doctoral Thesis

Study on light response of carotenoid production in oleaginous yeast *Rhodosporidium toruloides*

（油脂生産酵母 *Rhodosporidium toruloides* におけるカロテノイド生産の光応答に関する研究）

Submitted June 2021

Nagaoka University of Technology

Department of Bioengineering

Integrated Bioscience and Technology

PHAM KHANH DUNG

Under the Supervision of

Professor Wataru Ogasawara

Table of Contents

Chapter 1: Introduction

1.1. Background

The world's population continues to grow consistently. From 7.7 billion people worldwide in 2019, the report of the World Population Prospects, 2019, indicated that the global population would grow to around 8.5 billion in 2030, 9.7 billion in 2050 (United Nations 2019). This population growth results in other serious global environmental issues, such as the unsustainable use of natural resources and threats to ecosystems, which has resulted in adverse climate changes throughout history. Among these climatic issues is global warming, which resulted from human activity, and has been proceeding at an unprecedented rate over decades to millennia. The average surface temperature has also risen approximately to 1.4°F since the early 20th Century, as reported by the National center for environmental information (https://www.ncdc.noaa.gov/monitoring-references/faq/indicators.php#warming-climate).
This warming has therefore resulted in a global ocean heat rise of more than 0.6°F (0.33°C) since 1969 (from Global Climate change https://climate.nasa.gov/evidence/). The ice cores from Greenland, Antarctica and the glaciers show that the climate responds to changes in greenhouse gas levels. Carbon dioxide from human activity is also increasing faster than many decades ago. Furthermore, the sea level rise was detected, to have been rising at a rate of $\sim 3 \pm 0.4$ mm per year since 1993 (Nerem *et al.* 2018). Therefore, green growth and green economy have recently become global trending policy topics. The green economy is defined as "results in improved human well-being and social equality, while significantly reducing environmental risks and ecological scarcities", according to UN Environment Programme (https://www.unep.org/). The green economy is based on renewable energy to substitute fossil fuels and energy conservation for efficient energy use. This process ranges from low carbon use, to resource efficiency, socially inclusiveness and the rise of an innovative economy. Therefore, the bioeconomy, circular economy and clean tech all make up the green economy. The main point of the green economy is the use of renewable resources to replace non-renewable resources which leads to the development of technologies in bioproduction. Thus, ecosystem management at the landscape scale and utility organisms should be built. Bioeconomy is described as an economy based on the sustainable manufacturing of products, in whole or parts from renewable resources. Bioproducts are products made with some component of biological or renewable materials. Therefore, bioproducts are divided into three categories: bioenergy (biofuel, solid biomass, gaseous fuel such as biogas and syngas),

biomaterials (bioplastics, biofoams, biorubber, and biocomposites), biochemical (industrial basic, and specialty chemicals, including resins, pharmaceuticals - antibodies and vaccines, biocosmetics - soaps, body creams and lotions) (Thimmanagari, McDonald and Todd 2010). Among them, lipids that can be used as biofuel for bioenergy, material for bioplastics, or DHA (type of fatty acid) for pharmaceuticals have become a potential source in industrial application. Besides, carotenoids that have much utility in many industries have also received attention. Therefore, we focus on lipid and carotenoid production in this study.

1.2. Lipids

1.2.1. Lipids

Lipids are group components that do not interact appreciably with water. The main component of lipid is composed of triacylglycerol (TAG), in which three molecules of fatty acids are ester-bonded to the glycerin skeleton. Alternatively, fatty acid molecules contain carbon (C) atoms, which are linked in a chain and are characterized by a holding carboxyl group (-COOH) at one end of the chain. Fatty acids have different properties, depending on the length of the chain and the number and position of the carbon double bonds. Therefore, fatty acids are components of many complex lipid molecules such as fats and phospholipids. In addition to straight-chain hydrocarbons, fatty acids also contain double bonds, methyl branches or a three-carbon cyclopropane ring near the center of the carbon chain. Furthermore, two types of fatty acids exist, saturated fatty acids that do not have double bonds between their carbon elements, and unsaturated fatty acids that have carbon double bonds. The saturated group indicates that the maximum possible number of hydrogen atoms are bonded to each carbon in the molecule. However, the unsaturated group shows that fewer than the maximum possible number of hydrogen atoms are bonded to each carbon in the molecule. Thus, the number of double bonds indicate whether the fatty acid is monounsaturated or polyunsaturated.

1.2.2. Application of lipids

Lipids, including oil and fats can apply in many industries such as food, bioenergy, bioplastic and health care as supplements or pharmaceutical.

Edible oil is a lipid that is physically extracted from vegetables (seeds) and animals (tissues). For example, palm, oilseed rape, soybean, sunflower, olive, coconut oils, etc. Edible oil is used in frying, baking, and other types of cooking preparations. Furthermore, edible oil forms the daily supplement component that should be taken. They are the main source of

dietary fats that play an essential role in satisfying nutrition, growth and brain operation or nerve system. Additionally, edible oil from different sources has different characteristics. Shah, *et al* reported that the global market for bio-lubricants oil is expected to grow from $2 billion in 2020 to $2.4 billion (20%) in 2025 (Shah, Aragon and Calderon 2021).

Biodiesel is a bioenergy source produced by the chemical conversion of vegetable oils and fats from animals via transesterification processing. Recently, microalgae are photosynthetic aquatic plants that produce these oils for use in the production of biodiesel, thereby resulting in a renewable alternative source to fossil fuels. For example, biodiesel consumption in the U.S.A from about 260 million gallons in 2010 has grown to about 1.8 billion gallons in 2020 (U.S. Energy Information Administration 2021).

Bioplastics are polymers produced from starch crops and vegetable oils (a replacement for petroleum). Biodegradable plastics are also produced using renewable raw materials, microorganisms, petrochemicals or combinations of all. The oils for this process are mostly from fossils, however, they are now being replaced by crop oils or bio-oils (from microorganisms).

Functional oils are lipids including essential components like omega-3-6 and -9 fatty acids. The three main omega-3 fatty acid types are alpha-linolenic acid (ALA), eicosapentaenoic acid (EPA), and docosahexaenoic acid (DHA). While ALA is found mainly in plant oils such as flaxseed, soybean and canola oils, DHA and EPA are found in marine fish and algae. However, DHA was derived in low quantities from other fatty acids during metabolic processes in the body. Thus, they must be taken up from food or a supplement. DHA and EPA help to reduce the risk of chronic diseases, such as heart diseases. DHA was also reported to support brain functions and eye health (Allaire *et al.* 2016; Yamagata 2017). Higher intake of omega-3 fats such as DHA has been linked to a lower risk of several cancers as well, including colorectal, pancreatic, breast, and prostate cancers (Zárate *et al.* 2017; Ferrucci and Fabbri 2018). Similarly, DHA is essential for brain and eye development in special babies (Cecilie Braarud *et al.*; Swanson, Block and Mousa).

1.2.3. Microbial lipids

Microbial lipids are known as single cell oils that are produced by oleaginous microorganisms, including many species such as algae, filamentous fungi, yeasts, and bacteria (Ewing and Msangi 2009). These oleaginous microorganisms can accumulate a large volume of lipids in their cells, such as *Lipomyces starkeyi*, *Yarrowia lipolytica*, *Rhodosporidium*

toruloides, *Rhodotorula graminis*, *Rhodotorula glacialis*, *Chlorella protothecoides* and *Trichosporon coremiiforme.* They can also accumulate intracellular lipids from 20% to 80% (w/w) under certain cultivated conditions (Seeger 2010; Zhang *et al.* 2011; Galafassi *et al.* 2012; Huang *et al.* 2013; Axelsson and Gentili 2014; Dulermo *et al.* 2015a; Calvey *et al.* 2016) (**Table 1.1)**. Microbial lipids of some oleaginous microorganisms are valuable sources of polyunsaturated fatty acids that are used as additives for different food products and in nutraceuticals. In contrast, omega-3 and omega-6 fatty acids are commercially produced using different oleaginous microorganisms. Examples include γ-linolenic acid (GLA, C18:3, n−6), which is produced by *Mucor circinelloides*; dihomo-gamma-linoleic (DGLA) (20:3, n−6) by *Mortierella alpina* 1S-4; eicosapentaenoic acid (EPA) (20:5, n−3) by *Mortierella alpina* ST1358 and *Yarrowia lipolytica*; including docosahexaenoic acid (DHA, 22:6, n−3) by *Crypthecodinium cohnii*, and *Schizochytrium* (Schneider *et al.* 2013; Abedi and Sahari 2014; Ling *et al.* 2015; Okuda *et al.* 2015; Tang *et al.* 2015; Bellou *et al.* 2016a).

Most of the lipid accumulated in the cells of oleaginous microorganisms is occupied by Triacyl-glycerol (TAG), and is accumulated in intracellular organelles as "lipid droplets" that are formed from the endoplasmic reticulum (Garay, Boundy-mills and German 2014). TAGs are neutral lipids that are naturally formed through fatty acid biosynthetic pathways. TAGs are used in many fields like foods, animal feeds and feed stocks for chemical syntheses. Recently, derivatives of TAGs, such as long-chain fatty acid methyl esters and alkanes, have been gotten attention as biofuels (Zhu *et al.* 2012).

Among the oil-producing microorganisms, it has been reported that filamentous fungi and yeast show high oil contents (**Table 1.1**). Fungi has a higher growth rate than plants and microalgae, and it is possible to scale up lipids production using a culture tank, regardless of the surrounding environments and climates (Li, Du and Liu 2008; Ageitos *et al.* 2011; Bonturi *et al.* 2015). Besides, fungi uses more diverse sugars and other carbon sources for their growth and lipid accumulation such as monosaccharides (glucose and xylose), amino sugars (N-acetylglucosamine), disaccharides (lactose, galactose, mannose, cellobiose, and sucrose), alcohols, polysaccharides (starch and pectin) and organic acids (Zhang *et al.* 2011; Galafassi *et al.* 2012).

Table 1.1. Lipid content of some microorganisms

Species	**Lipid content %DCW**	**References**
Bacteria		
Bacillus cereus	18.06	(Karim *et al.* 2019)
Pseudomonas spp	52.7	(J. Brigham and Kurosawa 2011)
Microalgae		
Chlorella	16.1	(Darwish *et al.* 2020)
Botryococcus braunii	5.2	(Tran, Hong and Lee 2009)
Chlamydomonas reinhardtii	24.7	(Darwish *et al.* 2020)
Filamentous fungi		
Mucour circinelloides	46	(Mitra *et al.* 2012)
Aspergillus niger	1.4–2.5 g/L	Andre et al 2010
Fusarium oxysporum	42.6	(Matsakas, Giannakou and Vörös 2017)
Mortierella alpina	11.9 g/L	(Nie *et al.* 2014)
Yeast		
Lipomyces starkeyi	54.85	(Calvey *et al.* 2016)
Yarrowia lipolytica	53	(Niehus *et al.* 2018)
Cryptococcus podzolicus	53.8	(Qian *et al.* 2019)
Rhodotorula glutinis	47.24	(Maza *et al.* 2020)
Rhodosporidium toruloides	58.67–61.54	(Fei *et al.* 2016)
Rhodosporidium toruloides	67.5	(Li, Zhao and Bai 2007)

High lipid contents in the cell was reported in *Yarrowia*, *Rhodosporidium*, *Lipomyces* and *Sporobolomyce* species. As in the *Rhodotorula glutinis* ATCC 26085 and *Sporobolomyces roseus* B99040, total fatty acid was reported to be 19.7 and 14.3 µg/g dry weight respectively. Moreover, fatty acid components of lipid producing microorganisms were similar to those of vegetable oils (**Table 1.2**) from which C16:1, C16:0, C18:2 and C18:0 fatty acids from the main fatty acid types that were reported, comprising 2.08 %, 15.52%, 72.1%, 5.72% and 1.75%, 13.38%, 60.2%, 16.58%, respectively. The former was *R. glutinis* ATCC 26085, whereas, the latter was *S. roseus* B99040 (Davoli, Mierau and Weber 2004). Therefore, microbial lipids from microorganisms are promising source as an alternative oil source for not only biodiesel production but also the food industry.

Table 1.2. Fatty acid composition of various sources

Sources	**Fatty acid compositions**							**References**
	C14:0	C16:0	C16:1	C18:0	C18:1	C18:2	C18:3	
Palm oil	0.3–1.0	32.5–50.0	0.1–0.2	3.7–8.4	35.3–50.0	5.0–12.2	0.1-0.4	(Montoya *et al.* 2014)
Oilseed rape (Brassica napus)	-	4.31–5.12	-	2.14–2.67	57.85–64.63	15.71–18.41	4.87–7.25	(Sharafi *et al.* 2015)
Oilseed rape (Brassica napa)	-	2.23–3.92	-	1.18–1.84	15.20–26.72	11.25–17.69	14.95–16.09	(Sharafi *et al.* 2015)
Soybean oil	-	10.6–12.9	-	3.0–4.0	20.9–30.4	46.3–58.8	3.6–6.3	(Sharma *et al.* 2014)
Olive oil	<0.1	7.5–20.0	0.3–3.5	0.5–5.0	55.0–83.0	3.5–21.0	-	(Boskou, Blekas and Tsimidou 2006)
Chlorella	-	22.2	23.0	2.8	7.0	31.4	23.5	(Darwish *et al.* 2020)
Chlorella protothecoides	0.05	4.72	0.55	1.78	62.04	20.64	6.85	(Makareviciene *et al.* 2014)

C. vulgaris NIES-227	3.65	21.11	0.99	-	2.67	47.02	24.56	(Shen *et al.* 2015)
Chlamydomonas reinhardtii	-	23.8	2.7	2.3	14.7	3.8	46.5	(Darwish *et al.* 2020)
Cryptococcus podzolicus	0.1	21.1	-	5.5	61.5	8.1	1.8	(Qian *et al.* 2019)
Fusarium oxysporum	0.6	22	0.7	11	42	20	0.1	(Matsakas, Giannakou and Vörös 2017)
Lipomyces starkeyi	1.2	35.7	3.4	13.7	43.1	1.7	-	(Calvey *et al.* 2016)
Lipomyces starkeyi	-	32.9	4.3	4.2	50.4	5.2	0.1	(Matsuzawa *et al.* 2020)
Yarrowia lipolytica	-	14.9		11.1	55.1	18.5	-	(Niehus *et al.* 2018)
Rhodotorula glutinis R4	3.3	16.78	-	1.81	1.35	61.64	4.23	(Maza *et al.* 2020)
Rhodosporidium toruloides	1.3	25.1	-	10.1	45.9	10.5	3.3	(Fei *et al.* 2016)

1.2.4. Fact of oil supplements in Japan

Especially in Japan, the self-sufficiency rate of producing vegetable oils and fats is as low as 3%, and most of the vegetable oils and fats currently used in homes depend on overseas imports. Therefore, it is expected that the sharp rise in the price of oil seeds due to the increase in the world's population will become a future social problem for the Japanese food oil industry. Thus, it is essential to develop a new food oil production process unique to Japan. Recently, microorganisms which are capable of producing fats and oils have attracted attention. Oils and fats produced by oleaginous microorganisms have also been used as energy for biodiesel fuels.

Besides, oil supplements for biodiesel also are also limited in Japan. Furthermore, trade data shows that Japan's imports of biodiesel in 2016 grew by 19.7 percent (or 210,000 liters) from the previous year (Iijima and Paulson 2017). Biofuels (including biodiesel) are mainly used in homes, and to a lesser extent in the industry, while liquid biofuel for transport still plays limited roles (~2%). Additionally, on-road diesel demand in Japan has been robust at 34.0 billion liters in 2019, with a 1.0% increase in 2018 (Daisuke Sasatani, Rakhovskaya and Highli 2020). Moreover, Japan's biodiesel market is extremely limited, meeting just 0.04 percent of the national on-road transportation demand for diesel fuels, however, there is no renewable diesel market (Iijima and Paulson 2017). Consequently, new resource for biodiesels have become an urgent issue.

1.3. Carotenoids

Carotenoids are important groups of pigments that have over 600 structural compound types. They have 40 carbons in their formulas, with oxygenated or non-oxygenated molecules, conjugated double bonds, and rings at the end (Popova and Academy 2013; Yuan *et al.* 2015). Furthermore, they are divided into two classes; one which contains oxygen (xanthophylls), and another which does not contain oxygen (carotenes) (Britton 2004). Xanthophylls are synthesized in several photosynthetic and non-photosynthetic organisms, including plants and microorganisms. Furthermore, carotenoids are lipophilic molecules that provide yellowish, orange, or reddish pigmentations (Avalos *et al.* 2017). Thus, they are used in the food industry as a natural colorant pigment. Some carotenoids are precursors of vitamin A (β-carotene) or antioxidant agents (such as torulene, astaxanthin), both of which are used as vitamins and dietary supplements (Frengova and Beshkova 2009). Additionally, they are among the bioactive phytochemicals that are associated with reducing the risk of developing degenerative diseases such as cancers, cardiovascular diseases, cataracts, etc.

β-carotene is pigment that has been applied in the industries, medicines, health products, food additives, cosmetics, feed additives, and many other products. β-carotene is the fat-soluble, yellowish-orange colored part of carotenoid, having 11 conjugated double bonds and 2 retinyl groups (**Figure 1.1)**. The large number of double bonds in the polyene chain and ring makes β-carotene easily oxidized by free radicals. Therefore, β-carotene has antioxidant activities, and has been added to the foods due to its antioxidant property (Kim *et al.* 2010). In medical and or health care industries, the antioxidant activity of β-carotene helps to prevent the cancers, tumors and cardiovascular diseases. γ-carotene formed via the cyclization of lycopene through

an enzymatic reaction facilitated by lycopene ε-cyclase has been identified. γ-carotene is the isomer of β-carotene, structurally containing 11 conjugated double bonds, 1 non-conjugated double bond and 1 retinyl group (**Figure 1.1)**. γ-carotene functions as a β-carotene, though less than β-carotene because of its one less retinyl group. Thus, both β-carotene and γ-carotene are vitamin A precursors (Rodriguez-Concepcion and Stange 2013; Hempel *et al.* 2016).

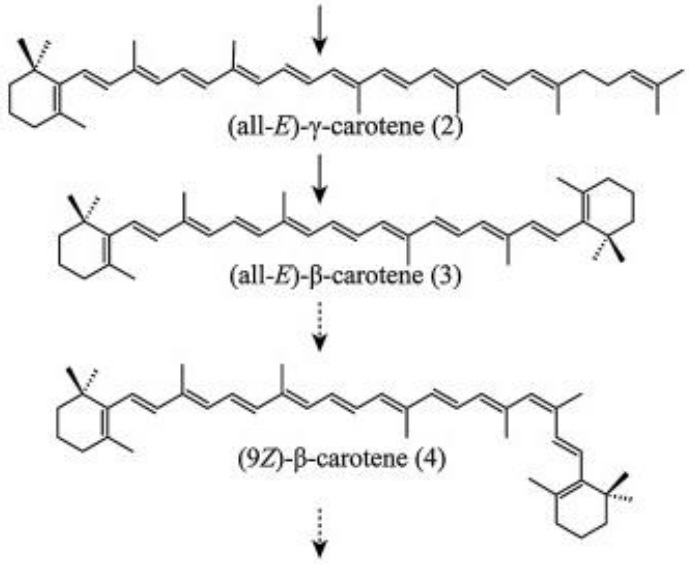

Figure 1.1. Structures of γ -carotene and β-carotene (Hempel *et al.* 2016)

Torulene and Torularhodin are acid pigments. An extra double bond in the 13C position converts γ-carotene to torulene. Then, substituting one methyl group with one carboxyl group forms torularhodin. Since these two carotenoids contain the β-ionone ring in their structure, which is the backbone of vitamin A, both of them serve as potential precursors of vitamin A. Torulene and torularhodin have shown stronger antioxidant activities, because of the presence of extraconjugated double bonds in the 13C position of their structure (Ungureanu and Ferdes 2012) that is absent in β-carotene or γ-carotene (**Figure 1.2)**. It was also reported that high torularhodin producing mutants can reduce the susceptibility to oxidative damage induced by active oxygen species (Sakaki *et al.* 2001).

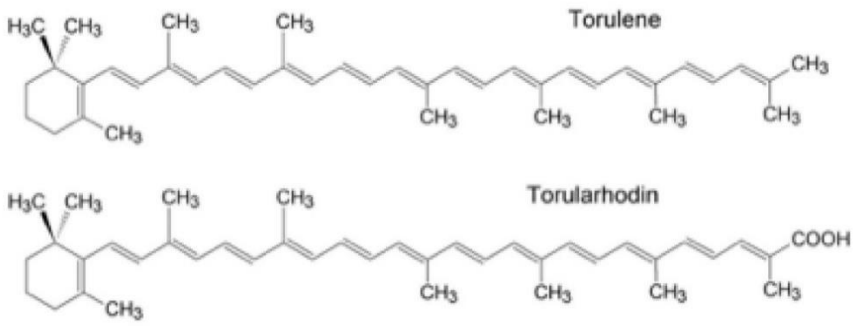

Figure 1.2. Structures of Torulene and Torularhodin (Zoz *et al.* 2015)

Astaxanthin is isoprenoids belonging to the conserved mevalonate pathway. β-carotene is hydroxylated and oxidized to astaxanthin, as catalyzed by astaxanthin synthase (Miao *et al.* 2011). The natural microorganism-producers of astaxanthin include microalgae, fungi (the basidiomycetous yeast, *Xanthophyllomyces dendrorhous*), and bacteria (*Paracoccus* spp. and *Brevundimonas* spp.) (Meyer and Preez 1993; Vázquez 2001; Schmidt *et al.* 2011; Ide *et al.* 2012; Han, Li and Hu 2013). Astaxanthin (3,3′-dihydroxy-β, β-carotene-4,4′-dione) is a ketocarotenoid having 13 conjugated double bonds arranged as alternating single-double bonds (**Figure 1.3).** These double bonds account for its strong antioxidant properties and its ability to act as reactive oxygen species and neutralizing free radicals (Brotosudarmo *et al.* 2020).

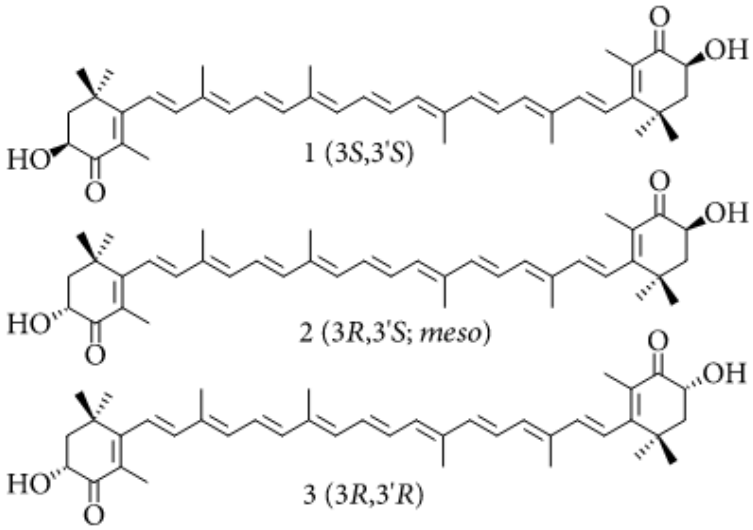

Figure 1.3. Structures of Astaxanthin (Brotosudarmo *et al.* 2020)

Canthaxanthin (β-β′-carotene-4, 4′ -dione) is a cosmopolitan keto-carotene applied in both direct and indirect food coloring (Hannibal *et al.* 2000). Canthaxanthin combined with β-

carotenoid is used in cosmetology and pharmacology as a dermal photo-protect (Goralczyk *et al.* 1997).

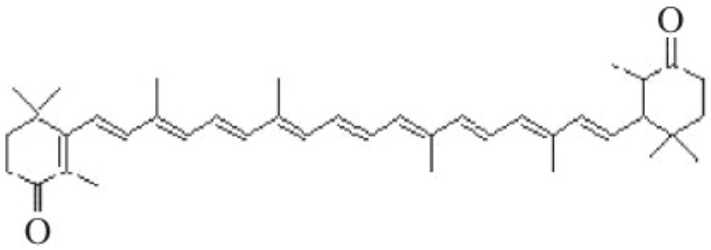

Figure 1.4. Structures of Canthaxanthin (Chandi and Gill 2011)

In microorganisms, some showed higher carotenoid productivity than others, and varied from algae, and filamentous fungi to yeast as shown in **Table 1.3**

Table 1.3. The carotenoid production yield of microorganisms

Strains	**Carotenoid yields**	**References**
Bacteria		
Flavobacterium	500 mg/L	(Sajilata, Singhal and Kamat 2008)
Sphingobacterium multivorum	10.6 mg/L	(Bhosale 2004)
Brevundimonas sp. *SD212*	7.4 mg/g	(Lu, Bu and Liu 2017)
Microalgae		
Chlorella zofingiensis	10.29 mg/L	(Ip and Chen 2005)
Chlorella protothecoides	0.6 g/ 100g biomass	(Campenni' *et al.* 2013)
Asterarcys quadricellulare	35±1.75 μg/mg	(Singh *et al.* 2019)
Dunaliella salina	15.1 mg/L	(García-González *et al.* 2003)
Filamentous fungi		
Aspergillus carbonarius	1298 μg /g total carotenoids	(Sanjay *et al.* 2007)
Aspergillus nidulans	125 μg/g of β-carotene	(Wiemann *et al.* 2018)

Xanthophyllomyces dendrorhous	487 µg/g total carotenoids	(Verwaal *et al.* 2007)
Fusarium fujikuroi	48 µg/g -0.15 mg/g after 144 h	(Rodríguez-Ortiz, Limón and Avalos 2009)
Sporidiobolus ruberrimus	0.51 g /L	(Cardoso *et al.* 2016)
Sporidiobolus roseus	278 µg/g of β-carotene	(Ananda and Vadlani 2010)
Sporidiobolus salmonicolor	1019 µg/L total carotenoids	(Valduga *et al.* 2009)
Sporidiobolus salmonicolor AL_1	torularhodin 458.3 ± 24.5 µg/g, torulene 273.7 ± 14.5 µg/g, β-carotene 129.2 ± 7.3 µg/g	(Dimitrova *et al.* 2013)
Sporidiobolus pararoseus	843 µg/ L	(Valduga *et al.* 2014)
Chlamydomonas reinhardtii	23.75 mg/g DCW	(Bohne and Linden 2002)
Chlamydomonas reinhardtii	25.9 mg/g DCW	(Tran *et al.* 2019)
Chlamydomonas reinhardtii	~6 mg/g	(Liu *et al.* 2013a)
Neurospora crassa	295.16 µg/g	(Nuraini, Sabrina and Latif 2009)
Neurospora intermedia	1.19 mg/g	(Gmoser *et al.* 2018)
Yeasts		
Yarrowia lipolytica	1.7 mg/g of lycopene	(Zhao *et al.* 2017)
Rhodotorula glutinis mutant 32	3.8 mg/g 5.4 mg/g (Optimization)	(Bhosale and Gadre 2001a) (Bhosale and Gadre 2001b)
Rhodotorula glutinis CCY 20-2-26	34 mg/L	(Marova *et al.* 2010)

Rhodotorula glutinis DBVPG 6081	112.2 µg/g	(Buzzini *et al.* 2007)
Rhodotorula graminis DBVPG 7021	122.6 µg/g	(Buzzini *et al.* 2005)

1.4.Oleaginous yeast *Rhodosporidium toruloides*

Rhodosporidium toruloides is a non-pathogenic, and red-colored (**Figure 1.5**) basidiomycetous fungus. This yeast can produce a large volume of lipids in the body that makes up a large amount of the lipid in its cell, with a dry cell weight value of 70%. Thus microbe has antioxidant activity as a secondary metabolite from various monosaccharides. Lipids of *R. toruloides* could be applied in the fuel industry as an alternative resource and in the food industry as an edible oil because their lipid is similar to that of vegetable oils in composition (**Table 1.2**). It, therefore, becomes a promising producer for renewable fuels and functional foods or chemistries (Zhu *et al.* 2012).

Figure 1.5. Morphology of *Rhodosporidium toruloides* NBRC 10032 on a YPD agar plate

R. toruloides also possesses the propensity to form large lipid droplets that are primarily present as triacylglycerols (TAGs) in the cells, thereby creating the single cell oil forms (**Figure 1.6** Left).

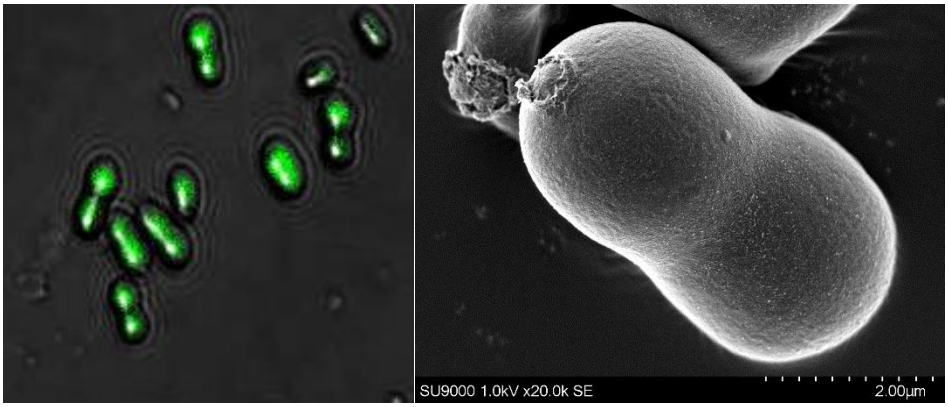

Figure 1.6. *Rhodosporidium toruloides* NBRC10032 cells by Microscopes x40
(Left: Green shows the lipid droplet in the cells)

R. toruloides also has the ability to produce carotenoids, including biotechnologically important enzymes (Politino *et al.* 1997; Botes 1999). Research on carotenoid production from *R. toruloides* has been conducted by many researchers. They reported that *R. toruloides* produced predominantly β-carotene, γ-carotene, torulene and torularhodin in various proportions dependent on cultural conditions (Buzzini *et al.* 2007; Saenge *et al.* 2011; Lee *et al.* 2014; Zhang, Zhang and Tan 2014). As mentioned above (section 1.3), these carotenoids produced by *R. toruloides* have many advantages to industries as foods, feeds, cosmetics, including pharmaceutical industries as pigments, vitamins, and dietary supplements and bioactive phytochemicals (Khanafari, Tayari and Emami 2008; Frengova and Beshkova 2009). Compared to other microorganisms, *R. toruloides* also shows high carotenoid yields (**Table 1.3**). The *Rhodotorula glutinis* (former name of *Rhodosporidium toruloides*) DBVPG 6081 had 112.2 µg/g cell dry mass of carotenoids that was distributed as 46.8% torularhodin, 30.57% torulene, 4.55% γ-carotene, and 18% of β-carotene. It was also reported that the *R. toruloides* DBVDG 6739 strain contained 122.6 µg/g cell dry mass of carotenoids with 16.23%, 42.17%, 7.34%, and 18.1% of torularhodin, torulene, γ-carotene and β-carotene, respectively (Buzzini *et al.* 2007). In other *Rhodotorula* strains, like the *R. glutinis* mutant 32, 5.4 mg/g dry cell was carotenoids including torularhodin, torulene, and β-carotenoid, which were 2.3%, 17% and 80%, respectively (Bhosale and Gadre 2001b). The advantage of carotenoids as food additives and special anti-cancer agents have encouraged research on the economic production of carotenoids from microorganisms. Also, because of the cultural conditions dependent on carotenoid production, various methods of media manipulation and cultural condition have been suggested for the improvement of carotenoid content.

1.5. General biosynthesis pathway

Oleaginous yeasts that produce lipids and carotenoids are used industrially as new energy resources, or in food. Research on the lipid and carotenoid production mechanism have been conducted. Therefore, the mechanism of lipid/carotenoid production in oleaginous yeast that has been considered so far will be described. Lipids that were produced by oleaginous yeast contained triacylglycerols (TAGs) and sterol ester (SE) in which one molecule of fatty acid was ester-bonded to the hydroxyl group of the sterol, and free fatty acid (FFA), which is fatty acid existing without an ester bond. A schematic diagram of the metabolic pathways related to lipid production and accumulation common to various species is shown below. Glucose taken up into cells is converted from glycolysis to ATP, NADH, FADH2, etc. through the citric acid cycle. Lipids are also accumulated in the metabolic pathway that branched from this energy synthesis pathway as well. Accumulated lipids are accumulated in intracellular organelles called lipid globules and are stored as raw materials for energy conversion and in cell membranes by the β-oxidation system. From Acetyl-CoA, these molecules not only enter to TAGs, FFA, or SE biosynthesis, but also enter carotenoid biosynthesis through the mevalonate and isoprene biosynthesis pathways (**Figure 1.7**).

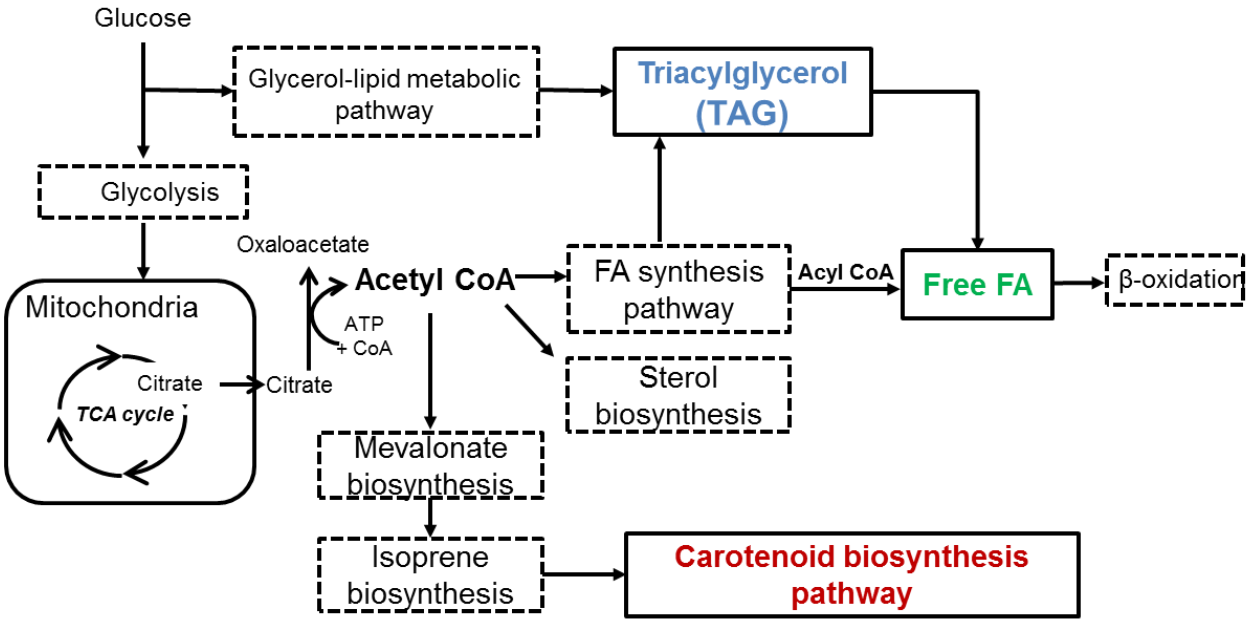

Figure 1.7. A schematic diagram of the metabolic pathways related to lipid production and carotenoid production

1.5.1. Glycolysis-TCA cycle

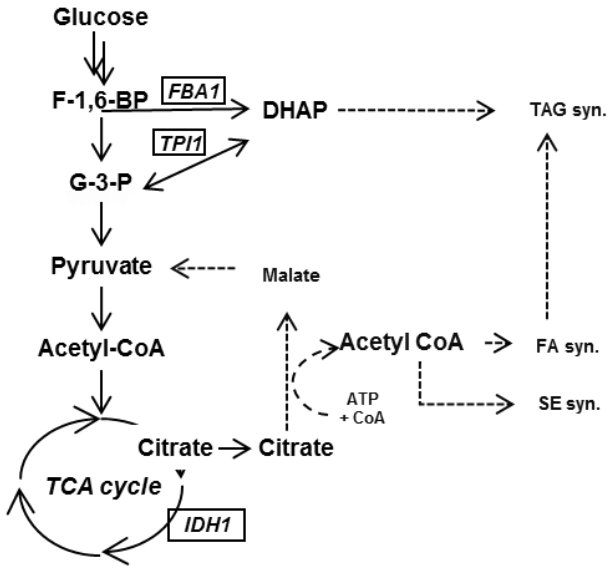

Figure 1.8. Glycolysis and TCA cycle pathway

Fructose-1,6-bisphosphate (F-1,6,BP), Glyceraldehyde-3-phosphate (G-3-P), Dihydroxyacetone phosphate (DHAP), Triacylglycerol (TAG), Tricarboxylic acid cycle (TCA cycle), Fructose-bisphosphate aldolase (*FBA1*), Triose phosphate isomerase (*TPI1*), Isocitrate dehydrogenase (*IDH1*)

Acetyl CoA that is major for lipid synthesis is formed after the monosaccharide (glucose) is converted via the glycolytic pathway and TCA cycle. TAG uses the dihydroxyacetone phosphate (DHAP) produced by cleaving fructose-1,6-bisphosphate (F-1,6-BP) in glycolysis as the glycerin skeleton. Simultaneously, pyruvate, which is converted from G-3-P, is also transported to mitochondria and converted into acetyl-CoA by the pyruvate dehydrogenase complex (Tai and Stephanopoulos 2013). When nitrogen sources are exhausted, a rapid decrease in intracellular adenosine monophosphate (AMP) levels, triggers an increase in the activity of adenosine monophosphate deaminase (AMPD). Low AMP concentration, therefore, suppresses the activity of isocitrate dehydrogenase (*IDH1*), resulting in the production of a large volume of citric acid in the mitochondria. After that, these citric acids are transported to the cytosol, where fatty acid and sterol synthesis occur. (Tang *et al.* 2009; Tai and Stephanopoulos 2013; Lazar, Liu and Stephanopoulos 2018).

1.5.2. TAG synthesis

The synthetic route from glycolysis to TAG synthesis is shown (**Figure 1.9**). First, a redox reaction between DHAP and glycerol 3-phosphate (Glycerol -3-P) is catalyzed by glycerol 3-phosphate dehydrogenase (*GPD1*). Glycerol-3-P is then acylated by glycerol-3-phosphate acyltransferase (*SCT1*/*GAT1*) to form lysophosphatidic acid (Lyso-PA). LPA is subsequently acylated by the LPA acyltransferase (*SLC1*) enzyme to release phosphatidic acid

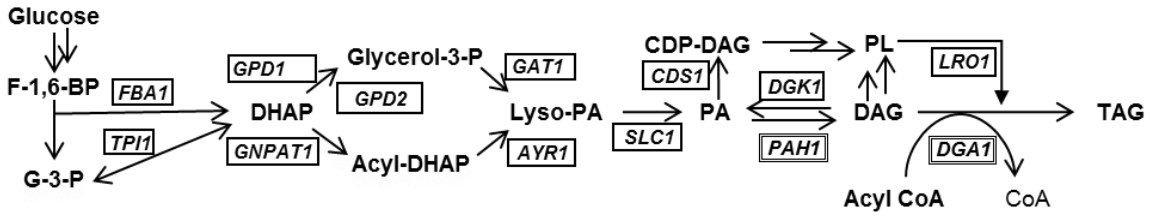

Figure 1.9. TAG synthesis pathway

Dihydroxyacetone phosphate (DHAP), Glycerol 3-phosphate (G-3-P), phosphatidic acid (PA), diacylglycerol (DAG), phospholipid (PL), Triacylglycerol (TAG), glycerol 3-phosphate dehydrogenase (*GPD1*) , glycerol 3-phosphate acyltransferase (*GNPAT1*), acyl *DHAP* reductase (*AYR1*), lysophosphatidic acid acyltransferase (*SLC1*), CDP-diacylglycerol synthase (*CDS1*), diacylglycerol kinase (*DGK1*), phosphatidic acid phosphatase, phospholipid diacylglycerol acyltransferase (*LRO1*).

(PA). Then, PA is dephosphorylated by PA phosphatase (*PAH1*) to form diacylglycerol. Finally, TAGs are synthesized by DAG acyltransferase (*DGA1*, *DGA2*), which uses acyl-CoA as the final acyl group donor, or by phospholipid DAG acyltransferase (*LRO1*), which uses glycerol-phospholipids as the acyl group donor (Tkachenko, Tigunova and Shulga 2013; Lazar, Liu and Stephanopoulos 2018).

1.5.3. Fatty acid synthesis

Fatty acid synthesis, which is the raw material, is indispensable for TAG synthesis. This fact is because the properties of the lipid production are determined by the length and degree of unsaturation of the synthesized fatty acid carbon chains. Citric acid, which is an intermediate metabolite of the citric acid cycle, is used for fatty acid synthesis **(Figure 1.10**). Furthermore, citric acid is cleaved into oxaloacetate and acetyl-CoA, which is a raw material for fatty acid, by the enzyme ATP citrate lyase (*ACL1*). This enzyme exists only in species that produce and accumulate large amounts of lipid and are absent in the non-oleaginous yeasts (Hynes and

Murray 2010; Dulermo *et al.* 2015b; Muniraj *et al.* 2015; Tang, Lee and Chen 2015). From acetyl-CoA, malonyl-CoA is carboxylated by the enzyme acetyl-CoA carboxylase (*ACC*) (Zhu

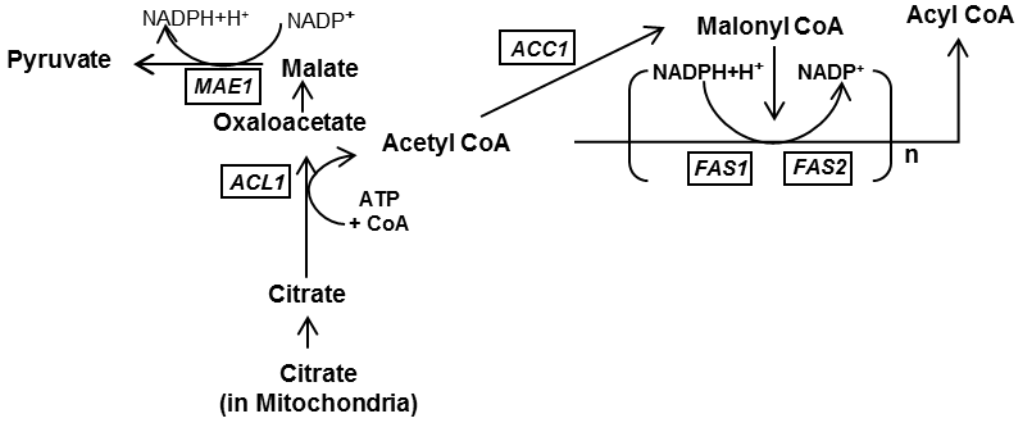

Figure 1.10. Fatty acid synthesis pathway

ATP citrate synthase (*ACL1*), acetyl-CoA carboxylase (*ACC1*), fatty acid synthase (*FAS1, 2*), malic enzyme (*MAE1*)

et al. 2012; Shi and Zhao 2017). Then, the fatty acid synthase (*FAS1*, *FAS2*) complex produces acyl-CoA using both acetyl-CoA and malonyl-CoA molecules. *MAE1* is a cytosolic enzyme involved in the conversion of L-malate and NADP+ into pyruvate, CO_2, and NADPH. Similarly, NADPH is essential for fatty acid synthesis and due to its capacity to produce NADPH, this enzyme was proposed to be one of the rate-limiting steps in fatty acid synthesis (Ratledge 2014; Dulermo *et al.* 2015b).

1.5.4. β oxidation

Under nutrient depletion conditions, TAG is degraded by TAG lipase (*TGL1*, *TGL2*) to release FFA. After that, FFA is converted to acyl-CoA by fatty acyl-CoA synthetase (*FAA1*, *FAA2*). Next, acyl-CoA oxidase (*POX1*, *POX2*), which is a β-oxidizing enzyme group, decomposes into acetyl-CoA by the action of acetyl CoA C-acyltransferase (*POT1*). The resultant molecule is then transported to peroxisomes(Tang, Lee and Chen 2015; Lazar, Liu and Stephanopoulos 2018) (**Figure 1.11**).

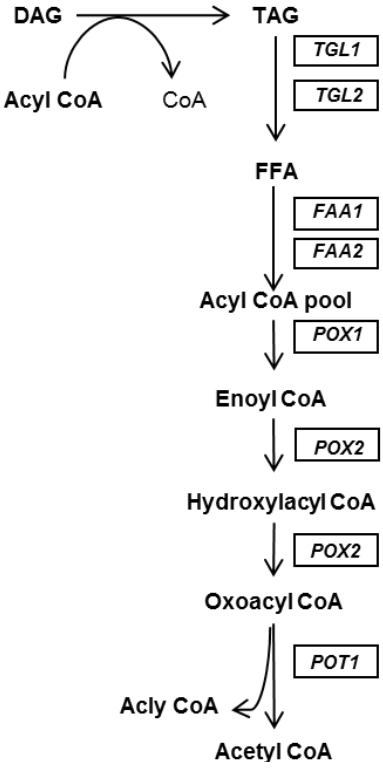

Figure 1.11. The β oxidation pathway

Diacylglycerol (DAG), Triacylglycerol (TAG), Free fatty acid (FFA), TAG lipase (*TGL1, 2*), fatty acyl-CoA synthetase (*FAA1, 2*), acyl-CoA oxidase (*POX1, 2*), acetyl CoA C-acyltransferase (*POT1*)

1.5.5. Sterol synthesis

Acetyl-CoA synthesized in the fatty acid synthesis pathway is also used as a raw material for sterol synthesis. The synthesized sterol is ester-bonded to fatty acid by the action of acyl-CoA-sterol acyltransferase (*ARE1, 2*) and converted into SE, which is a lipid

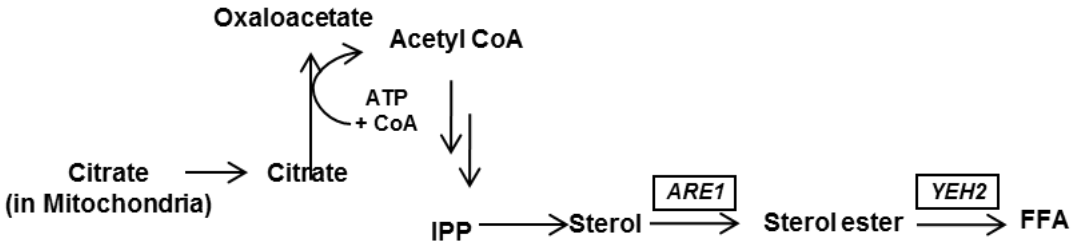

Figure 1.12. Sterol synthesis pathway

Isopentenyl-pyrophosphate (IPP), free fatty acid (FFA), acyl-CoA-sterol acyltransferase (*ARE1, 2*), yeast steryl ester hydrolase (*YEH2*)

component that converts to FFA using the yeast steryl ester hydrolase (*YEH2*) enzyme (**Figure 1.12**). Then, the synthesized lipid components are accumulated as fat globules in the cells of

oleaginous yeast, after which they are stored until use as an energy source or a cell membrane raw material. (Beopoulos, Chardot and Nicaud 2009).

Carotenoid biosynthesis is known as the starting pathway in phytoene, the first colorless carotenoid in the carotenoid pathway. The biosynthesis of isopentenyl pyrophosphate (IPP) is proposed to happen via two distinct routes; The Mevalonate pathway (MVA pathway) and the Methylerythritol Phosphate pathway (MEP pathway). In the MVA pathway, IPP is synthesized from the condensation of three Acetyl-CoA molecules; whereas, in the MEP pathway, IPP is synthesized through the condensation of pyruvate and D-glyceraldehyde 3-phosphate. The MVA pathway is found in animals, fungi, and the cytoplasm of phototrophic organisms. However, the MEP pathway is found in most eubacteria, unicellular green algae, and chloroplasts of phototrophic organisms (plant).

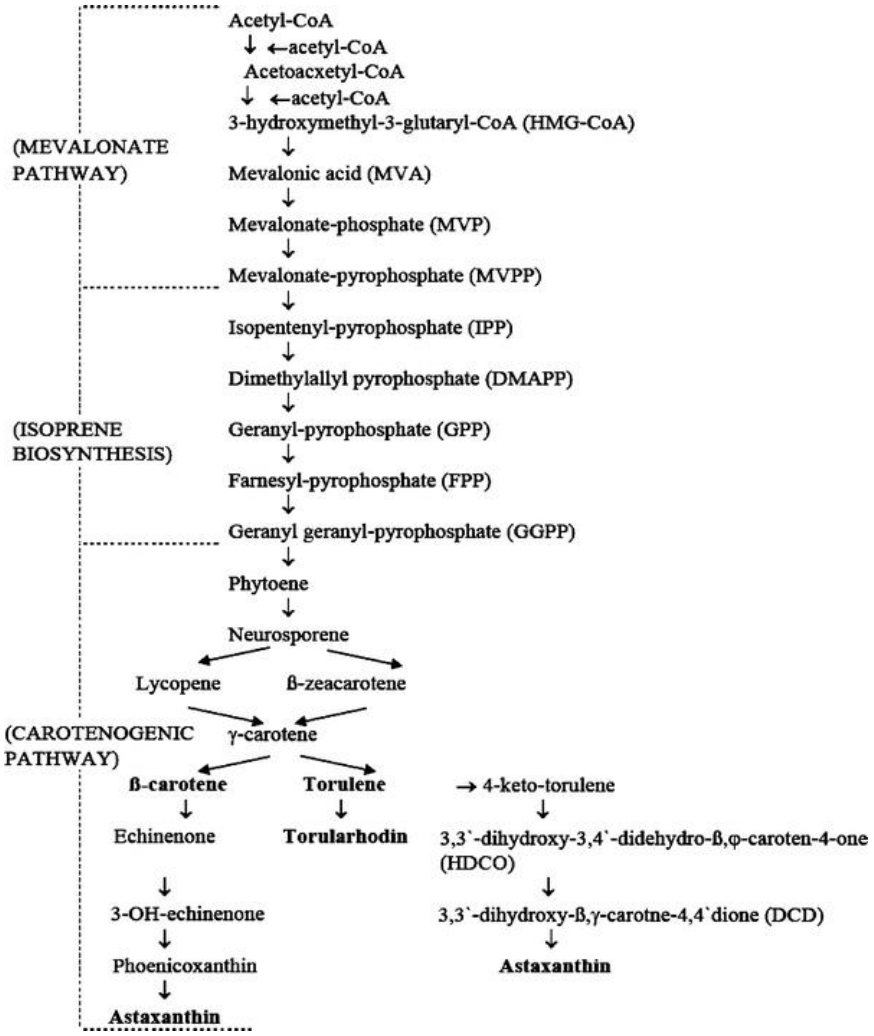

Figure 1.13. Biosynthetic pathways from acetyl-CoA to β-carotene, torulene and torularhodin in *Rhodotorula* species and astaxanthin in *P. rhodozyma*/*X. dendrorhous* (Frengova and Beshkova 2009).

1.5.6. Mevalonic acid biosynthesis

The mevalonic acid biosynthetic pathway, which is the biosynthetic pathway from acetyl-CoA to dimethylallyl pyrophosphate (IPP), is shown **(Figure 1.14**). First, three molecules of acetyl CoA are simultaneously converted to hydroxymethylglutaryl-CoA (HMG-CoA) by hydroxymethylglutaryl-CoA synthase (*HMGS*), and HMG-CoA is then converted to mevalonic acid (MVA) by HMG-CoA reductase (*HMGR*). Additionally, MVA is converted to isopentenyl-pyrophosphate by mevalonate kinase (*MVAK1*), diphosphomevalonate kinase (*MVAK2*) and diphosphomevalonate decarboxylase (*MVAD*). The synthesis of this acetyl-CoA to IPP is a continuous reaction through Mevalonate-5-phosphate (MVA-P) and Mevalonate-5-pyrophosphate (MVA-PP) (Loto *et al.* 2012; Bröker *et al.* 2018).

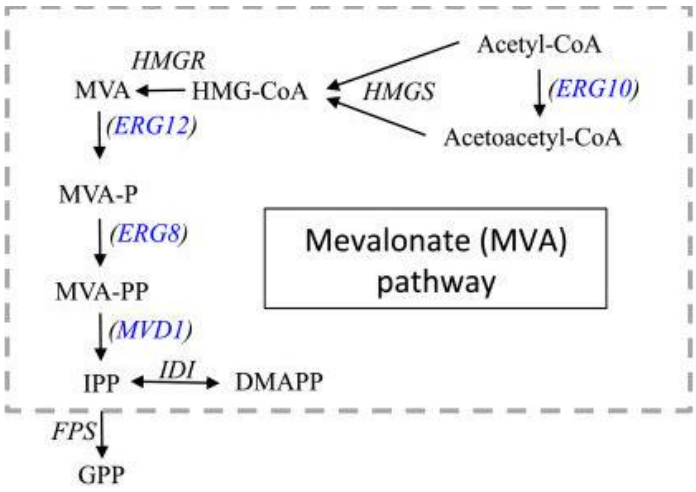

Figure 1.14. The mevalonate pathway in *X. dendrorhous.* 3-hydroxy-3-methylglutaryl-CoA (HMG-CoA), Mevalonate (MVA), Mevalonate-5-phosphate (MVA-P), Mevalonate-5-pyrophosphate (MVA-PP), Isopentenyl-pyrophosphate (IPP), Dimethylallyl-pyrophosphate (DMAPP), Geranyl-pyrophosphate (GPP), HMG-CoA synthase (*HMGS*), HMG-CoA reductase (*HMGR*) (Blue shown genes in the *Saccharomyces cerevisiae* respectively) (Loto *et al.* 2012).

1.5.7. Isoprene biosynthesis

The isoprenoid biosynthetic pathway, which is the biosynthetic pathway from IPP to phytoene, is shown (**Figure 1.15**). The IPP molecule is converted to dimethylallyl-pyrophosphate (DMAPP) by isopentenyl-diphosphate delta-isomerase (*IDI*). After that, DMAPP and IPP are bound by farnesyl diphosphate synthase (*FDPS*), then converted to geranyl-pyrophosphate (GPP). GPP is subsequently converted to geranyl geranyl-pyrophsphate (GGPP), which is formed by the addition of 20 carbon atoms by the geranylgeranyl diphosphate synthase (*GGPSI, crtE*) enzyme. Two GGPP molecules are then

bound by phytoene synthase (*CAR2, crtYB*) to synthesize phytoene, which is the first biosynthetic product of carotenoids, which is formed by 40 carbon atoms.

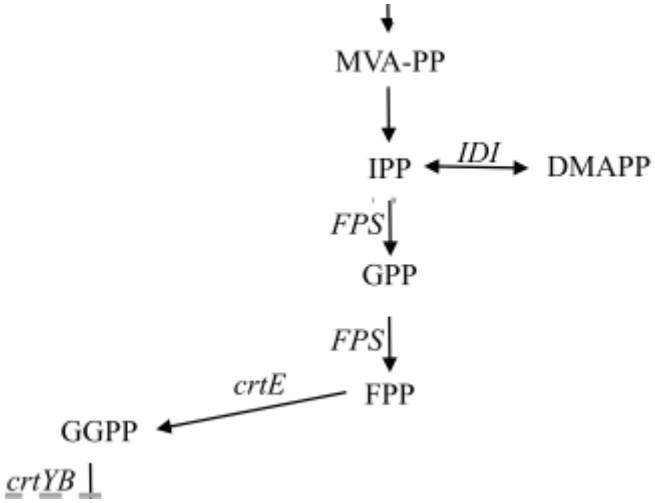

Figure 1.15. The isoprene biosynthetic pathway (Loto *et al.* 2012)

1.5.8. Carotenoid biosynthesis

After the MVA pathway and isoprene biosynthesis, C20 compound GGPP leads to the phytoene- the first C40 carotene component in the carotenoid biosynthesis pathway by phytoene synthase (*CAR2/CarB*). Phytoene biosynthesized by the isoprenoid biosynthetic pathway is then converted to lycopene by phytoene desaturase (*CAR1/CarRA*). After that, lycopene is converted to γ-carotene, and β-carotene by lycopene cyclase (*CAR2/CarB*). Neurosporaxanthin and astaxanthin are also biosynthesized from γ-carotene (Avalos *et al.* 2017). Lycopene is an all-*trans* compound, thus, the isomerization of the first or second double-bond of the phytoene occurs at the same stage of the desaturation process (Mata-Gómez *et al.* 2014). Lycopene also acts as a precursor of cyclic carotenoids and undergoes several metabolic reactions to form β-carotene, γ-carotene, torulene, torularhodin and astaxanthin.

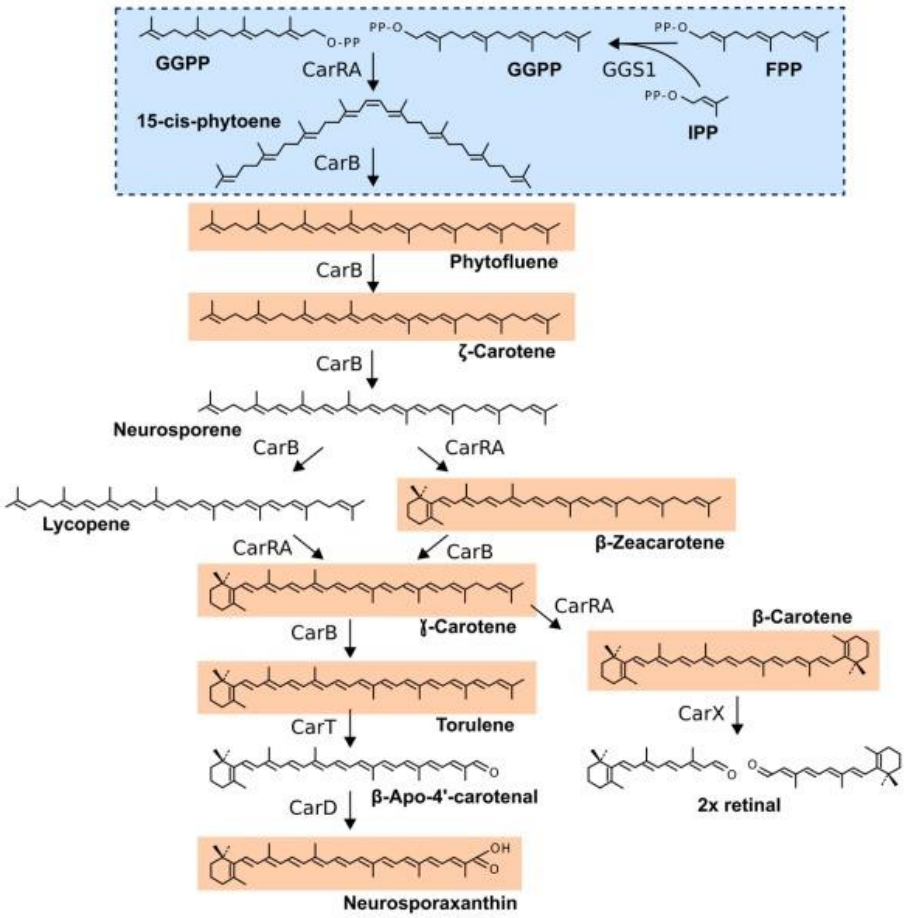

Figure 1.16. The carotenoid biosynthesis pathway and genes: *CarRA.* , *CarB.* , *CarT.* , *CarD* in *Saccharomyces cerevisiae* (Avalos *et al.* 2017)

1.6. Factors affecting lipid/carotenoid production

Lipid and carotenoid production by microorganisms have more advantages over other methods, including the less effect by seasonal and geographical variations and the potential to achieve high rates of production. Besides, they can accumulate lipids/carotenoids from low-cost natural substrates (such as carbohydrates) (Lin, Jain and Yan 2014; Lin *et al.* 2017). However, the lipid and carotenoid production process is influenced by many factors including choice of carbon source, nitrogen source, light, temperature, pH, aeration, metal ion and salts (Alcantara and Sanchez 1999; Mata-Gómez *et al.* 2014).

Carbon source is the most studied parameter to influence to growth or lipid and carotenoid production. Glucose and other fermentable sugars are metabolized by the glycolytic

pathway, then through alcoholic fermentation, even in the presence of oxygen (Hannibal *et al.* 2000). Ethanol as a carbon source is carried through acetyl-CoA oxidation to the citric acid cycle, where it was reported to increase pigments synthesis (Gu, An and Johnson 1997; Orosa *et al.* 2005; Marcoleta *et al.* 2011). With the knowledge that glucose, sucrose and xylose supports rapid growth and pigment production, the influence of these carbon sources on growth and pigment production was tested in the many strains (Alcantara and Sanchez 1999).

C/N ratio was also mentioned as a key factor when studying in the lipid production or lipid/carotenoid production. During nitrogen starvation conditions, the depletion reduces intracellular AMP concentration. Since AMP is a complex substrate of isocitrate dehydrogenase (*IDH*) in the citric acid cycle, the activity of *IDH*, which uses isocitrate (citric acid derivative), as a substrate also decreases. As a result, a large amount of isocitric acid is released, which is then converted to acetyl CoA for use as the main substrate for fatty acid biosynthesis (Tang *et al.* 2009). Therefore, the high C/N ratio was reported to support high lipid production. It was also reported that in *R. glutilis*, both carotenoids and lipids accumulated in cultures that contained a high carbon to nitrogen ratio. Therefore, it is suggested that carotenoids were produced under conditions that also promoted lipid synthesis (Braunwald *et al.* 2013; Elfeky *et al.* 2019), The high C/N ratio was also reported to promote lipid production *Yarrowia lipolytica* (Ledesma-Amaro, Dulermo and Nicaud 2015; Bellou *et al.* 2016b).

Light was reported for carotenoid production through carotenogenesis. Due to the effect of light and the possible roles of fatty acid metabolism in carotenoid production in *Dunaliella salina*, it appeared that carotenoid overproduction was associated with lipid globule formation and a decrease fatty acid unsaturation (Lamers *et al.* 2010). The source and intensity of light affects in the carotenoid or lipid production in different ways (Zhang, Zhang and Tan 2014). Therefore, lipid unsaturation and xanthophylls are required to provide proper structure and function for the membrane environment , thus protecting it against light (Zakar *et al.* 2017).

Temperature is another parameter that affects growing cells and metabolite production, as the effect of temperature depends on the microorganism, which in turn affects the number of products (Bhosale and Gadre 2001b; Vijayalakshmi *et al.* 2001; Aksu and Tuğba Eren 2005; Orosa *et al.* 2005).The xanthophyll- and polyunsaturated lipid-deficient ROAD mutant of *Synechocystis* spp., has also been used as a model to study the effect of low temperatures on the saturation level of glycerolipids. Results indicated that the maximum biomass was 17.9 g/L at a relatively higher temperature group of 30 h, whereas, that of 15.8 g/L had a relatively lower

temperature group at 45 h. Meanwhile, higher carotenoid productivity was obtained at 30°C than that at 24°C (Zhang, Zhang and Tan 2014).

pH. Optimal pH has been reported for growth, including lipid and carotenoid production by the yeast *R. toruloides* NCYC 921 (Dias *et al.* 2015, 2016) or *R. mucilaginosa* (da Silva *et al.* 2020).

Aeration factor. This factor affects growth rate, cell mass and carotenogenesis. Metal ions and salts have also impacted in stimulating carotenoids production (Hayman *et al.* 1974; Buzzini *et al.* 2005).

Metal ion and salts. The effects of different concentrations of MgSO4·7H2O, FeCl3 · 6H2O, ZnSO4·7H2O, CuSO4·5H2O and MnSO4·5H2O was optimized for lipid and GLA production by *Cunninghamella* sp. Mg, Fe and Zn were shown to have a profound effects on lipid production (Muhid *et al.* 2008). Furthermore, Buzzini *et al* reported that the trace elements showed a selective influence on the carotenoid profile in *R. gramini*s (Buzzini *et al.* 2005).

Among these factors, the information for carbon and nitrogen sources, temperature, pH, aeration, metal ion and salts factor were reported in many papers. The light factor was reported in few studies, whereas most studies reported for only lipid or carotenoid production microorganisms and rarely in both carotenoid and lipid production. Besides, carotenogenesis is a photo protective mechanism; therefore, the carotenoid production in microorganisms serve as a defense mechanism of cells from light or other environmental stresses (Mata-Gómez *et al.* 2014). Unsaturated fatty acids are antioxidants that protect cells. Thus, light was suggested to relate to carotenoid and lipid production, and more attention focuses on the lipid carotenoid producer (carotenoid oleaginous microorganism), such as microorganisms shown in **Table 1.4** below).

Table 1.4. List of microorganisms that can produce both lipids and carotenoids

Strains	**References**
Microalgae	
Tetraselmis	(Dahmen-Ben Moussa *et al.* 2017)
Dunaliella	(Chagas *et al.* 2015; Bonnefond *et al.* 2017)
Chlorella	(Campenni' *et al.* 2013)

Yeast	
Sporidiobolus	(Khodaiyan *et al.* 2007; Han *et al.* 2016; Chaiyaso and Manowattana 2018)
Yarrowia	(Beopoulos *et al.* 2008; Matthäus *et al.* 2014; Rakicka *et al.* 2015; Bellou *et al.* 2016b; Shabbir Hussain *et al.* 2016; Bruder *et al.* 2020)
Rhodotorula/Rhodosporidium	(Perrier, Dubreucq and Galzy 1995; Braunwald *et al.* 2013; Zhang, Zhang and Tan 2014; Dias *et al.* 2016; Singh *et al.* 2016; Zhang *et al.* 2016; Pi *et al.* 2018)

Rhodosporidium toruloides belong the oleaginous yeast that also produces carotenoids. Therefore, we studied the effect of light on carotenoid and lipid production in the *Rhodosporidium toruloides* strain.

Research about the light factor

Light is a particularly important factor because carotenogenesis is a photoprotective mechanism; microorganisms produce carotenoids as an antioxidant which performs a role in protecting cells from light or other environmental stresses (Mata-Gómez *et al.* 2014). Thus, the carotenoid production is dependent on the period and intensity of exposed light. Two important aspects of photo-induction have previously been reported. The first is that conditions that increase microbial growth also increase carotenoid production, whereas, the second is that increased activity of the enzymes essential to carotenoid biosynthesis results in an associated increase in cellular accumulation of these carotenoids (Frengova and Beshkova 2009). Therefore, light becomes interesting in researches, and was reported in various strains. Light affects carotenoid yield and changes the carotenoid composition dependent species, such as *Euglena gracilis*, *Nicotiana tabacum*, *Xanthophyllomyces dendrorhous*, *Haematococcus pluvialis*, *Cryptococcus neoformans*, *Rhodotorula glutinis*, *Synechocystis* sp *etc* (Constantopoulos and Bloch 1967; Takeda *et al.* 1996; Sakaki *et al.* 2001; Vázquez 2001; Steinbrenner and Linden 2003; Idnurm and Heitman 2005; Takano *et al.* 2005; Stachowiak and Czarnecki 2007; Zhang *et al.* 2015; Zakar *et al.* 2017). There is evidence that fungal growth and carotenoid production were influenced by exposure to light (Linden, Ballario and Macino

1997; Khanafari, Tayari and Emami 2008). In *Rhodotorula glutilis*, increased biomass concentration and carotenoid formation have been observed in light-grown cultures (Zhang, Zhang and Tan 2014) and *R. toruloides* carotenogenesis is light inducible (Takano *et al.* 2005).

1.7. Aim of the studies

In this study, the effects of light on the carotenoid and lipid production of *R. toruloides* NBRC10032 was investigated. *R. toruloides* NBRC10032 was identified as the strong lipid producer screened from the National Institute of Technology and Evaluation (NITE, Chiba, Japan). Besides, *R. toruloides* NBRC10032 has the ability of carotenoid production in the red-yeast groups. Furthermore, carotenoids are components that are localized in the lipid body of oleaginous yeasts. Thus, NBRC10032 is a suitable strain for carotenoid production. Therefore, by comparing microbial growth and gene expression patterns, I demonstrated that carotenoid biosynthesis was controlled at the transcription level in response to light. This process occurred via a two-step response in which temporary gene activation occurred early in the cultivation period (1 h), and later (72 h) in the main carotenogenic genes, geranylgeranyl diphosphate synthase, phytoene desaturase, and phytoene synthase/lycopene cyclase (encoding by *GGPSI*, *CAR1*, and *CAR2*, respectively). Moreover, *CRY1* (encoding the putative Cryptochrome DASH, the blue-light receptor) was expressed exponentially in the early light-exposure period. Therefore, unravelling the regulatory mechanisms involved in carotenoid production, namely, *CRY1* disruption (to analyze its function) and comparative genome analysis of mutants (to obtain new insights into responses to light) were approached. Additionally, deleting *CRY1* using gene targeting revealed that this gene partially contributed to carotenoid production. Therefore, comparative genome analysis of high carotenoid-producing mutants resulted in the detection of genes possessing single nucleotide polymorphism (SNP). Our results also show a strong possibility that NBRC 10032 is a homozygous diploid strain.

1.8. References

Abedi E, Sahari MA. Long-chain polyunsaturated fatty acid sources and evaluation of their nutritional and functional properties. *Food Sci Nutr* 2014;**2**:443–63.

Ageitos JM, Vallejo JA, Veiga-Crespo P *et al.* Oily yeasts as oleaginous cell factories. *Appl Microbiol Biotechnol* 2011;**90**:1219–27.

Aksu Z, Tuğba Eren A. Carotenoids production by the yeast *Rhodotorula mucilaginosa*: Use of agricultural wastes as a carbon source. *Process Biochem* 2005;**40**:2985–91.

Alcantara S, Sanchez S. Influence of carbon and nitrogen sources on *Flavobacterium* growth and zeaxanthin biosynthesis. *J Ind Microbiol Biotechnol* 1999;**23**:697–700.

Allaire J, Couture P, Leclerc M *et al.* A randomized, crossover, head-to-head comparison of eicosapentaenoic acid and docosahexaenoic acid supplementation to reduce inflammation markers in men and women: the Comparing EPA to DHA (ComparED) Study 1-3. *Am J Clin Nutr* 2016;**104**:280–7.

Ananda N, Vadlani P V. Production and optimization of carotenoid-enriched dried distiller's grains with solubles by *Phaffia rhodozyma* and *Sporobolomyces roseus* fermentation of whole stillage. *J Ind Microbiol Biotechnol* 2010;**37**:1183–92.

Avalos J, Pardo-Medina J, Parra-Rivero O *et al.* Carotenoid Biosynthesis in *Fusarium*. *J Fungi* 2017;**3**, DOI: 10.3390/jof3030039.

Axelsson M, Gentili F. A single-step method for rapid extraction of total lipids from green microalgae. *PLoS One* 2014;**9**:17–20.

Bellou S, Triantaphyllidou IE, Aggeli D *et al.* Microbial oils as food additives: Recent approaches for improving microbial oil production and its polyunsaturated fatty acid content. *Curr Opin Biotechnol* 2016a;**37**:24–35.

Bellou S, Triantaphyllidou IE, Mizerakis P *et al.* High lipid accumulation in *Yarrowia lipolytica* cultivated under double limitation of nitrogen and magnesium. *J Biotechnol* 2016b;**234**:116–26.

Beopoulos A, Chardot T, Nicaud JM. *Yarrowia lipolytica*: A model and a tool to understand the mechanisms implicated in lipid accumulation. *Biochimie* 2009;**91**:692–6.

Beopoulos A, Mrozova Z, Thevenieau F *et al.* Control of Lipid Accumulation in the Yeast *Yarrowia lipolytica*. *Appl Environ Microbiol* 2008;**74**:7779–89.

Bhosale P. Environmental and cultural stimulants in the production of carotenoids from microorganisms. *Appl Microbiol Biotechnol* 2004;**63**:351–61.

Bhosale P, Gadre R V. β-Carotene production in sugarcane molasses by a *Rhodotorula glutinis* mutant. *J Ind Microtechnology* 2001a;**26**:327–32.

Bhosale P, Gadre R V. Optimization of carotenoid production from hyper-producing *Rhodotorula glutinis* mutant 32 by a factorial approach. *Lett Appl Microbiol* 2001b;**33**:12–6.

Bohne F, Linden H. Regulation of carotenoid biosynthesis genes in response to light in *Chlamydomonas reinhardtii*. *Biochim Biophys Acta* 2002;**1579**:26–34.

Bonnefond H, Moelants N, Talec A *et al.* Coupling and uncoupling of triglyceride and beta-carotene production by Dunaliella salina under nitrogen limitation and starvation. *Biotechnol Biofuels* 2017;**10**:1–10.

Bonturi N, Matsakas L, Nilsson R *et al.* Single cell oil producing yeasts Lipomyces starkeyi and Rhodosporidium toruloides: Selection of extraction strategies and biodiesel property prediction. *Energies* 2015;**8**:5040–52.

Boskou D, Blekas G, Tsimidou M. *Olive Oil Composition*., 2006.

Botes AL. Affinity purification and characterization of a yeast epoxide hydrolase. *Biotechnol Lett* 1999;**21**:511–7.

Braunwald T, Schwemmlein L, Graeff-Hönninger S *et al.* Effect of different C/N ratios on carotenoid and lipid production by *Rhodotorula glutinis*. *Appl Microbiol Biotechnol* 2013;**97**:6581–8.

Britton G. *Carotenoids Handbook*. 1st ed. Britton G, Liaen-Jensen S, Pfander H (eds.). Birkhäuser Basel, 2004.

Bröker JN, Müller B, van Deenen N *et al.* Upregulating the mevalonate pathway and repressing sterol synthesis in *Saccharomyces cerevisiae* enhances the production of triterpenes. *Appl Microbiol Biotechnol* 2018;**102**:6923–34.

Brotosudarmo THP, Limantara L, Setiyono E *et al.* Structures of Astaxanthin and Their Consequences for Therapeutic Application. *Int J Food Sci* 2020;**2020**:14–7.

Bruder S, Melcher FA, Zoll T *et al.* Evaluation of a *Yarrowia lipolytica* Strain Collection for Its Lipid and Carotenoid Production Capabilities. *Eur J Lipid Sci Technol* 2020;**122**, DOI:

10.1002/ejlt.201900172.

Buzzini P, Innocenti M, Turchetti B *et al.* Carotenoid profiles of yeasts belonging to the genera *Rhodotorula*, *Rhodosporidium*, *Sporobolomyces*, and *Sporidiobolus*. *Can J Microbiol* 2007;**53**:1024–31.

Buzzini P, Martini A, Gaetani M *et al.* Optimization of carotenoid production by Rhodotorula graminis DBVPG 7021 as a function of trace element concentration by means of response surface analysis. *Enzyme Microb Technol* 2005;**36**:687–92.

Calvey CH, Su YK, Willis LB *et al.* Nitrogen limitation, oxygen limitation, and lipid accumulation in *Lipomyces starkeyi*. *Bioresour Technol* 2016;**200**:780–8.

Campenni' L, Nobre BP, Santos CA *et al.* Carotenoid and lipid production by the autotrophic microalga *Chlorella protothecoides* under nutritional, salinity, and luminosity stress conditions. *Appl Microbiol Biotechnol* 2013;**97**:1383–93.

Cardoso LAC, Jäckel S, Karp SG *et al.* Improvement of *Sporobolomyces ruberrimus* carotenoids production by the use of raw glycerol. *Bioresour Technol* 2016;**200**:374–9.

Cecilie Braarud H, Markhus MW, Skotheim S *et al.* Maternal DHA Status during Pregnancy Has a Positive Impact on Infant Problem Solving: A Norwegian Prospective Observation Study. , DOI: 10.3390/nu10050529.

Chagas AL, Rios AO, Jarenkow A *et al.* Production of carotenoids and lipids by *Dunaliella tertiolecta* using CO2 from beer fermentation. *Process Biochem* 2015;**50**:981–8.

Chaiyaso T, Manowattana A. Enhancement of carotenoids and lipids production by oleaginous red yeast *Sporidiobolus pararoseus* KM281507. *Prep Biochem Biotechnol* 2018;**48**:13–23.

Chandi GK, Gill BS. Production and characterization of microbial carotenoids as an alternative to synthetic colors: A review. *Int J Food Prop* 2011;**14**:503–13.

Constantopoulos G, Bloch K. Effect of Light Intensity of *Euglena gracilis*. *J Biol chemitry* 1967;**242**:3538–42.

Dahmen-Ben Moussa I, Chtourou H, Karray F *et al.* Nitrogen or phosphorus repletion strategies for enhancing lipid or carotenoid production from Tetraselmis marina. *Bioresour Technol* 2017;**238**:325–32.

Daisuke Sasatani, Rakhovskaya M, Highli R. *Biofuels Annual - Japan.*, 2020.

Darwish R, Gedi MA, Akepach P *et al. Chlamydomonas reinhardtii* is a potential food supplement with the capacity to outperform *Chlorella* and *Spirulina*. *Appl Sci* 2020;**10**:6736.

Davoli P, Mierau V, Weber RWS. Carotenoids and fatty acids in red yeasts *Sporobolomyces roseus* and *Rhodotorula glutinis*. *Appl Biochem Microbiol* 2004;**40**:392–7.

Dias C, Silva C, Freitas C *et al.* Effect of Medium pH on *Rhodosporidium toruloides* NCYC 921 Carotenoid and Lipid Production Evaluated by Flow Cytometry. *Appl Biochem Biotechnol* 2016;**179**:776–87.

Dias C, Sousa S, Caldeira J *et al.* New dual-stage pH control fed-batch cultivation strategy for the improvement of lipids and carotenoids production by the red yeast Rhodosporidium toruloides NCYC 921. *Bioresour Technol* 2015;**189**:309–18.

Dimitrova S, Pavlova K, Lukanov L *et al.* Production of metabolites with antioxidant and emulsifying properties by antarctic strain *Sporobolomyces salmonicolor* AL1. *Appl Biochem Biotechnol* 2013;**169**:301–11.

Dulermo R, Gamboa-Meléndez H, Ledesma-Amaro R *et al.* Unraveling fatty acid transport and activation mechanisms in *Yarrowia lipolytica*. *Biochim Biophys Acta - Mol Cell Biol Lipids* 2015a;**1851**:1202–17.

Dulermo T, Lazar Z, Dulermo R *et al.* Analysis of ATP-citrate lyase and malic enzyme mutants of *Yarrowia lipolytica* points out the importance of mannitol metabolism in fatty acid synthesis. *Biochim Biophys Acta - Mol Cell Biol Lipids* 2015b;**1851**:1107–17.

Elfeky N, Elmahmoudy M, Zhang Y *et al.* Lipid and carotenoid production by Rhodotorula glutinis with a combined cultivation mode of nitrogen, sulfur, and aluminium stress. *Appl Sci* 2019;**9**, DOI: 10.3390/app9122444.

Ewing M, Msangi S. Biofuels production in developing countries: assessing tradeoffs in welfare and food security. *Environ Sci Policy* 2009;**12**:520–8.

Fei Q, O'Brien M, Nelson R *et al.* Enhanced lipid production by *Rhodosporidium toruloides* using different fed-batch feeding strategies with lignocellulosic hydrolysate as the sole carbon source. *Biotechnol Biofuels* 2016;**9**:1–12.

Ferrucci L, Fabbri E. Inflammageing: chronic inflammation in ageing, cardiovascular disease, and frailty HHS Public Access. 2018, DOI: 10.1038/s41569-018-0064-2.

Frengova GI, Beshkova DM. Carotenoids from *Rhodotorula* and *Phaffia*: yeasts of biotechnological importance. *J Ind Microbiol Biotechnol* 2009;**36**:163–80.

Galafassi S, Cucchetti D, Pizza F *et al.* Lipid production for second generation biodiesel by the oleaginous yeast *Rhodotorula graminis*. *Bioresour Technol* 2012;**111**:398–403.

Garay LA, Boundy-mills KL, German JB. Accumulation of Hgh-Value Lipids in Single-Cell Microorganisms: A Mechanistic Approach and Future Perspectives. *J Agric Food Chem* 2014;**62**:2709–27.

García-González M, Moreno J, Cañavate JP *et al.* Conditions for open-air outdoor culture of *Dunaliella salina* in southern Spain. *J Appl Phycol* 2003;**15**:177–84.

Gmoser R, Ferreira JA, Lundin M *et al.* Pigment production by the edible filamentous fungus *Neurospora intermedia*. *Fermentation* 2018;**4**, DOI: 10.3390/fermentation4010011.

Goralczyk R, Buser S, Bausch J *et al.* Occurrence of birefringent retinal inclusions in cynomolgus monkeys after high doses of canthaxanthin. *Investig Ophthalmol Vis Sci* 1997;**38**:741–52.

Gu WL, An GH, Johnson EA. Ethanol increases carotenoid production in *Phaffia rhodozyma*. *J Ind Microbiol Biotechnol* 1997;**19**:114–7.

Han D, Li Y, Hu Q. Astaxanthin in microalgae: Pathways, functions and biotechnological implications. *Algae* 2013;**28**:131–47.

Han M, Xu Z yuan, Du C *et al.* Effects of nitrogen on the lipid and carotenoid accumulation of oleaginous yeast *Sporidiobolus pararoseus*. *Bioprocess Biosyst Eng* 2016;**39**:1425–33.

Hannibal L, Lorquin J, D'Ortoli NA *et al.* Isolation and characterization of canthaxanthin biosynthesis genes from the photosynthetic bacterium *Bradyrhizobium* sp. strain ORS278. *J Bacteriol* 2000;**182**:3850–3.

Hayman EP, Yokoyama H, Chichester CO *et al.* Carotenoid biosynthesis in Rhodotorula glutinis. *J Bacteriol* 1974;**120**:1339–43.

Hempel J, Schädle CN, Leptihn S *et al.* Structure related aggregation behavior of carotenoids and carotenoid esters. *J Photochem Photobiol A Chem* 2016;**317**:161–74.

Huang C, Chen X fang, Xiong L *et al.* Microbial oil production from corncob acid hydrolysate by oleaginous yeast *Trichosporon coremiiforme*. *Biomass and Bioenergy* 2013;**49**:273–8.

Hynes MJ, Murray SL. ATP-citrate lyase is required for production of cytosolic acetyl

coenzyme A and development in *Aspergillus nidulans*. *Eukaryot Cell* 2010;**9**:1039–48.

Ide T, Hoya M, Tanaka T *et al.* Enhanced production of astaxanthin in *Paracoccus* sp. strain N-81106 by using random mutagenesis and genetic engineering. *Biochem Eng J* 2012;**65**:37–43.

Idnurm A, Heitman J. Light controls growth and development via a conserved pathway in the fungal kingdom. *PLoS Biol* 2005;**3**:0615–26.

Iijima M, Paulson J. Japan Biofuels Annual 2017. 2017.

Ip PF, Chen F. Production of astaxanthin by the green microalga *Chlorella zofingiensis* in the dark. *Process Biochem* 2005;**40**:733–8.

J. Brigham C, Kurosawa K. Bacterial Carbon Storage to Value Added Products. *J Microb Biochem Technol* 2011;**s3**:0–13.

Karim A, Islam MA, Yousuf A *et al.* Microbial Lipid Accumulation through Bioremediation of Palm Oil Mill Wastewater by *Bacillus cereus*. *ACS Sustain Chem Eng* 2019;**7**:14500–8.

Khanafari A, Tayari K, Emami M. Light Requirement for the Carotenoids Production by *Mucor hiemalis*. *Iran J Basic Med Sci* 2008;**11**:25–32.

Khodaiyan F, Razavi SH, Emam-Djomeh Z *et al.* Effect of culture conditions on canthaxanthin production by Dietzia natronolimnaea HS-1. *J Microbiol Biotechnol* 2007;**17**:195–201.

Kim JK, Kim JI, Lee NK *et al.* Extraction of β-carotene produced from yeast *Rhodosporidium* sp. and its heat stability. *Food Sci Biotechnol* 2010;**19**:263–6.

Kitahara Y, Yin T, Zhao X *et al.* Isolation of oleaginous yeast (*Rhodosporidium toruloides*) mutants tolerant of sugarcane bagasse hydrolysate. *Biosci Biotechnol Biochem* 2014;**78**:336–42.

Lamers PP, Van De Laak CCW, Kaasenbrood PS *et al.* Carotenoid and fatty acid metabolism in light-stressed *Dunaliella salina*. *Biotechnol Bioeng* 2010;**106**:638–48.

Lazar Z, Liu N, Stephanopoulos G. Holistic Approaches in Lipid Production by Yarrowia lipolytica. *Trends Biotechnol* 2018;**36**:1157–70.

Ledesma-Amaro R, Dulermo T, Nicaud JM. Engineering *Yarrowia lipolytica* to produce biodiesel from raw starch. *Biotechnol Biofuels* 2015;**8**, DOI: 10.1186/s13068-015-0335-7.

Lee JJL, Chen L, Shi J *et al.* Metabolomic profiling of *Rhodosporidium toruloides* grown on glycerol for carotenoid production during different growth phases. *J Agric Food Chem* 2014;**62**:10203–9.

Li Q, Du W, Liu D. Perspectives of microbial oils for biodiesel production. *Appl Microbiol Biotechnol* 2008;**80**:749–56.

Li Y, Zhao Z (Kent), Bai F. High-density cultivation of oleaginous yeast *Rhodosporidium toruloides* Y4 in fed-batch culture. *Enzyme Microb Technol* 2007;**41**:312–7.

Lin X, Gao N, Liu S *et al.* Characterization the carotenoid productions and profiles of three Characterization the carotenoid productions and profiles of three *Rhodosporidium toruloides* mutants from *Agrobacterium tumefaciens*-mediated transformation. *Yeast* 2017;**34**:335–42.

Lin Y, Jain R, Yan Y. Microbial production of antioxidant food ingredients via metabolic engineering. *Curr Opin Biotechnol* 2014;**26**:71–8.

Linden H, Ballario P, Macino G. Blue light regulation in *Neurospora crassa*. *Fungal Genet Biol* 1997;**22**:141–50.

Ling X, Guo J, Liu X *et al.* Impact of carbon and nitrogen feeding strategy on high production of biomass and docosahexaenoic acid (DHA) by *Schizochytrium* sp. LU310. *Bioresour Technol* 2015;**184**:139–47.

Liu J, Gerken H, Huang J *et al.* Engineering of an endogenous phytoene desaturase gene as a dominant selectable marker for *Chlamydomonas reinhardtii* transformation and enhanced biosynthesis of carotenoids. *Process Biochem* 2013;**48**:788–95.

Loto I, Gutiérrez MS, Barahona S *et al.* Enhancement of carotenoid production by disrupting the C22-sterol desaturase gene (CYP61) in *Xanthophyllomyces dendrorhous*. *BMC Microbiol* 2012;**12**, DOI: 10.1186/1471-2180-12-235.

Lu Q, Bu YF, Liu JZ. Metabolic engineering of *Escherichia coli* for producing astaxanthin as the predominant carotenoid. *Mar Drugs* 2017;**15**, DOI: 10.3390/md15100296.

Makareviciene V, Skorupskaite V, Levisauskas D *et al.* The optimization of biodiesel fuel production from microalgae oil using response surface methodology. *Int J Green Energy* 2014;**11**:527–41.

Marcoleta A, Niklitschek M, Wozniak A *et al.* Glucose and ethanol-dependent transcriptional

regulation of the astaxanthin biosynthesis pathway in Xanthophyllomyces dendrorhous. *BMC Microbiol* 2011;**11**:190.

Marova I, Carnecka M, Halienova A *et al.* Production of carotenoid-/ergosterol-supplemented biomass by red yeast *Rhodotorula glutinis* grown under external stress. *Food Technol Biotechnol* 2010;**48**:56–61.

Mata-Gómez LC, Montañez JC, Méndez-Zavala A *et al.* Biotechnological production of carotenoids by yeasts: An overview. *Microb Cell Fact* 2014;**13**:1–11.

Matsakas L, Giannakou M, Vörös D. Effect of synthetic and natural media on lipid production from *Fusarium oxysporum*. *Electron J Biotechnol* 2017;**30**:95–102.

Matsuzawa T, Kamisaka Y, Maehara T *et al.* Identification and characterization of two fatty acid elongases in *Lipomyces starkeyi*. *Appl Microbiol Biotechnol* 2020;**104**:2537–44.

Matthäus F, Ketelhot M, Gatter M *et al.* Production of lycopene in the non-carotenoid-producing yeast *Yarrowia lipolytica*. *Appl Environ Microbiol* 2014;**80**:1660–9.

Maza DD, Viñarta SC, Su Y *et al.* Growth and lipid production of *Rhodotorula glutinis* R4, in comparison to other oleaginous yeasts. *J Biotechnol* 2020;**310**:21–31.

Meyer PS, Preez JC. Effect of acetic acid on astaxanthin production by *Phaffia rhodozyma*. *Biotechnol Lett* 1993;**15**:919–24.

Miao L, Chi S, Tang Y *et al.* Astaxanthin biosynthesis is enhanced by high carotenogenic gene expression and decrease of fatty acids and ergosterol in a *Phaffia rhodozyma* mutant strain. *FEMS Yeast Res* 2011;**11**:192–201.

Mitra D, Rasmussen ML, Chand P *et al.* Value-added oil and animal feed production from corn-ethanol stillage using the oleaginous fungus *Mucor circinelloides*. *Bioresour Technol* 2012;**107**:368–75.

Montoya C, Cochard B, Flori A *et al.* Genetic architecture of palm oil fatty acid composition in cultivated oil palm (Elaeis guineensis Jacq.) compared to its wild relative E. oleifera (H.B.K) Cortés. *PLoS One* 2014;**9**, DOI: 10.1371/journal.pone.0095412.

Muhid F, Nawi WNNW, Kader AJA *et al.* Effects of metal ion concentrations on lipid and gamma linolenic acid production by Cunninghamella sp. 2A1. *Online J Biol Sci* 2008;**8**:62–7.

Muniraj IK, Uthandi SK, Hu Z *et al.* Microbial lipid production from renewable and waste

materials for second-generation biodiesel feedstock. *Environ Technol Rev* 2015;**4**:1–16.

Nerem RS, Beckley BD, Fasullo JT *et al.* Climate-change-driven accelerated sea-level rise detected in the altimeter era. *Proc Natl Acad Sci U S A* 2018;**115**:2022–5.

Nie ZK, Ji XJ, Shang JS *et al.* Arachidonic acid-rich oil production by Mortierella alpina with different gas distributors. *Bioprocess Biosyst Eng* 2014;**37**:1127–32.

Niehus X, Casas-Godoy L, Rodríguez-Valadez FJ *et al.* Evaluation of *Yarrowia lipolytica* Oil for Biodiesel Production: Land Use Oil Yield, Carbon, and Energy Balance. *J Lipids* 2018;**2018**:1–6.

Nuraini, Sabrina, Latif SA. Improving the quality of tapioca by product through fermentation by *Neurospora crassa* to produce β carotene rich feed. *Pakistan J Nutr* 2009;**8**:487–90.

Okuda T, Ando A, Negoro H *et al.* Eicosapentaenoic acid (EPA) production by an oleaginous fungus Mortierella alpina expressing heterologous the Δ17-desaturase gene under ordinary temperature. *Eur J Lipid Sci Technol* 2015;**117**:1919–27.

Orosa M, Franqueira D, Cid A *et al.* Analysis and enhancement of astaxanthin accumulation in Haematococcus pluvialis. *Bioresour Technol* 2005;**96**:373–8.

Perrier V, Dubreucq E, Galzy P. Fatty acid and carotenoid composition of *Rhodotorula strains*. *Arch Microbiol* 1995;**164**:173–9.

Pi HW, Anandharaj M, Kao YY *et al.* Engineering the oleaginous red yeast *Rhodotorula glutinis* for simultaneous β-carotene and cellulase production. *Sci Rep* 2018;**8**:2–11.

Politino M, Tonzi SM, Burnett W V *et al.* Purification and characterization of a cephalosporin esterase from *Rhodosporidium toruloides*. *Appl Environ Microbiol* 1997;**63**:4807–11.

Popova AV, Academy B. Carotenoid-Lipid Interactions. *Advances in Planar Lipid Bilayers and Liposomes Vol.17*. 2013, 215–36.

Qian X, Gorte O, Chen L *et al.* Co-production of single cell oil and gluconic acid using oleaginous *Cryptococcus podzolicus* DSM 27192. *Biotechnol Biofuels* 2019;**12**:1–9.

Rakicka M, Lazar Z, Dulermo T *et al.* Lipid production by the oleaginous yeast *Yarrowia lipolytica* using industrial by-products under different culture conditions. *Biotechnol Biofuels* 2015;**8**, DOI: 10.1186/s13068-015-0286-z.

Ratledge C. The role of malic enzyme as the provider of NADPH in oleaginous microorganisms: A reappraisal and unsolved problems. *Biotechnol Lett* 2014;**36**:1557–68.

Rodriguez-Concepcion M, Stange C. Biosynthesis of carotenoids in carrot: An underground story comes to light. *Arch Biochem Biophys* 2013;**539**:110–6.

Rodríguez-Ortiz R, Limón MC, Avalos J. Regulation of carotenogenesis and secondary metabolism by nitrogen in wild-type *Fusarium fujikuroi* and carotenoid-overproducing mutants. *Appl Environ Microbiol* 2009;**75**:405–13.

Saenge C, Cheirsilp B, Suksaroge TT *et al.* Efficient Concomitant Production of Lipids and Carotenoids by Oleaginous Red Yeast *Rhodotorula glutinis* Cultured in Palm Oil Mill Effluent and Application of Lipids for Biodiesel Production. *Biotechnol Bioprocess Eng* 2011;**16**:23–33.

Sajilata MG, Singhal RS, Kamat MY. The Carotenoid Pigment Zeaxanthin-A Review. *Compr Rev FOOD Sci FOOD Saf* 2008;**7**:29–49.

Sakaki H, Nakanishi T, Tada A *et al.* Activation of Torularhodin Production by *Rhodotorula glutinis* Using Weak White Light Irradiation. *J Biosci Bioeng* 2001;**92**:294–7.

Sanjay KR, Kumaresan N, Manohar B *et al.* Optimization of carotenoid production by *Aspergillus carbonarius* in submerged fermentation using a response surface methodology. *Int J Food Eng* 2007;**3**, DOI: 10.2202/1556-3758.1295.

Schmidt I, Schewe H, Gassel S *et al.* Biotechnological production of astaxanthin with *Phaffia rhodozyma/Xanthophyllomyces dendrorhous*. *Appl Microbiol Biotechnol* 2011;**89**:555–71.

Schneider T, Graeff-Hönninger S, French WT *et al.* Lipid and carotenoid production by oleaginous red yeast *Rhodotorula glutinis* cultivated on brewery effluents. *Energy* 2013;**61**:34–43.

Seeger A. Single cell oils of the cold-adapted oleaginous yeast Rhodotorula glacialis DBVPG 4785. *Metall Trans* 2010;**9**:1–6.

Shabbir Hussain M, M Rodriguez G, Gao D *et al.* Recent advances in bioengineering of the oleaginous yeast *Yarrowia lipolytica*. *AIMS Bioeng* 2016;**3**:493–514.

Shah R, Aragon N, Calderon J. Bio-based (edible) oils: feedstock for lubricants of the future. *Am Oil Chem Soc* 2021.

Sharafi Y, Majidi MM, Goli SAH *et al.* Oil content and fatty acids composition in *Brassica* Species. *Int J Food Prop* 2015;**18**:2145–54.

Sharma S, Kaur M, Goyal R *et al.* Physical characteristics and nutritional composition of some new soybean (Glycine max (L.) Merrill) genotypes. *J Food Sci Technol* 2014;**51**:551–7.

Shen XF, Chu FF, Lam PKS *et al.* Biosynthesis of high yield fatty acids from *Chlorella vulgaris* NIES-227 under nitrogen starvation stress during heterotrophic cultivation. *Water Res* 2015;**81**:294–300.

Shi S, Zhao H. Metabolic engineering of oleaginous yeasts for production of fuels and chemicals. *Front Microbiol* 2017;**8**:1–16.

da Silva J, Honorato da Silva FL, Santos Ribeiro JE *et al.* Effect of supplementation, temperature and pH on carotenoids and lipids production by Rhodotorula mucilaginosa on sisal bagasse hydrolyzate. *Biocatal Agric Biotechnol* 2020;**30**:101847.

Singh DP, Khattar JS, Rajput A *et al.* High production of carotenoids by the green microalga *Asterarcys quadricellulare* PUMCC 5.1.1 under optimized culture conditions. *PLoS One* 2019;**14**:1–19.

Singh G, Jawed A, Paul D *et al.* Concomitant production of lipids and carotenoids in *Rhodosporidium toruloides* under osmotic stress using response surface methodology. *Front Microbiol* 2016;**7**:1–13.

Stachowiak B, Czarnecki Z. Effect of Light on Carotenoid Yield in Fed Cultures of *Phaffia Rhodozyma* CBS 5626. *Polish J Food Nutr Sci* 2007;**57**:129–31.

Steinbrenner J, Linden H. Light induction of carotenoid biosynthesis genes in the green alga *Haematococcus pluvialis*: Regulation by photosynthetic redox control. *Plant Mol Biol* 2003;**52**:343–56.

Swanson D, Block R, Mousa SA. Omega-3 Fatty Acids EPA and DHA: Health Benefits Throughout Life 1,2. , DOI: 10.3945/an.111.000893.

Tai M, Stephanopoulos G. Engineering the push and pull of lipid biosynthesis in oleaginous yeast *Yarrowia lipolytica* for biofuel production. *Metab Eng* 2013;**15**:1–9.

Takano H, Obitsu S, Beppu T *et al.* Light-induced carotenogenesis in *Streptomyces coelicolor* A3(2): Identification of an extracytoplasmic function sigma factor that directs photodependent transcription of the carotenoid biosynthesis gene cluster. *J Bacteriol* 2005;**187**:1825–32.

Takeda S, Ida K, Inumaru K *et al.* Light-induced Changes in Carotenoid Composition in

Cultured Green Cells of *Nicotiana tabacum*. *Biosci Biotechnol Biochem* 1996;**60**:1864–7.

Tang W, Zhang S, Wang Q *et al.* The isocitrate dehydrogenase gene of oleaginous yeast Lipomyces starkeyi is linked to lipid accumulation. *Can J Microbiol* 2009;**55**:1062–9.

Tang X, Chen H, Chen YQ *et al.* Comparison of biochemical activities between high and low lipid-producing strains of *Mucor circinelloides*: An explanation for the high oleaginicity of strain WJ11. *PLoS One* 2015;**10**:1–12.

Tang X, Lee J, Chen WN. Engineering the fatty acid metabolic pathway in *Saccharomyces cerevisiae* for advanced biofuel production. *Metab Eng Commun* 2015;**2**:58–66.

Thimmanagari M, McDonald I, Todd J. http://www.omafra.gov.on.ca/english/crops/facts/10-013w.htm. *Minist Agric Food Rural Aff* 2010.

Tkachenko AF, Tigunova OA, Shulga SM. Microbial lipids as a source of biofuel. *Cytol Genet* 2013;**47**:343–8.

Tran HL, Hong SJ, Lee CG. Evaluation of extraction methods for recovery of fatty acids from *Botryococcus braunii* LB 572 and *Synechocystis* sp. PCC 6803. *Biotechnol Bioprocess Eng* 2009;**14**:187–92.

Tran QG, Cho K, Kim U *et al.* Enhancement of B-carotene production by regulating the autophagy-carotenoid biosynthesis seesaw in *Chlamydomonas reinhardtii*. *Bioresour Technol* 2019;**292**:121937.

U.S. Energy Information Administration. *May 2021 Monthly Energy Review*., 2021.

Ungureanu C, Ferdes M. Evaluation of antioxidant and antimicrobial activities of torularhodin. *Adv Sci Lett* 2012;**18**:50–3.

United Nations. *World Population Prospects 2019: Highlights*., 2019.

Valduga E, Rausch Ribeiro AH, Cence K *et al.* Carotenoids production from a newly isolated *Sporidiobolus pararoseus* strain using agroindustrial substrates. *Biocatal Agric Biotechnol* 2014;**3**:207–13.

Valduga E, Valério A, Treichel H *et al.* Optimization of the production of total carotenoids by *Sporidiobolus salmonicolor* (CBS 2636) using response surface technique. *Food Bioprocess Technol* 2009;**2**:415–21.

Vázquez M. Effect of the Light on Carotenoid Profiles of *Xanthophyllomyces dendrorhous* Strains (formerly *Phaffia rhodozyma*). *Food Technol Biotechnol* 2001;**39**:123–8.

Verwaal R, Wang J, Meijnen JP *et al.* High-level production of beta-carotene in *Saccharomyces cerevisiae* by successive transformation with carotenogenic genes from *Xanthophyllomyces dendrorhous*. *Appl Environ Microbiol* 2007;**73**:4342–50.

Vijayalakshmi G, Shobha B, Vanajakshi V *et al.* Response surface methodology for optimization of growth parameters for the production of carotenoids by a mutant strain of *Rhodotorula gracilis*. *Eur Food Res Technol* 2001;**213**:234–9.

Wiemann P, Soukup AA, Folz JS *et al.* Coin: Co-inducible nitrate expression system for secondary metabolites in *Aspergillus nidulans*. *Fungal Biol Biotechnol* 2018;**5**:1–10.

Yamagata K. Docosahexaenoic acid regulates vascular endothelial cell function and prevents cardiovascular disease. *Lipids Health Dis* 2017;**16**:1–13.

Yuan H, Zhang J, Nageswaran D *et al.* Carotenoid metabolism and regulation in horticultural crops. *Hortic Res* 2015;**2**, DOI: 10.1038/hortres.2015.36.

Zakar T, Herman E, Vajravel S *et al.* Lipid and carotenoid cooperation-driven adaptation to light and temperature stress in *Synechocystis* sp. PCC6803. *Biochim Biophys Acta - Bioenerg* 2017;**1858**:337–50.

Zárate R, Jaber-Vazdekis N, Tejera N *et al.* Significance of long chain polyunsaturated fatty acids in human health. *Clin Transl Med* 2017;**6**, DOI: 10.1186/s40169-017-0153-6.

Zhang G, French WT, Hernandez R *et al.* Microbial lipid production as biodiesel feedstock from N-acetylglucosamine by oleaginous microorganisms. *J Chem Technol Biotechnol* 2011;**86**:642–50.

Zhang L, Ma G, Yamawaki K *et al.* Effect of blue LED light intensity on carotenoid accumulation in citrus juice sacs. *J Plant Physiol* 2015;**188**:58–63.

Zhang S, Skerker JM, Rutter CD *et al.* Engineering *Rhodosporidium toruloides* for increased lipid production. *Biotechnol Bioeng* 2016;**113**:1056–66.

Zhang Z, Zhang X, Tan T. Lipid and carotenoid production by *Rhodotorula glutinis* under irradiation/high-temperature and dark/low-temperature cultivation. *Bioresour Technol* 2014;**157**:149–53.

Zhao C, Gao Q, Chen J *et al.* Metabolomic changes and metabolic responses to expression of heterologous biosynthetic genes for lycopene production in *Yarrowia lipolytica*. *J Biotechnol* 2017;**251**:174–85.

Zhu Z, Zhang S, Liu H *et al.* A multi-omic map of the lipid-producing yeast *Rhodosporidium toruloides*. *Nat Commun* 2012;**3**:1–11.

Zoz L, Carvalho JC, Soccol VT *et al.* Torularhodin and torulene: Bioproduction, properties and prospective applications in food and cosmetics - A review. *Brazilian Arch Biol Technol* 2015;**58**:278–88.

Chapter 2: Effect of light on oleaginous yeast *Rhodosporidium toruloides*

2.1. Introduction

Carotenogenesis is a photoprotective mechanism; therefore, microorganisms produce carotenoids as antioxidant agents which have a role in protecting cells from light or other environmental stresses (Mata-Gómez *et al.* 2014). There is evidence that fungal growth and carotenoid production are influenced by exposure to light (Linden, Ballario and Macino 1997; Khanafari, Tayari and Emami 2008). In *R. glutilis*, increased biomass concentration and carotenoid formation have been observed in light-grown cultures (Zhang, Zhang and Tan 2014) and in *R. toruloides* carotenogenesis is light-inducible (Takano *et al.* 2005). Additionally, Braunwald *et al*., reported that in *R. glutilis*, both carotenoids and lipids accumulated in cultures that contained high carbon to nitrogen ratios and that carotenoids were produced under conditions that also promoted lipid synthesis (Braunwald *et al.* 2013). Thus, it is important to understand the bioregulation of both carotenoids and lipids to determine the optimal conditions for microbial carotenoid production. When glucose enters glycolysis, it is converted into pyruvate. In the oleaginous yeast, the conversion of pyruvate to acetyl CoA for the TCA cycle delivers citrate to the next step, acetyl CoA. This molecule is then serves as a precursor for the fatty acid biosynthesis pathway or the mevalonate biosynthesis pathway that continues to the carotenoid biosynthesis pathway (**Figure 2.1**). A relationship is proposed to exist between the carotenoid and lipid biosynthesis pathways. Therefore, in this chapter, we investigated the effects of light on lipid and carotenoid production of *R. toruloides* NBRC 10032.

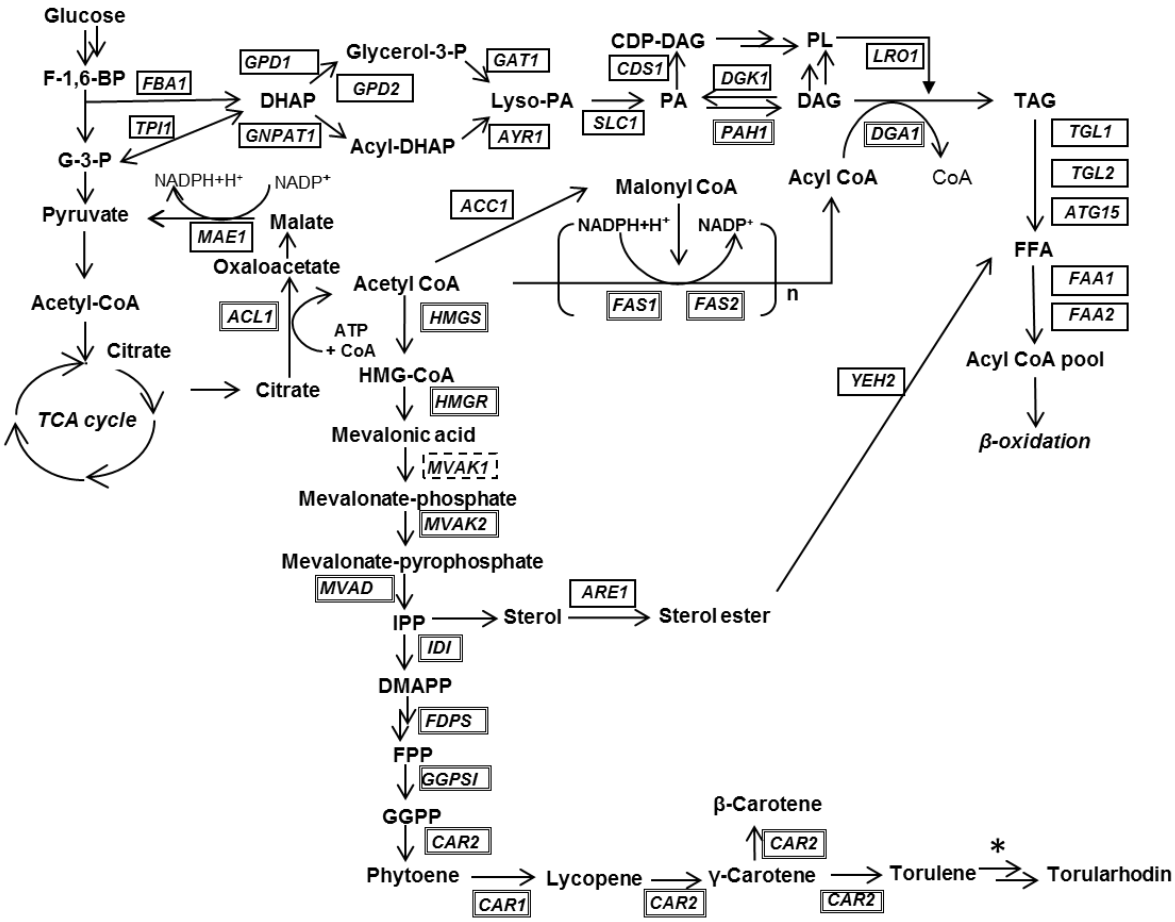

Figure 2.1. Biosynthesis pathway in *R. toruloides*. *FBA1* (fructose-biphosphate aldolase), *TPI1* (triosephosphate isomerase), *GPD1*,2 (glycetol-3-phosphhate dehydrogenase), *GNPAT1* (glyceronephosphate O-acyltransferase), *GAT1* (glycerol-3-phosphate/ dihydroxyacetonephosphate acyltransferase), *AYR1* (acyl-DHAP reductase), *SLC1* (lysophosphatididate acyltransferase), *CDS1* (phosphatidate cytidylyltransferase), *DGK1* (diacylglycerol kinase), *PAH1* (phosphatididate phosphatase), *LRO1* (phospholipid diacylglycerol acyltransferase), *DGA1* (acyl-CoA:diacylglycerol acyltransferase), *MAE1* (malic enzyme), *ACL1* (ATP-citrate lyase), *ACC1* (acetyl-CoA carboxylase), *FAS1*,*2* (fatty acid synthase), *TGL1*,*2* (triacylglycerol lipase), *ATG15* (triacylglycerol lipase), *ARE1*,*2* (acyl-CoA dehydroxyacyl-CoA dehydrogenase), *YEH2* (yeast steryl ester hydrolase), *FAA1*,*2* (acyl-CoA synthase), *HMGS* (hydroxylmethylglutaryl-CoA synthase), *HMGR* (hydroxymethalglutaryl-CoA reductase), *MVAK1* (mevalonate kinase), *MVAK2* (phosphomevalonate kinase), *MVAD* (diphosphomevalonate decarboxylase), *ARE1* (acyl-CoA-sterol acyltransferase), *IDI* (isopentenyl-diphosphate isomerase), *FDPS* (farnesyl diphosphate synthase), *GGPSI* (geranylgeranyl diphosphate synthase, type III), *CAR2* (phytoene synthase), *CAR1* (phytoene desaturase). F-1,6-BP, fructose-1,6-bisphosphate; G-3-

P, glyceraldehyde-3-phosphate; Glycerol-3-P, Glycerol-3-phosphate; DHAP, dihydroxyacetone phosphate; PA, phosphatidic acid; CDP-DAG, cytidine diphosphate-diacylglycerol; PL, phospholipid; DAG, diacylglycerol; TAG, triacylglycerol; FFA, free fatty acid; CoA, coenzyme A; HMG-CoA, 3-hydroxy-3-methylglutaryl-CoA;IPP, isopentenyl-pyrophosphate; DMAPP, dimethylallyl-pyrophosphate; FPP, farnesyl-pyrophosphate; GGPP, geranyl geranyl-pyrophosphate. *In this step, it was proposed that hydroxylation and oxidation happened; however, gene(s) correlated with this step has not been identified (Kot *et al.* 2016).

2.2. Materials and methods

2.2.1. Yeast strain and culture conditions

The *R. toruloides* NBRC10032 strain was obtained from the National Institute of Technology and Evaluation (NITE, Chiba, Japan). *R. toruloides* was grown on Yeast Peptone D-Glucose (YPD) agar plates (1% Yeast extract, 1% Peptone, 2% D-Glucose, 2% Agar) at 30°C for 4 days, after which the setup was maintained at 4°C. Plates were subsequently sub-cultured every month. The YPD medium was used for pre-cultivation and LS10 medium (0.805% Powder Yeast extract, Kyokuto Seiyaku Co., Tokyo, Japan, 15% D-Glucose, 0.047% NH_2CONH_2, 0.15% $MgSO_4 \cdot 7H_2O$, 0.04% KH_2PO_4, 1.9×10^{-6} mmol/L $ZnSO_4$, 1.22×10^{-4} mmol/L $MnCl_2$, 1×10^{-4} mmol/L $MnCl_2$, 1×10^{-4} mmol/L $CuSO_4$ and 1.5 mmol/L $CaCl_2$, Nacalai Tesque, Tokyo, Japan) was used for lipid accumulation. Next, yeast cells were pre-cultivated for 24 h in YPD medium using L-shaped test tubes and then cultured in 200 mL Erlenmeyer flasks containing 50 mL LS10 medium, at an initial optical density (O.D.) of 660 nm = 0.1. The experiment was conducted in a dark room. Dark conditions were achieved by wrapping samples in aluminum foil (two layers, 24 μm thick in total), whereas, light conditions were achieved using a 27-Watt fluorescent lamp.

Samples used for the analysis of gene expression during the earlier cultivation stages were subsequently produced from the cells cultured in the LS10 medium (15% glucose) in the dark for 24 h, after which the cultures were transferred to either light or dark conditions and sampled at appropriate times post-induction.

2.2.2. Biochemical analysis

The yeast growth rate was measured using ultraviolet-visible spectroscopy (UV-Vis) UV mini-1240 (Shimadzu, Kyoto, Japan), and the O.D. of each culture was recorded at a

wavelength of 660 nm. Dry cell weight (DCW) was then quantified in lyophilized cells derived from 1 mL broth. Next, Glucose CII Test Wako kit (Wako Pure Chemical Industries Ltd., Osaka, Japan) was used to determine the glucose concentrations of the culture supernatant to provide a measure of glucose consumption over the growth period.

Lipids were extracted in mixture solvents (Petroleum ether: Ethanol = 1:3) from cells using Multi Beads Shocker (Yasui Kikai, Osaka, Japan). Dry cells were then suspended in 200 µL of the solvent mixture with 500 mg of glass beads (0.5 mm diameter), which were disrupted in the Multi Beads Shocker (conditions: 4°C, 2500 rpm, 30 cycles of 30 s ON time and 30 s OFF time). 800 µL of the solvent mixture was subsequently added to the resultant cell lysate and centrifuged at 14,000 rpm and a temperature of 4°C for 10 min. Next, the supernatant was aliquoted into 1 mL samples in new microtubes, after which an additional 1 mL of the solvent mixture was added to the cell debris. This procedure was repeated to ensure that all cellular lipids were extracted. Lipid content was then quantified using the E-test Wako TG kit (Wako Pure Chemical Industries Ltd., Osaka, Japan).

To determine the fatty acid composition, lipids were extracted in a mixture of chloroform and methanol (2:1, v/v) as described by Folch et al. (Folch, Lees and Stanley 1957) using the Multi Beads Shocker (conditions: 4°C, 2500 rpm, 30 cycles of 30 s ON time and 0 s OFF time). After, 500 µL of the solvent mixture was added to the resultant cell lysate, which was then shaken (250 rpm at room temperature) for 10 min, then the resultant solution was collected in new microtubes. This final step was repeated to ensure that all cellular lipids were extracted. Subsequently, 1 mL of the supernatant was collected after centrifuging at 14,000 rpm at 4°C for 10 min. Then, the solvent was removed using an ultra-small centrifugal concentrator (TAITEC, Saitama, Japan), and methyl esterification was conducted using a fatty acid methylation kit (Nacalai Tesque, Tokyo, Japan). The final lipid content of the total DCW was determined with gas chromatography (GC) using a GC-2014 instrument (Shimadzu, Kyoto, Japan) having a DB-23 column (Agilent Technologies, CA, US).

Carotenoids were extracted as well from dry cells in 100% acetone using the Multi Beads Shocker. Dry cells were mixed with 200 µL of acetone and 500 mg glass beads (0.5 mm diameter), followed by treatment using the Multi Beads Shocker (conditions: 4°C, 2500 rpm, 30 cycles of 30 s ON time and 30 s OFF time). After cell disruption, 800 µL of acetone was added. The mixture was centrifuged at 4°C and a speed of 14,000 rpm for 10 min. Next, 1 mL of the supernatant was collected in a new microtube and a further 1 mL of acetone was added

to the cell debris to obtain all cellular carotenoids. Infinite M200 PRO (TECAN, Kanagawa, Japan) was then used to measure 100 µL of the carotenoid samples into a 96-well glass plate at 488 nm. Carotenoid production was expressed as the absorbance of samples at 488 nm/ g-DCW.

2.2.3. Quantification of gene expression amounts

Yeast cells for total RNA extraction were initially cultured in the dark for 24 h, transferred to either light or dark conditions, then sampled at appropriate times post transfer. Subsequently, total RNA was extracted from frozen mycelia by a modified hot-phenol method using TRIzol®LS (Invitrogen, Carlsbad, USA) and an RNA spin (GE Healthcare, Chicago, USA). Total RNA (1 µg) was reverse-transcribed, after which complementary DNA was synthesized using a Transcriptor First-Strand cDNA Synthesis Kit (Roche Applied Science, Bavaria, Germany). Next, quantitative real-time polymerase chain reaction (qRT-PCR) was performed using a Light Cycler® 480 SYBR Green I Master kit (Roche Applied Science, Bavaria, Germany) with 0.5 µM forward primer, 0.5 µM reverse primer and 2 µL cDNA (100-fold dilution of synthesized cDNA) in a final volume of 20 µL. After, thermal cycling was conducted under the following conditions: 5 min at 95°C followed by 45 cycles of 10 s at 60°C, and 10 s at 72°C. Then, the relative expression levels were calculated as the ΔCt power of 2, in which the ΔCt value was obtained by subtracting the Ct value of the housekeeping gene (*ACT1*, the gene encoding actin) from that of the target gene. PCR primers for expression analysis are listed in **Table 2.1**.

Table 2.1. The list of PCR primers for gene expression analysis in *R. toruloides*

Gene	Fw	Rv
ACL1	ACCCAGACCCAGACCTACGA	TGGTGAAGTTGGCGATGC
PAH1	ACGGCTGATGTGCTCAGGT	CGTTCACTGCGTGTCGTTC
DGA1	CATCTGCTCCGTCTCGATG	TTCGTCGCTTGAGGGTGA
FAS1	CCATTCGTGGTATGTTCTCGAC	GTGAACGGAACCCAGAGGA
FAS2	ACGTCGAGGGCCAGCAATA	CATCGTCTCGGTGAGCTTG
HMGS	CATCGACTTTGACTACGTTTGCT	CCTTGGACACGGACGAGAA
HMGR	TCGTCTGGGATGCGTTCTG	AGAGAGGTCGGCGGAAGAGT
MVAK2	ATTGTCGGCGAAGGAGTGGT	TTCGTCTGCTCGGGAGGTTC
MVAD	TCCTCCAGCACCGCATCAAG	AGTCGGCCATGGTCTCTTCC
IDI	CCCACTTGACATCGCTGACC	CCCACTTGACATCGCTGACC
FDPS	GCCCGAAGATGCCGTCAATC	CGAGAGCAACGGGGAGGTAG
GGPSI	TCTTCCAGATCCGCGACGAC	GTGTCGGAGCGGATCGAGTG
CAR2	CATCGAGAAGGGCACCAAG	ACGAGGCCGAAGACAATCA
CAR1	TCGAGGAGAAGCCCGTTAG	TGGTCGCGGAAGATTGAG
WC1	ACGCAGGTCTCGCTGATCAA	GACCTGGAAGCCGACGAAGA
WC2	TTCGACCTCCACCCAACACC	GCTGTTTCGGGTCTGAAGCG
CRY1	CTTCTGTGGCGTGACTACTTCCT	CTGCTTGCTTCGGGTCTGT
ACT1	GTCCCCATCTCTACGAGGGCTA	CGTCGTCGTGAACGTGTACC

2.2.4. Genome Sequencing of R. toruloides

Frozen yeast cells were disrupted using a Multi Beads Shocker, then suspended in extraction buffer (50 mM Tris-HCl pH 7.5, 10 mM EDTA·2Na, 1% SDS). After adding 3 M potassium acetate, the mixture was centrifuged, after which the supernatant was purified through RNase treatment, phenol-chloroform treatment and ethanol precipitation. Finally, the precipitated genomic DNA was dissolved in TE buffer.

The genome sequence was analyzed using the PacBio and Illumina Miseq platform. Assembly of the PacBio on control filtered subreads (raw reads) was performed using Canu ver. 1.6, in which the putative genome size was set as 20 Mb. Contig sequences were polished by aligning raw reads to each contig using the pbalign ver. 0.3.1, then corrections or sequence errors was conducted using the Genomic Consensus Ver. 2.20 applied variant Caller (quiver algorithm). This step was repeated five times. To correct of the contig sequences, Miseq read,

Illumina short reads were used to trim, using the Trimmomatic ver. 0.38. Trimmed short reads were aligned to contig by bwa ver.0.7.12, after which error correction was performed by Pilon ver. 1.22. This step was repeated five times as well. Among the protein sequences of *R. toruloides* NP11, IFO1236, NBRC 0880 opened at the JGI website (https://mycocosm.jgi.doe.gov/mycocosm/home). Conserved sequences in more than one strain were also extracted and mapped to the contig sequence. DNA sequences that were mapped to the whole length of the protein were used as samples. Gene model optimization was performed by training program of AUGUSTUS ver. 3.3.1. Finally, AUGUSTUS was applied to the contig sequence for gene prediction.

2.2.5. HPLC analysis

The carotenoid solution obtained after acetone extraction was filtered by a DISMIC®-03CP filter with a pore size of 0.45μm (Toyo Roshi Kaisha, Japan). Carotenoids were analyzed by an HPLC system equipped with a UV/Vis detector SPD-20A (Shimadzu, Japan). The separation C18 column used was Shim-pack XR-ODS (2.2 μm particles size, 75 × 3 mm, Shimadzu GLC, Japan). The method was modified by Roland W.S Weber (2007) and P. Davoli (2004) (Davoli, Mierau and Weber 2004; Weber, Anke and Davoli 2007). The flow rate was 1 mL/min with a gradient ranging from 70%–100% acetone. Absorbance at 450 nm was recorded.

2.2.6. Microarray analysis

Gene Expression Microarray was conducted using the Agilent Array software provided by Agilent, which we then used to create a custom microarray (Agilent), carrying all the putative genes of the *R. toruloides* NBRC 10032 strain. A total of 6 probes were designed so that the probe length was 60–mer, and 2–3 probes per gene corresponded. Then, they were placed on the microarray chip substrate. The analysis was outsourced to Cell Innovator. Agilent's GeneSpring Software was used for data analysis.

2.3. Results

2.3.1. Influence of light on R. toruloides phenotype

The influence of light on yeast growth was examined by culturing cells under light irradiation or continuous dark condition. Samples were withdrawn every 24 h to analyze the turbidity, glucose consumption, DCW, carotenoid production and lipid production. As a result, the red colorization of cells was observed by light irradiation after 24 h (**Figure 2.2a**).

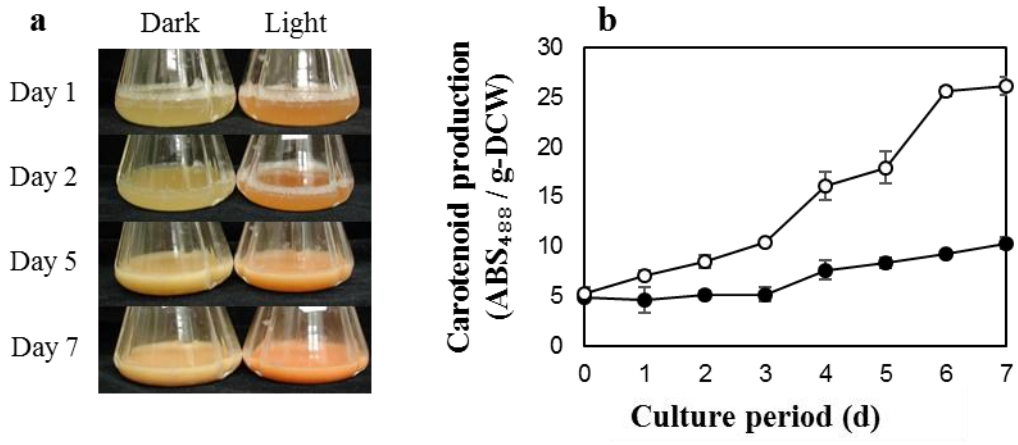

Figure 2.2. Carotenoid production of *R. toruloides* NBRC 10032

a. The color change of cultures over time b. Carotenoid production in the light (white circle) and during the dark (black circle).

The maximum absorption wavelengths of β-carotene, torulene and torularhodin were 450 (or 454) nm, 482 (or 485) nm and 492 nm, respectively (Lichtenthler 1987; Hornero-Méndez and Minguez-Mosquera 2001; Davoli and Weber 2002; El-Banna, El-Razek and El-Mahdy 2012). Also, the maximum absorption wavelength of the extracted carotenoids were analyzed over a range of 350-650 nm. Spectral shape exhibited considerable variation but in both light and dark conditions, the maximum absorbance was 488 nm (**Figure 2.3**). Therefore, the value of ABS 488 nm per g-DCW was used as a measure of carotenoid production. The carotenoid sample from light irradiated cells showed a much higher absorbance than that from cells cultivated in the dark. Indeed, the cell-free extract after six days of cultivation showed that cells grown in the light exhibited a five-fold greater production of carotenoids compared to those grown in the dark (**Figure 2.2b**).

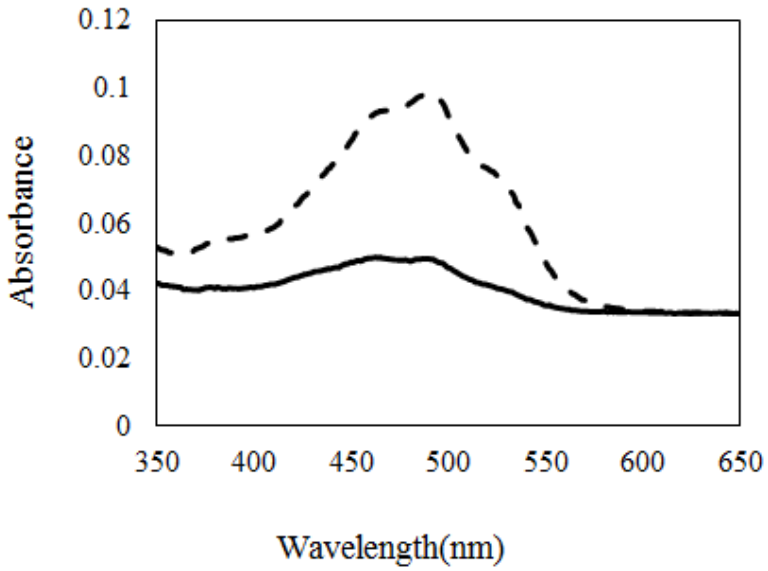

Figure 2.3. The maximum wavelength peak of absorbance of carotenoid production in *R. toruloides.* Line is dark condition and dash line is light condition.

The major carotenoids in *R. toruloides* were analyzed by HPLC. Because of the unavailability of commercial standards for γ-carotene, torulene and torularhodin, the peak area of each carotenoid was directly used for calculating of composition due to similarity in structure and the extinction coefficient between β-carotene, γ-carotene, torulene and torularhodin (Shi *et al.* 2013). From the results, β -carotene and torulene were suggested as the major pigments in the *R. toruloides* NBRC 10032 (**Figure 2.4, Table 2.2**). Therefore, in the dark condition, the amount of β-carotene and torulene were seemed to be similar. However, in the light condition, the peak of β-carotene was higher than that in the dark (**Figure 2.4**). From the carotenoid composition **(Table 2.2**), the ratio of β-carotene was higher under the light. Interestingly, torulene composition under dark was higher than that under the light. This might imply that metabolic steps to β-carotene biosynthesis were affected by light irradiation.

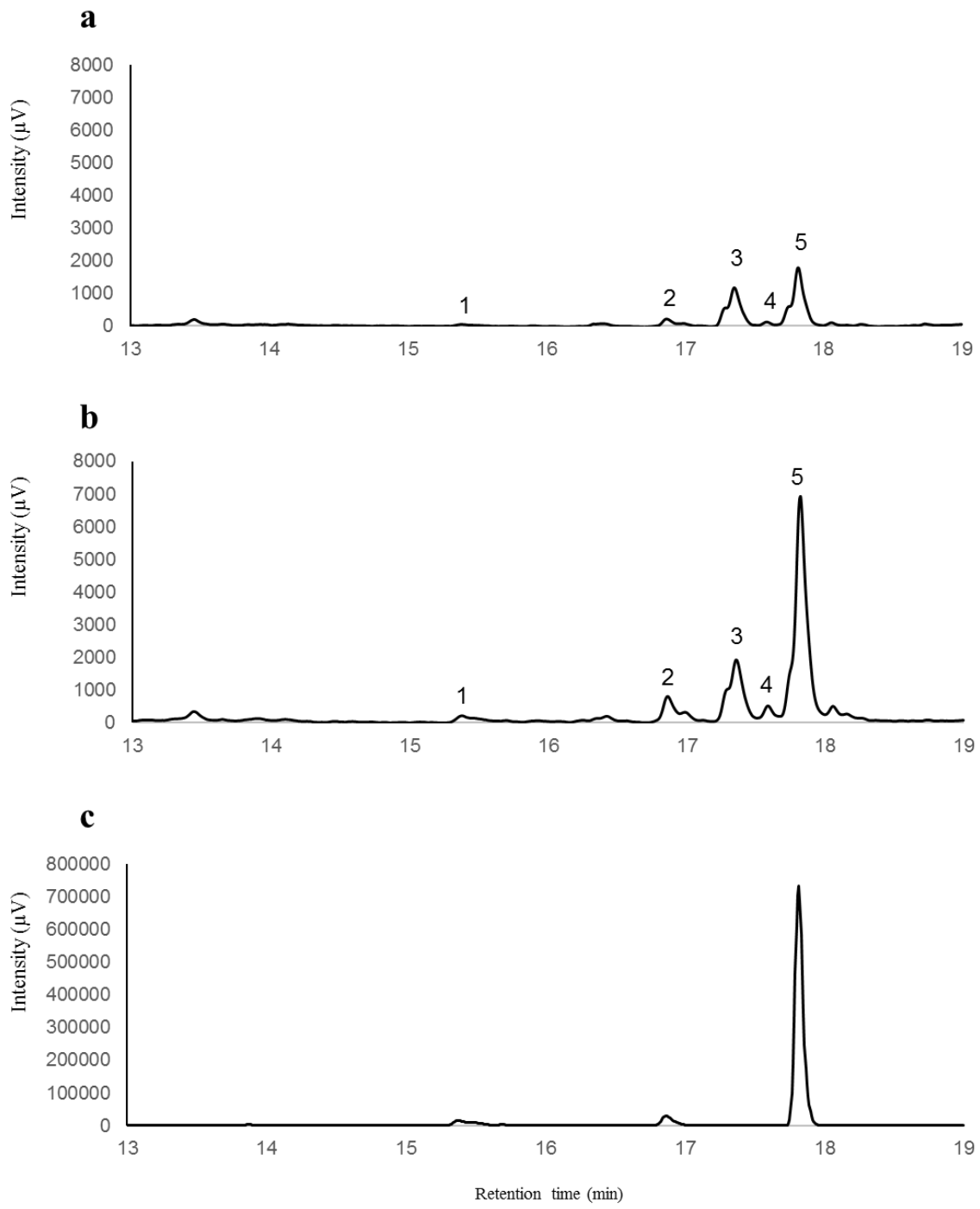

Figure 2.4. HPLC chromatogram of the pigment profile of NBRC 10032

a) in the dark b) in the light condition c) β-carotene standard

Refer to Roland W.S Weber and P. Davoli reported (Davoli, Mierau and Weber 2004; Weber, Anke and Davoli 2007), that the peak (3) might be suggested as the torulene, peak (4) as γ-carotene, peak (5) as β-carotene, while peak (1) was proposed as torularhodin. The peak (2) is an unknown carotenoid.

Table 2.2. Carotenoid composition of *R. toruloides* cells grown under light or dark conditions.

Carotenoids	Dark	Light
β-carotene	37.00 ±1.03	48.72 ±1.77
γ-carotene	1.48 ±0.34	3.54 ±0.03
Torulene	27.24 ±0.67	15.05 ±0.22
Torularhodin	1.16 ±0.23	3.39 ±0.35
Others	33.12 ±2.28	29.29 ±1.92

The detail in the effect of light in the carotenoid composition, components of carotenoid was analyzed in the day by day. Results in the **Figure 2.5** indicated that the torulene content was increased in the day 2 (after first step) and then in the day 6 (after second step) in the light condition compare to dark condition. It was suggested that the non-light effect condition, the β-carotene is a priority product.

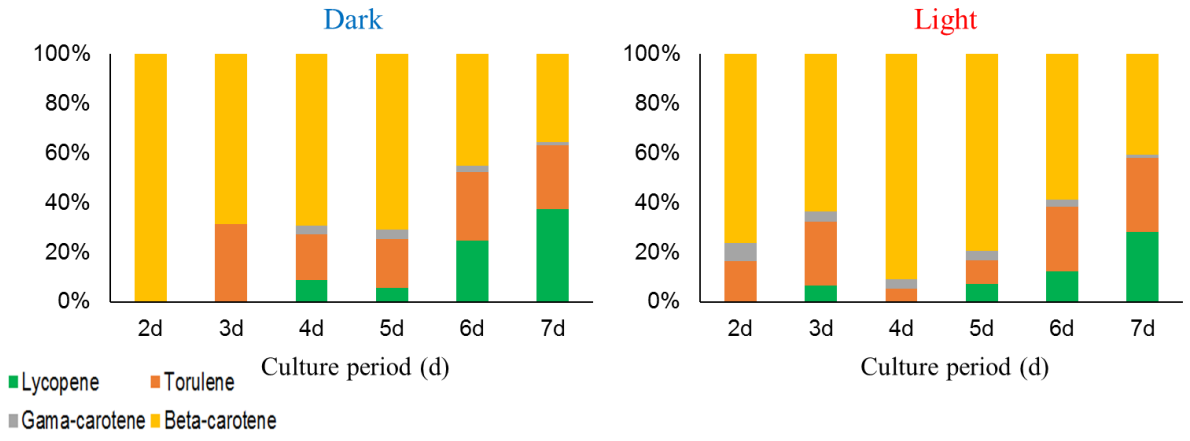

Figure 2.5. Carotenoid composition under dark and light condition follow cultural time Green is lycopene, grey is γ-carotene, yellow is β-carotene and orange is torulene.

The effect of light irradiation on fungal growth and lipid accumulation was analyzed in several different phenotypes of *R. toruloides*. Our data show that cell density and DCW were both higher in the samples grown in the dark (**Figure 2.6a, b**). Thus, there was no significant

difference in overall glucose consumption between 0-7 days. However, the samples grown in the light consumed the glucose a little earlier (**Figure 2.6c**). Also, although higher amounts of overall lipid production were observed in the dark-grown samples, lipid content per cell was the same under light and dark conditions (**Figure 2.6a**).

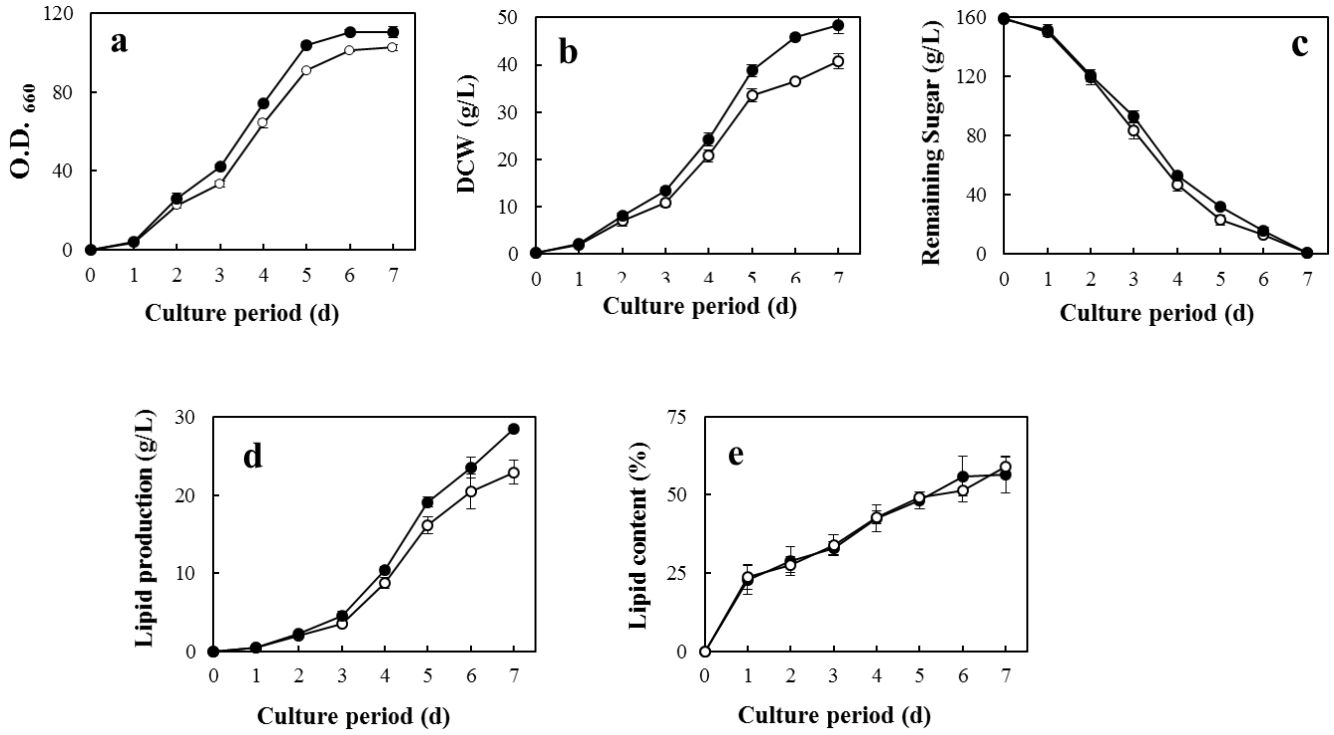

Figure 2.6. Growth rate parameter and lipid production of *R. toruloides* NBRC 10032 in the light (white circle) and dark (black circle). a. Optimal density; b. Biomass calculated by dry cell weight; c. Glucose consumption; d. Lipid production; e. % Lipid content calculated by lipid production (g)/ DCW (g).

A comparison of lipid composition derived from both growth conditions showed that the percentage of unsaturated fatty acids (C16:1, C18:3) was greater in light-grown samples (**Table 2.3**). Double bonds in the unsaturated fatty acid are known to act as antioxidants against harmful factors. Thus, an increase in the amount of unsaturated fatty acid in response to light could be a natural defense response in *R. toruloides*.

Table 2.3: Fatty acid composition of *R. toruloides* NBRC 10032 cells grown under light or dark conditions.

Fatty acids		Light		Dark	
Myristic	C14:0	3.49	±2.20	4.42	±4.27
Palmitic	C16:0	19.83	±2.92	19.69	±2.08
Palmitoleic	C16:1	3.61	±3.54	1.56	±0.28
Stearic	C18:0	6.73	±1.54	7.62	±1.27
Oleic	C18:1	57.11	±4.99	60.41	±2.31
Linoleic	C18:2	1.52	±0.33	1.65	±0.61
α-Linolenic	C18:3	4.49	±5.50	1.12	±0.66
Arachidic	C20:0	0.42	±0.04	0.63	±0.07
Behenic	C22:0	1.43	±1.00	1.46	±0.74
Lignoceric	C24:0	1.37	±0.56	1.44	±0.07

2.3.2. Determination of genome sequence of R. toruloides NBRC 10032

Expression analysis was performed on the genes related to the biosynthesis of carotenoids, fatty acids and TAGs in order to determine whether the observed light-responsive phenotypes were regulated at the transcription level. First, the genome of the strain NBRC 10032, which was used in this study, was sequenced by a combination of next-generation sequencers. The *de novo* assembly of the sequence reads resulted in a 19.4 Mb of sequence with an average coverage of 84 × and 49 × by MiSeq and PacBio platform, respectively. Thirty-nine assembled contigs were observed, and one of them was the mitochondrial DNA. Therefore, they were deposited at the DNA data bank of Japan (DDBJ) (accession No. BJWK01000001 to BJWK01000039) (**Table 2.4**). Among them, it is possible that 7 contigs had a telomere in both termini because TTAGGG sequence repeats were detected in both. Therefore, the NBRC 10032 strain could have at least 7 contigs with the full length of the chromosome sequence. Furthermore, from *R. toruloides* that are available in public databases were used as a model for predicting NBRC 10032 genes. In addition, two sets of RNA sequences were utilized for intron prediction. The final number of predicted genes was 6,909.

Table 2.4. Summary of *Rhodosporidium toruloides* NBRC 10032 genome assemble

	Pacbio	**Miseq**
Total reads	106,267	6,766,670
Total reads nucleotides	945,880,994	1,634,224,578
Average nucleotides per read	8,901.0	241.5
Coverage	49	84
Predicted genome size	19.4 Mb	
Contigs	39	
Total contig length	19,799,019	

I

In the genome sequence data of the NBRC 10032 strain, the number of predicted genes were fewer than those of other reports for *Rhodosporidium*. Therefore, to identify genes that NBRC 10032 did not possess, bidirectional BLAST analysis was carried out and 1058 genes were extracted. The genes were classified based on the information from NP11 annotation (https://mycocosm.jgi.doe.gov/Rhoto1/Rhoto1.home.html), and comprised 248 enzymes, 29 transporters, 18 transcription factors, 20 ribosomal proteins, 340 functional proteins and 403 hypothetical proteins (**Figure 2.7**).

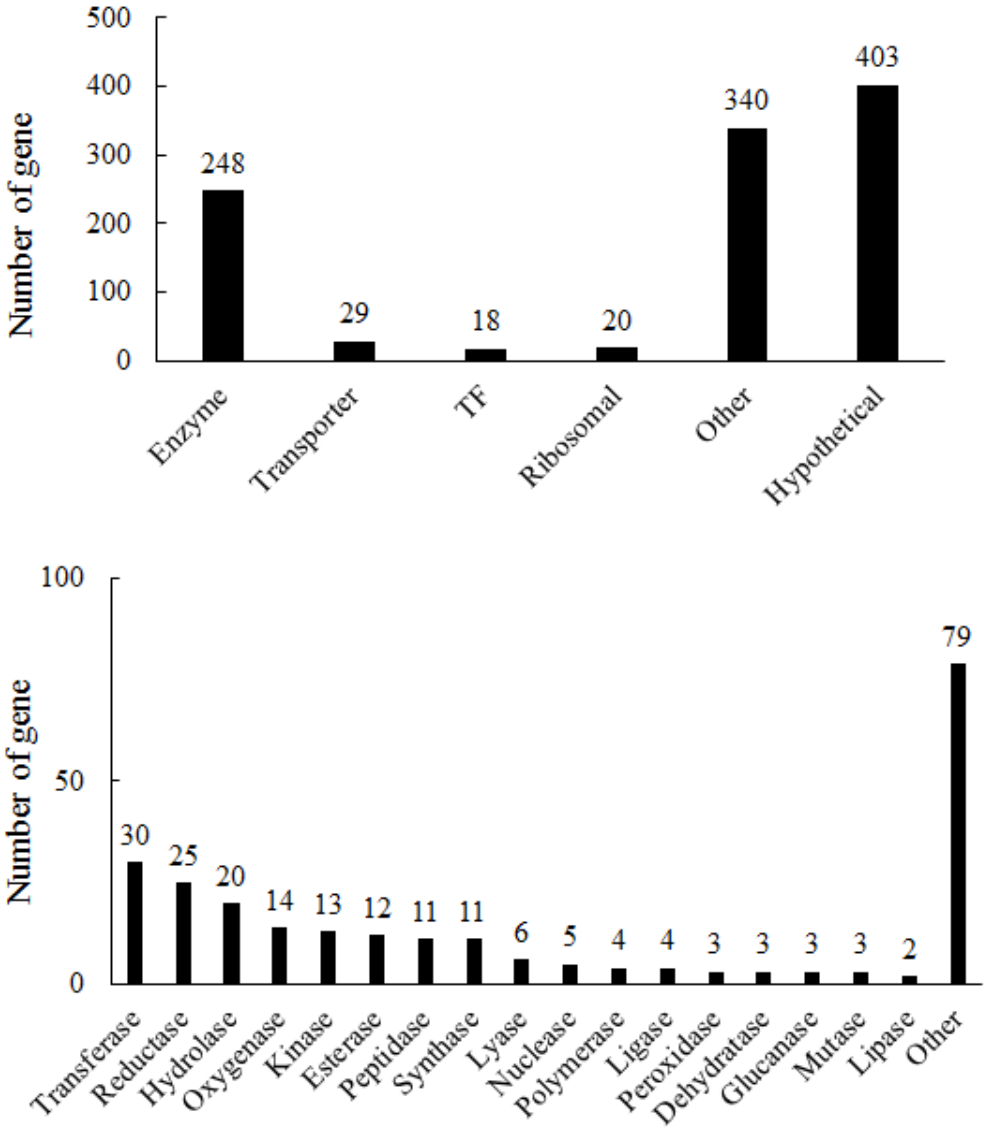

Figure 2.7. The genome sequence data of the NBRC 10032 strain

We were able to identify genes related to carotenoid biosynthesis, fatty acid biosynthesis and triacylglycerol biosynthesis by BLAST (**Figure 2.1, Table 2.5**). However, *MVAK1* encoding mevalonate kinase was predicted in the form of two fusion genes but the boundary was unclear, so it could not be identified.

Table 2.5. The list of genes related to lipid and carotenoid production

Gene	Locus tag	homologous protein	origin	similarity	accession No.
FBA1	c08g3716	fructose-bisphosphate aldolase, class II	*Rhodotorula toruloides* NP11	92	XP_016276434
TPI1	c12g4957	triosephosphate isomerase (TIM)	*Rhodotorula toruloides* NP11	97	XP_016272801
GPD1	c11g4624	glycerol-3-phosphate dehydrogenase (NAD+)	*Rhodotorula toruloides* CECT1137	97	CDR45301
GPD2	c13g4972	glycerol-3-phosphate dehydrogenase	*Rhodotorula toruloides* NP11	94	XP_016274442
GNPAT1	c04g1836	acyltransferase	*Rhodotorula toruloides* NBRC 0880	97	PRQ76347
GAT1	c02g1222	1-acylglycerol-3-phosphate acyltransferase	*Rhodotorula toruloides* NP11	92	XP_016274778
AYR1	c16g5697	1-acylglycerone phosphate reductase	*Rhodotorula toruloides* NP11	96	XP_016276583
SLC1	c05g2574	lysophosphatidic acid acyltransferase	*Rhodotorula toruloides* NP11	85	XP_016269607
CDS1	c20g6383	phosphatidate cytidylyltransferase	*Rhodotorula toruloides* NP11	93	XP_016272777
PAH1	c01g0050	Lipin1	*Rhodotorula toruloides* NP11	95	XP_016275833
CDK1	c09g3865	diacylglycerol kinase	*Rhodotorula toruloides* NP11	84	XP_016275030
DGA1	c01g0279	2-acylglycerol O-acyltransferase 2	*Rhodotorula toruloides* NP11	88	XP_016272211
LRO1	c01g0295	phospholipid:diacylglycerol acyltransferase	*Rhodotorula toruloides* NP11	94	XP_016272194
ACL1	c10g4086	ATP-citrate synthase	*Rhodotorula toruloides* NP11	99	PRQ71611
ACC1	c06g2756	acetyl-CoA carboxylase	*Rhodotorula toruloides* NP11	99	XP_016272252
FAS1	c06g2877	fatty acid synthase subunit alpha, fungi type	*Rhodotorula toruloides* NP11	98	XP_016272387
FAS2	c06g2783	fatty acid synthase	*Rhodotorula toruloides* NBRC 0880	98	PRQ77602
MAE1	c18g5981	malic enzyme, mitochondrial	*Rhodotorula toruloides* NP11	90	XP_016274603
ATG15	c02g0921	triacylglycerol lipase ATG15-like protein	*Rhodotorula toruloides* NP11	88	XP_016277052
TGL1	c05g2252	triacylglycerol lipase	*Rhodotorula toruloides* NP11	96	XP_016273358
TGL2	c02g1194	lipase2	*Rhodotorula toruloides* NP11	83	XP_016274811
FAA1	c02g0660	long-chain acyl-CoA synthetase	*Rhodotorula toruloides* NP11	94	XP_016276749
FAA2	c14g3230	long-chain acyl-CoA synthetase	*Rhodotorula toruloides* NP11	94	XP_016270694
ARE1	c03g1314	sterol O-acyltransferase	*Rhodotorula toruloides* NP11	85	XP_016273566
YEH2	c05g2305	ab-hydrolase associated lipase	*Rhodotorula toruloides* NP11	96	XP_016273427
HMGS	c03g1528	hydroxymethylglutaryl-CoA synthase	*Rhodotorula toruloides* NP11	96	XP_016272158
HMGR	c12g4753	hydroxymethylglutaryl-CoA reductase (NADPH)	*Rhodotorula toruloides* NP11	97	XP_016270872
MVAK2	c06g2809	phosphomevalonate kinase	*Rhodotorula toruloides* ATCC 204091	87	EGU11315
MVAD	c04g2148	diphosphomevalonate decarboxylase	*Rhodotorula toruloides* NP11	95	XP_016275120
IDI	c06g2941	isopentenyl diphosphate isomerase	*Rhodotorula toruloides* NBRC 0880	96	PRQ73450
FDPS	c21g6428	farnesyl diphosphate synthase	*Rhodotorula toruloides* NP11	97	XP_016272719
GGPSI	c01g0314	geranylgeranyl diphosphate synthase, type III	*Rhodotorula toruloides* NP11	96	XP_016271675
CAR2	c06g2720	phytoene synthase	*Rhodotorula toruloides* NP11	92	XP_016275546
CAR1	c06g2717	phytoene dehydrogenase	*Rhodotorula toruloides* NP11	96	XP_016275543
ACT1	c05g2525	actin	*Rhodotorula toruloides* NP11	100	XP_016271443
WC-1	c03g1335	white collar 1	*Rhodotorula toruloides* NP11	87	XP_016273590
WC-2	c08g3546	white collar 2	*Rhodotorula toruloides* NP11	93	XP_016276236
CRY1	c01g0030	Cryptochrome DASH	*Rhodotorula toruloides* NP11	94	XP_016275855

2.3.3. Expression analysis of major genes related to lipid or carotenoid biosynthesis

Since the enhancement of carotenoid productivity by light irradiation was observed, the gene expression profile of NBRC 10032 was investigated. For expression analysis, cells were cultured under light and dark conditions and RNA was extracted. The general pathway of carotenoid biosynthesis has two main steps: phytoene synthesis and phytoene desaturation. In non-photosynthetic organisms, *CrtE* genes encode geranylgeranyl diphosphate synthase, *CrtYB* genes encode the enzyme phytoene synthase and *CtrI* genes encodes phytoene desaturase. The latter is the enzyme that performs four consecutive desaturations to produce lycopene (Sieiro *et al.* 2003; Lodato *et al.* 2007; Verwaal *et al.* 2007). The genes *CAR1* and *CAR2* which were identified in the *R. toruloides* genome were homologues of phytoene desaturase and phytoene synthase, respectively (**Figure 2.1**). Thus, the expression of *CAR1* and *CAR2* was analyzed. After three days the transcription levels of *CAR2* and *CAR1* genes in light-grown cells increased by approximately 2- and 3-folds of that in dark-grown cells, respectively (**Figure 2.8**).

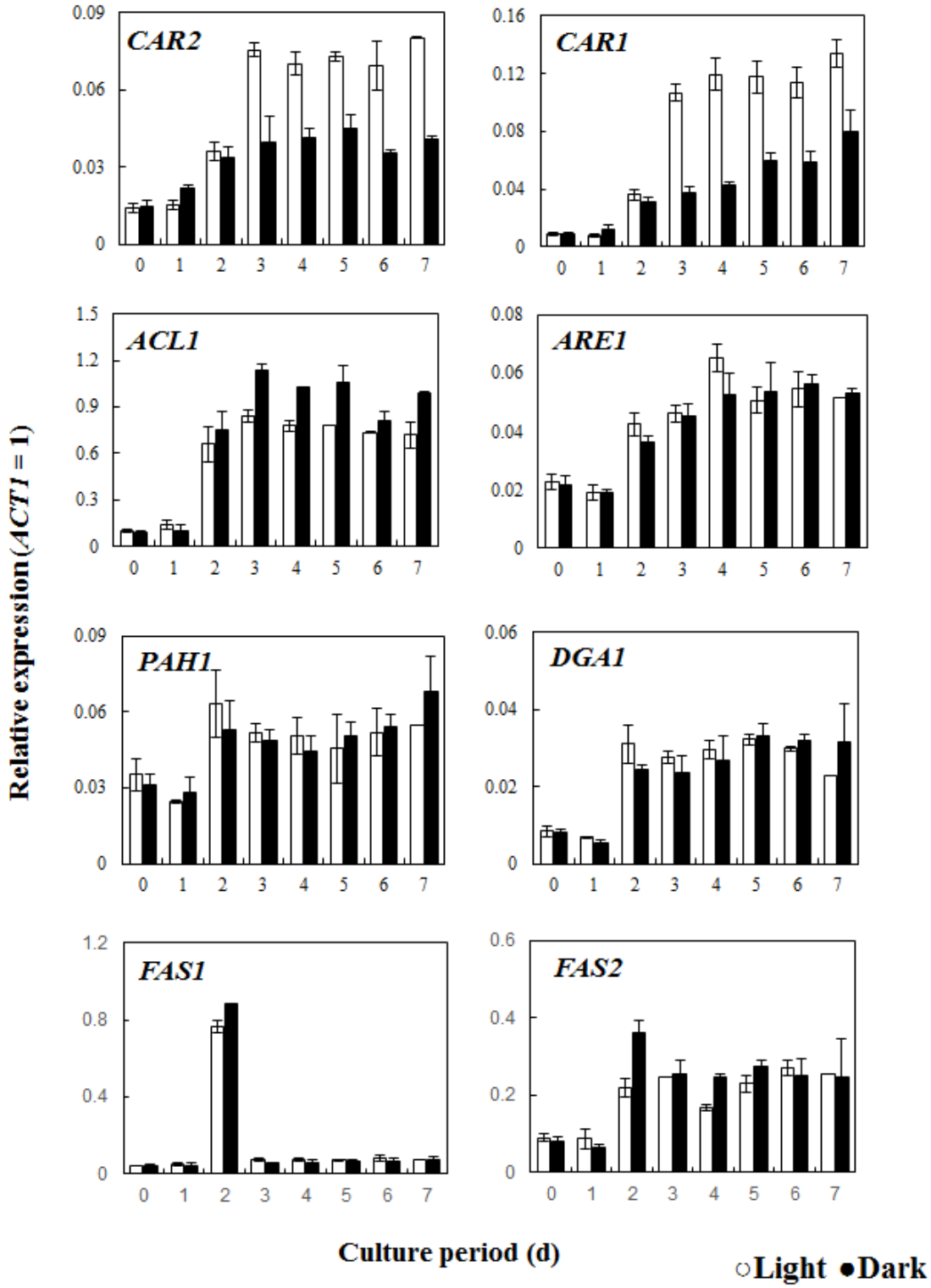

Figure 2.8. Effect of light irradiation on the expression of the genes related to carotenoid and lipid biosynthetic pathways. Quantity Real-time PCR analyses for genes, *CAR2*, *CAR1* and *ACL1*, *ARE1*, *PAH1*, *DGA1*, *FAS1*and *FAS2* in RNA samples grown in the dark (black) and exposed to light (white) for the time indicated (d).

We performed qRT-PCR analysis on several genes involved in the lipid biosynthesis pathway (**Figure 2.1**). ATP citrate lyase (*ACL1*) is the primary enzyme responsible for the synthesis of acetyl CoA. This is an essential precursor to many biologically important molecules including triacylglycerols, fatty acids and carotenoids. It was therefore hypothesized that increased carotenoid production in response to light irradiation could be because the expression of the *ACL1* gene was enhanced by light, or that the genes in the fatty acid (*FAS1, FAS2*) or triacylglycerol (*PAH1*, *DGA1*) or sterol (*ARE1*) biosynthesis pathways were down expressed. However, results showed that the expression profiles for the genes *FAS1*, *FAS2, PAH1, DGA1* and *ARE1* observed in light and dark conditions were very similar (**Figure 2.8**). The only gene that exhibited a difference in expression between the light and dark samples was *ACL1*. In this study, the overall amount of lipids (**Figure 2.2**) and the transcription level of other lipid producing genes were unchanged (**Figure 2.8**), however, fatty acid composition showed differences between light- and dark-grown cells.

2.3.4. Expression of the carotenoid biosynthesis genes in the early cultivation stage

The expression of genes involved in carotenoid biosynthesis was analyzed. The level of transcription of *CAR1* and *CAR2* was detectably greater at day three of the light samples. However, cultures became visibly red after one day of light irradiation, indicating that carotenoid levels had increased (**Figure 2.2a**). Furthermore, carotenoids were presented in the cultures after one day of growth in the light and the levels were greater than those detected in dark-grown cultures (**Figure 2.2b**). These results implied that carotenoid biosynthesis had already occurred during the first day of light irradiation. Therefore, a light stimulating experiment was performed in which dark-grown cells were transferred to light growing conditions and the expression of the genes involved in carotenoid biosynthesis (*CAR2* and *CAR1*) was analyzed. We found that the level of transcription of *CAR1* and *CAR2* was significantly increased after one hour of light irradiation and that the amount of transcripts then decreased after a further two hours. The difference in gene transcription was thus observed again at 72 h (**Figure 2.9**). Results showed that the expression of *CAR1* and *CAR2* was higher in light- compared to dark-grown cells, being three and two folds higher, respectively. This result suggests that *CAR1* and *CAR2* were regulated by a two-step photo response mechanism.

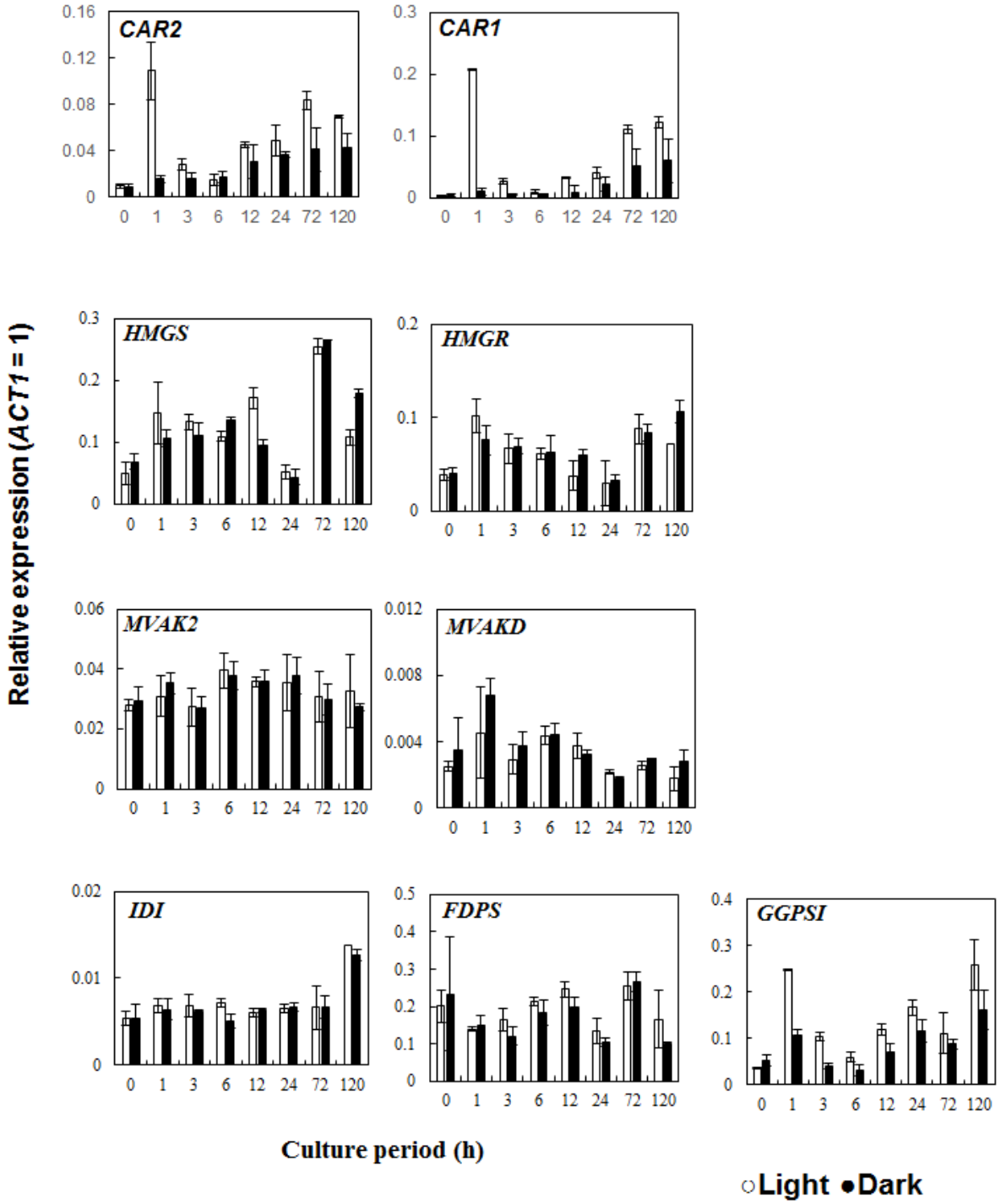

Figure 2.9. Effect of light irradiation on the expression of the genes for mevalonate and carotenoid biosynthetic pathways during the early stages of culture growth. qRT-PCR analyses for *HMGS*, *HMGR*, *MVAK2*, *MVAKD*, *IDI*, *FDPS*, *GGPSI* and *CAR2* and *CAR1* genes in RNA samples grown in the dark (black) and exposed to light (white) per time were indicated (h).

To determine which step of the biosynthetic pathway leading to phytoene was affected by light, genes involved in the mevalonate pathway were also analyzed. In order to do this, the following genes were included: *HMGS*, *HMGR*, *MVAK2*, *MVAD*, *IDI*, *FDPS* and *GGPSI*, which encode 3-hydroxy-3-methylglutaryl-CoA synthase, 3-hydroxy-3-methylglutaryl-CoA reductase, phosphomevalonate kinase, mevalonate pyrophosphate decarboxylase, isopentenyl pyrophosphate isomerase, farnesyl diphosphate synthase and geranylgeranyl diphosphate synthase, respectively (**Figure 2.1**). A two-step transcription activation profile was also observed in the *GGPSI* gene during exposed to light irradiation (**Figure 2.9**), however results showed that the expression of genes involved in the upstream of the pathway leading to geranylgeranyl diphosphate did not differ in response to light. Phytoene synthesis is the step that produces the precursor to the carotenoid pathway (**Figure 2.1**).

2.3.5. Light response control factors

Carotenoids are groups of pigments that absorb violet to blue-green light. Differences in the effect of various wavelengths of light on carotenoid formation and composition have been reported previously (An and Johnson 1990; Takano *et al.* 2005; Khanafari, Tayari and Emami 2008). Therefore, the effect of specific wavelengths of light was studied in *R. toruloides*. Cultures grown on agar were irradiated with blue, red and white light with a dark condition as control. *R. toruloides* colonies were darker red in color when exposed to blue and white light (**Figure 2.10**) than red light and dark-grown cultures. This finding suggested that *R. toruloides* is sensitive to blue light.

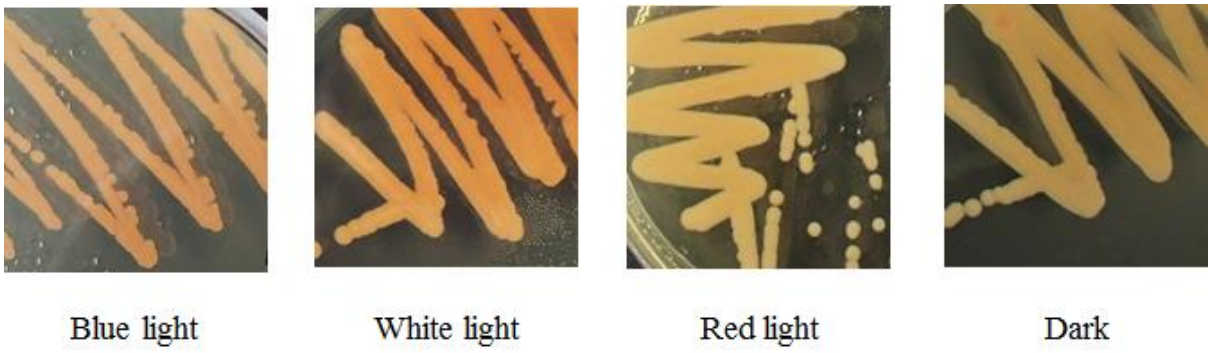

Figure 2.10. The color variation of *R. toruloides* under various wavelengths of visible light

The filamentous fungus *Neurospora crassa* possesses the white-collar complex (WCC), which is a protein complex formed by the proteins WC1 and WC2. It is widely known as the primary photoreceptor system for blue light (Linden, Ballario and Macino 1997; Corrochano

2007). The protein complex, WC1 and WC2 are also involved in promoting carotenoid biosynthesis by light irradiation (He *et al.* 2002; Iigusa, Yoshida and Hasunuma 2005; Belozerskaya *et al.* 2012). It has also been reported that WCC plays a role as a receptor and transcription factor, and that the complex is involved in promoting of carotenoid biosynthesis by light irradiation. Furthermore, cryptochrome DASH has been reported as a blue light receptor (Ahmad *et al.* 1998; Froehlich *et al.* 2010; Yu *et al.* 2010; Yang *et al.* 2016), and has recently been reported to bind FAD as a coenzyme. It is proposed to have evolved from a DNA repair enzyme, dependent on light absorption. It has also been identified as the blue light receptor in plants, with conservation in microorganisms (Facella *et al.* 2006; Yu *et al.* 2010; Gong *et al.* 2015). Therefore, from the draft genome sequence of *R. toruloides*, two genes encoded a protein that showed homology to *WC1* (37%) and *WC2* (36%) from *N. crassa.* We also founded a gene that encoded a protein exhibiting high homology (41%) to Cryptochrome DASH from the carotenoid producing yeast *X. dendrorhous* is *CRY1* in *R. toruloides*. Therefore, these genes were analyzed for the expression.

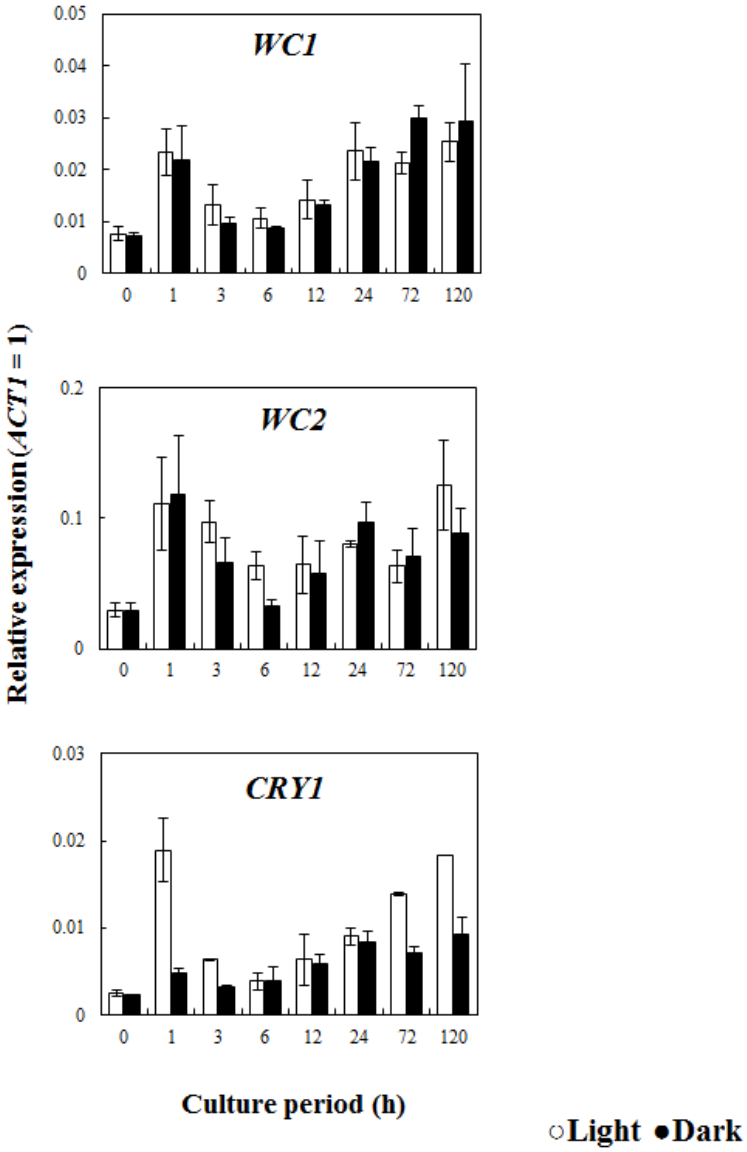

Figure 2.11. Effect of the light irradiation on the expression of the genes *WC1*, *WC2* and *CRY1*. Dark (black) condition and light (white) irradiation

Analysis of the expression response of the genes responsible for encoding *WC1*, *WC2*, and Cryptochrome DASH (*CRY1*) was performed by qRT-PCR. *WC-1* and *WC2* constitutively expressed under light and dark conditions (**Figure 2.11**). Besides, *CRY1* was expressed exponentially at one hour of light irradiation, after which it decreased. However, at 72 h of light irradiation, significant enhancement of gene expression was observed (**Figure 2.11**).

2.3.6. Identification of photo response genes by comprehensive gene expression analysis

From section 2.3.4, extremely increased expression at only 1 h by light showed that the light response happened within 1h light exposure in this strain. Thus, it suggested that the genes regulated the carotenoid biosynthesis pathway in this strain. To better understand this fact, comprehensive expression analysis was performed on the NBRC 10032 genes at 1 h during light irradiation, and compared to 1 h during dark condition and 0 h (dark condition).

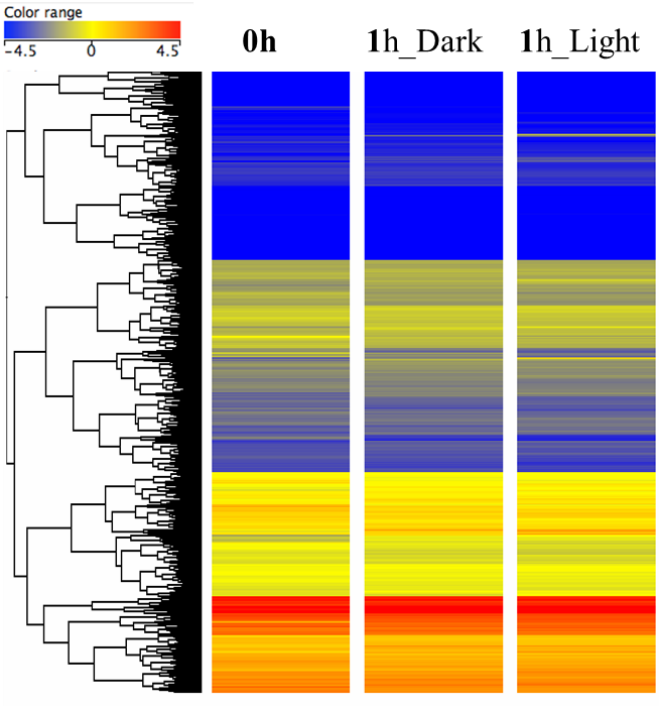

Figure 2.12.

The heat map indicated the comprehensive gene expression. Blue as the expression intensity is low, and Red as the expression intensity is high.

Total RNA was extracted from cells from 0 h and 1 h of light induction. Microarray data was analyzed and genes were clustered by their expression amounts (**Figure 2.12)**. Blue indicated low intensity expression, whereas red indicated the high intensity expression. Compared with 0 h, gene expression of most genes appeared unchanged in both continuous dark condition (1h_Dark) and light condition (1h_Light). However, 48 and 23 genes showed a 5-fold or more expression amount within 1 h of light irradiation and at 1 h of dark condition, respectively, compared to 0 h expression. Among them, 16 genes existed in both conditions, and only 32 genes show a 5-fold variation expression by light irradiation (**Figure 2.13**). These genes were therefore suggested as the light response genes.

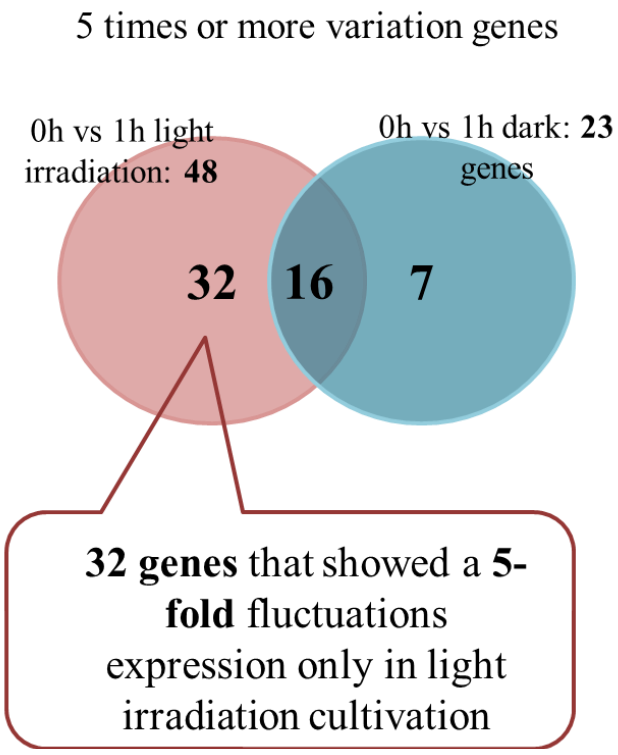

Figure 2.13. Gene groups showing a 5-fold or more varied expression only in the light irradiation-induced culture using a Venn diagram

2.3. Discussions

The effect of light on the *R. toruloides* NBRC 10032 strain in the growth rate, including the lipid and carotenoid production led to some interesting data. Redder colorations was observed when NBRC 10032 was cultured under light irradiation suggested higher carotenoid production or changes in the carotenoid composition. The short time to see the color change r also showed the strong influence of the light on the carotenoids of NBRC 10032.

The carotenoid samples from light irradiated cells showed a much higher absorbance than that from cells cultivated in the dark. Indeed, the cell-free extract after six days of cultivation showed that cells grown in the light exhibited a 5-fold greater production of carotenoids than those grown in the dark (**Figure 2.2b**). It has been reported previously that the fungus *Mucor hiemalis* produced more carotenoids when grown in the light. Furthermore, carotenoid production in blue and white light was 2.5 and 3-fold higher than that measured in the dark-grown sample, respectively (Khanafari, Tayari and Emami 2008). Similar results have also been reported in *R. glutinis* (Sakaki *et al.* 2001; Yen and Yang 2012; Zhang, Zhang and Tan 2014). Therefore, we proposed that *Rhodosporidium* species possess a light-responsive mechanisms for carotenoid production.

The effect of light irradiation on fungal growth and lipid accumulation was also analyzed in several phenotypes of NBRC 10032. Although higher amounts of overall lipid production were observed in the dark-grown samples, lipid content per cell was the same under light and dark conditions (**Figure 2.6d, e**). Growth inhibition by light has previously been reported in other fungi such as *R. glutilis* and *Phaffia rhodozyma* (Sakaki *et al.* 2001; Vázquez 2001; El-Banna, El-Razek and El-Mahdy 2012). However, contrasting results were reported by Zhang *et al.*, where samples of *R. glutilis* grown in the light exhibited lower biomass, and had similar total lipid content to those grown in the dark (Zhang, Zhang and Tan 2014). The lower biomass, but similar lipid content and glucose consumption might therefore suggest that this strain used glucose for carotenoid producing, not for growth or lipid producing when exposed to light. Besides, comparing lipid composition derived from both growth conditions showed that the percentage of unsaturated fatty acids was greater in light-grown samples. Double bonds in the unsaturated fatty acid are known as well to act as antioxidants against harmful factors. Thus, increasing the amount of unsaturated fatty acids in response to light exposure could be a natural defense response in *R. toruloides*. According to previous studies, co-consumption of dietary lipids, in the form of fats containing rich unsaturated fatty acids, might promote the bioavailability of fat-soluble micronutrients and phytochemicals in Caco-2 cells (Failla *et al.* 2014). Furthermore, fatty acid unsaturation significantly affects the antioxidant role of β-carotenoid by inhibiting lipid peroxidation in homogenous solutions (Palozza, Luberto and Bartoli 1995). Therefore, oils derived from *R. toruloides*, and having high carotenoid and unsaturated fatty acid content offers great potential as a new source of functional edible oils.

Genomic DNA and transcriptome sequences of the *R. toruloides* NP11 strain had revealed that it has a 20.2 Mb genome and 8,171 protein-coding genes (Zhu *et al.* 2012). Other reports have shown that the NBRC 0880 and CECT1137 strains have 7,920 and 8,206 predicted proteins, respectively (Zhang *et al.* 2016). However, in the genome sequence data of the NBRC 10032 strain, the number of predicted genes were fewer than those of other reports for *Rhodosporidium*. To identify genes that NBRC 10032 did not possess, a bidirectional BLAST analysis was carried out and 1058 genes were extracted, then identified by BLAST.

The expression of *CAR1* and *CAR2* in light-grown cells were higher than that in the dark (**Figure 2.8**). In the carotenogenic fungus *Xanthophyllomyces dendrorhous,* overall carotenoid content was increased by overexpressing *CrtE*, *CrtYB* and *CrtI* that encode

geranylgeranyl diphosphate synthase, phytoene synthase, phytoene desaturase, respectively (Verdoes *et al.* 2003). It has also been reported that carotenoids were produced in *Saccharomyces cerevisiae* when carotenoid biosynthesis genes (*CrtE, CrtYB* and *CrtI,* derived from *X. dendrorhous*) were overexpressed (Verwaal *et al.* 2007). Furthermore, albino transformants were observed after deletion of the *CAR2* gene in *R. toruloides* (Koh *et al.* 2014). Therefore, it was possible that the observed increase in carotenoid production in *R. toruloides* was due to enhanced expression of *CAR1* and *CAR2* in response to exposure to light. The expression of *ACL1* was enhanced by light, in similar pattern as that of *CAR1* and *CAR2*. This gene plays an essential role in fatty acid synthesis of the lipid producing yeast *Yarrowia lipolytica,* (Liu *et al.* 2013b; Wang *et al.* 2014; Dulermo *et al.* 2015b). Additionally, *ACL1* inactivated mutants of *Y. lipolytica* W29, fatty acid content was shown to be dramatically lower and an increase was observed in the proportion of unsaturated fatty acids (Dulermo *et al.* 2015b). Therefore, in this study, the overall amount of lipids (**Figure 2.2**) and the transcription levels of other lipid producing genes were unchanged (**Figure 2.8**), but the fatty acid composition showed differences between light- and dark-grown cells. These findings suggest that light does not directly affect lipid production but that it could be influential in determining the fatty acid composition.

In the detail of carotenoid biosynthesis genes, expression of *CAR1* and *CAR2* was higher in light grow cells than in dark grown cells. In addition, their expression was a two-step response. Light irradiation led to the generation of reactive oxygen species that are harmful to microorganisms. Thus, it is possible that *R. toruloides* produced carotenoids in response to light irradiation as part of the defense system against oxidative stress, resulting in the observed two-step transcriptional response being a defense system against acute or sustained light irradiation. Furthermore, the two-step transcription activation profile was also observed in *GGPSI* when exposed to light irradiation (**Figure 2.9**), but the expression of genes involved in the upstream of the pathway leading to geranylgeranyl diphosphate did not differ in response to light. Alternatively, phytoene synthesis is the step that produces the precursor to the carotenoid pathway (**Figure 2.1**). It condenses two GGPP molecules to form phytoene, a colorless C40 carotenoid with only three conjugated double bonds. *GGPSI* is the first light response gene in carotenoid biosynthesis. It has been hypothesized that the increased expression levels of *GGPSI* could lead to associated increase in the amount of GGPP which in turn stimulated carotenoid synthesis.

The WCC composed of WC1 and WC2, were known as the primary photoreceptor system for blue light in the filamentous fungus *Neurospora crassa* (Linden, Ballario and Macino 1997; C.Froehlich *et al.* 2002; He *et al.* 2002). Also, cryptochrome DASH which has been reported as a blue light receptor in plants and has been shown as well to have been conserved in microorganisms (Facella *et al.* 2006; Froehlich *et al.* 2010; Yu *et al.* 2010; Chaves *et al.* 2011; Gong *et al.* 2015). WC1 has ability to sense light and to bind to the promoters of light-inducible genes. Meanwhile WCC might role in transcriptional activation (C.Froehlich *et al.* 2002; He *et al.* 2002). *CRY1* was expressed exponentially by light irradiation through the same expression pattern profile for carotenoid genes. It has been speculated that the *CRY1* gene plays a role in photoreceptive responses. In the filamentous fungus *Fusarium fujikuroi*, *WcoA* which encodes a protein that is highly homologous to *WC1* , and serves as a photoreceptor and *cryD*, also acts as DASH cryptochrome gene (Estrada and Avalos 2008; Castrillo and Avalos 2015). *WcoA* played a role as light-signaling, and acted together with *cryD* when suddenly stimulated by light, to promote the expression of carotenoid genes (Castrillo and Avalos 2015). Froehlich *et al*., reported that the transcript and protein levels of CRY (Cryptochromes) were both strongly and rapidly induced by light in a *wc-1*-dependent manner (Froehlich *et al.* 2010) in *Neurospora crassa*. The interdependent transcriptional relationships between *Cmwc-1* (encoding white-collar) and *Cmcry-DASH* (encoding DASH cryptochrome) was also reported in *Cordyceps militaris* (Zhang *et al.* 2020).

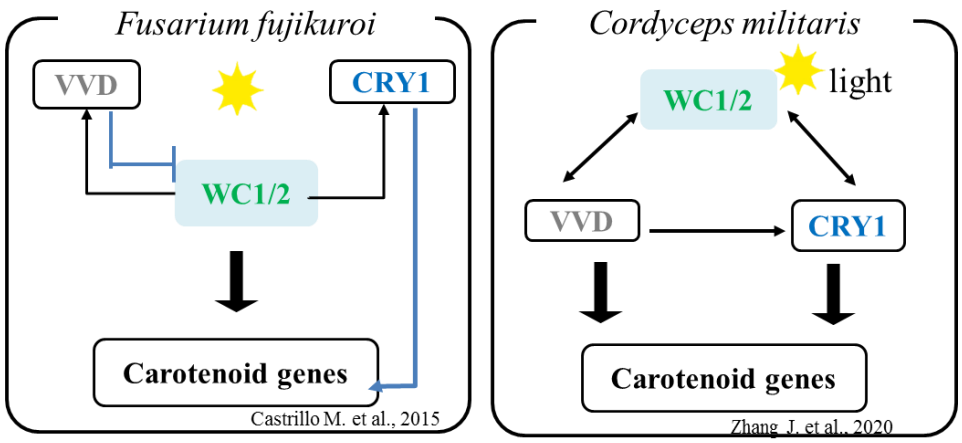

Figure 2.14. The interaction relation in photoreceptor genes. WC1/2. White-collar complex; CRY1. Cryptochromes DASH; VVD. Vivid-like photoreceptors (small VIVID-like protein, small flavin binding proteins).

In the case of *R. toruloides* NBRC 10032, the *CRY1* gene is also proposed to serve as light-signaling functions when it is over expressed during the first hour. Rapid response in *CRY1* promotes the expression of carotenoid genes as well, resulting in rapid carotenoid producing. Further research is thus required to determine the role of *WC1* and *CRY1* in *R. toruloides* cell responses to light, and these should include molecular genetic strategies such as gene deletion or overexpression.

The activation of carotenoid genes and light receptor genes resulted in the increasing carotenoid production. The almost was β-carotene content after one day of dark cultivation, while not only β-carotene, the γ-carotenoid and torulene also were produced in the light cultivation. It was suggested the non-light effect condition, the β-carotene is a priority product. The increasing of torulene content was observed in the day 2 and day 6 by light that was respective to two-step of carotenoid gene expression. That was suggested the light affected in the carotenoid composition. And, the mechanism in the carotenoid composition control might exist.

Table 2.6. List of the 32 genes having a 5-fold fluctuation expression by light

Annotation	(+: increased gene, - Dropened gene)
hydroxymethylglutaryl-CoA synthase	-
proteinof caleosin family	+
### Not characterized ###	+
proteinof choline transporter-like family	+
FAD dependent oxidoreductase	+
### Not characterized ###	+
deoxyribodipyrimidine photo-lyase	+
phytoene dehydrogenase(*CAR1*)	+
DUF427-domain-containing protein	+
geranylgeranyl diphosphate synthase, type III(*GGPSI*)	+
### Not characterized ###	+
Allergen	+
cell division control protein Cdc54	+
short-chain dehydrogenase/reductase SDR family protein	+
D-arabinono-1,4-lactone oxidase	+
beta-Ig-H3/Fasciclin	+
Ribonuclease	+
minichromosome maintenance protein 6	+
proteinof bacterial rhodopsin family	+
### Not characterized ###	+
GATA transcription factor	+
UV DNA damage endonuclease	+
mnng and nitrosoguanidine resistance protein	+
Hypothetical Protein RTG_01011	+
Proteophosphoglycan ppg4	+
phenolic acid decarboxylase	+
Proteophosphoglycan 5	+
phytoene synthase*(CAR2)*	+
zinc-type alcohol dehydrogenase	+
SH3 domain protein	+
arabinose-5-phosphate isomerase	+
START domain containing protein	+

In the comprehensive gene expression results, a list of these 32 genes having 5-fold or more variation expression only in light irradiation was found and shown in **Table 2.6**. Link to the qRT-PCR analysis, genes acting in the carotenoid biosynthesis *GGPSI*, *CAR2*, and *CAR1* showed an increase in transcription levels by light irradiation. The oxidoreductase enzyme, such as flavin adenine dinucleotide (FAD) dependent oxidoreductase, D-arabinono-1,4-lactone oxidase, and the zinc-type alcohol dehydrogenase enzyme also increased the transcription levels in the light irradiation. The FAD dependent oxidoreductase enzyme is a FAD

flavoenzyme that is among the FAD (NAD-H) binding domain superfamily. D-arabinono-1,4-lactone oxidase belongs oxidoreductase and has one FAD cofactor (like Cryptochrome DASH). This cofactor also shows that *R. toruloides* are sensitive to oxidative stress caused by light irradiation. Besides, deoxyribodipyrimidine photo-lyase and UV DNA damage endonuclease enzymes showed an increase in transcription by light irradiation. Deoxyribodipyrimidine photo-lyase enzymes involved in repair of UV radiation induced DNA damage as well, and has FAD cofactor binding sites. UV DNA damage endonuclease enzyme, is related to DNA repair by DNA damage factors. It is suggested that *R. toruloides* also retains a general DNA damage repair mechanism by light irradiation. Therefore, it is hypothesized that a protective mechanism against DNA damage and oxidative stress caused by light irradiation, which promotes antioxidant production such as carotenoid. And, the present of FAD in the binding site of these enzyme suggested the photo carotenogenesis was consistent with the participation of a flavin based photoreceptor.

And comparing the promoter region in these light activated genes, three motifs were extracted (**Figure 2.15**). It is possible that these motifs were regulatory region responsible for light.

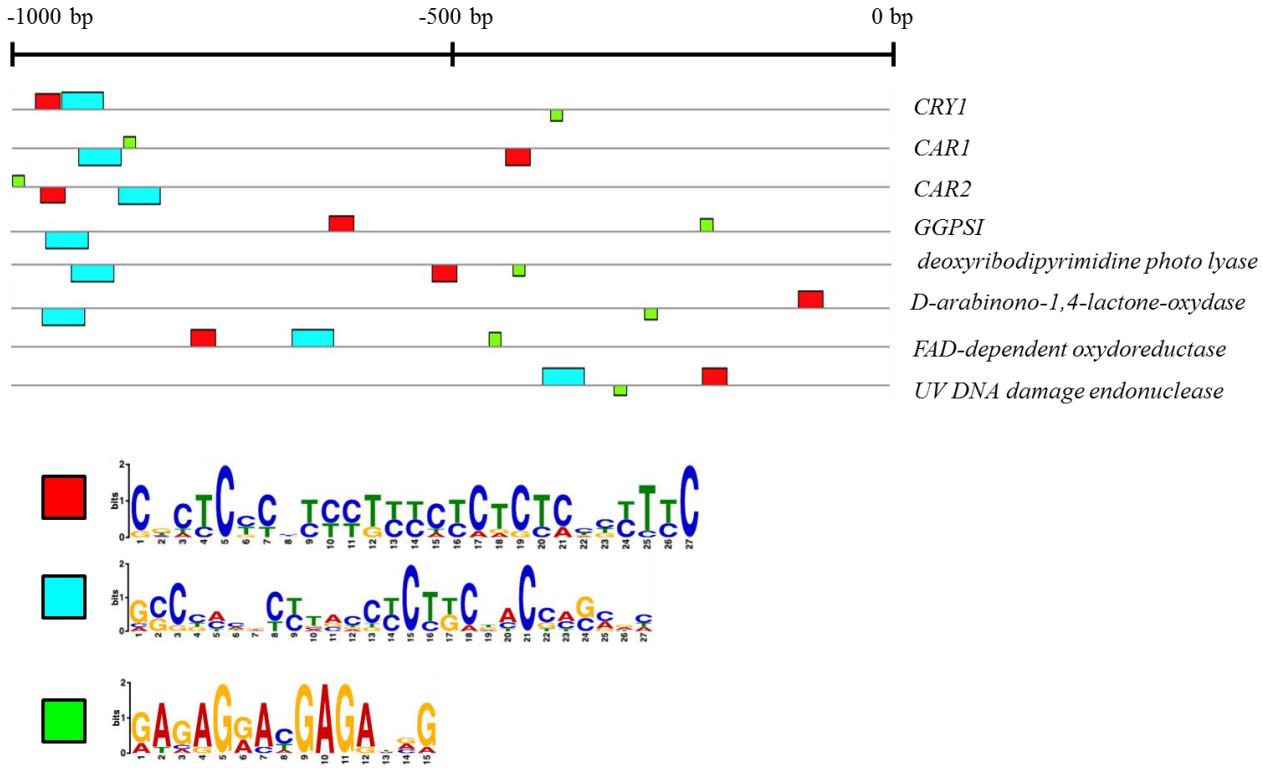

Figure 2.15. Comparison of promoter region of the light activated genes

2.5. References

Ahmad M, Jarillo JA, Smirnova O *et al.* The CRY1 blue light photoreceptor of *Arabidopsis* interacts with phytochrome a in vitro. *Mol Cell* 1998;**1**:939–48.

An GH, Johnson EA. Influence of light on growth and pigmentation of the yeast *Phaffia rhodozyma*. *Antonie Van Leeuwenhoek* 1990;**57**:191–203.

Belozerskaya TA, Gessler NN, Isakova EP *et al. Neurospora crassa* Light Signal Transduction Is Affected by ROS. *J Signal Transduct* 2012;**2012**:1–13.

Braunwald T, Schwemmlein L, Graeff-Hönninger S *et al.* Effect of different C/N ratios on carotenoid and lipid production by *Rhodotorula glutinis*. *Appl Microbiol Biotechnol* 2013;**97**:6581–8.

Castrillo M, Avalos J. The flavoproteins CryD and VvdA cooperate with the white collar protein WcoA in the Control of photocarotenogenesis in *Fusarium fujikuroi*. *PLoS One* 2015;**10**:1–22.

Chaves I, Pokorny R, Byrdin M *et al.* The cryptochromes: Blue light photoreceptors in plants and animals. *Annu Rev Plant Biol* 2011;**62**:335–64.

Corrochano LM. Fungal photoreceptors: sensory molecules for fungal development and behaviour. *Photochem Photobiol Sci* 2007;**6**:725–36.

Davoli P, Mierau V, Weber RWS. Carotenoids and fatty acids in red yeasts *Sporobolomyces roseus* and *Rhodotorula glutinis*. *Appl Biochem Microbiol* 2004;**40**:392–7.

Davoli P, Weber RWS. Carotenoid pigments from the red mirror yeast, *Sporobolomyces roseus*. *Mycologist* 2002;**16**:102–8.

Dulermo T, Lazar Z, Dulermo R *et al.* Analysis of ATP-citrate lyase and malic enzyme mutants of *Yarrowia lipolytica* points out the importance of mannitol metabolism in fatty acid synthesis. *Biochim Biophys Acta - Mol Cell Biol Lipids* 2015;**1851**:1107–17.

El-Banna AA, El-Razek AMA, El-Mahdy AR. Some Factors Affecting the Production of Carotenoids by *Rhodotorula glutinis* var. *glutinis*. *Food Nutr Sci* 2012;**03**:64–71.

Estrada AF, Avalos J. The White Collar protein WcoA of *Fusarium fujikuroi* is not essential for photocarotenogenesis, but is involved in the regulation of secondary metabolism and conidiation. *Fungal Genet Biol* 2008;**45**:705–18.

Facella P, Lopez L, Chiappetta A *et al. CRY-DASH* gene expression is under the control of the circadian clock machinery in tomato. *FEBS Lett* 2006;**580**:4618–24.

Failla ML, Chitchumronchokchai C, Ferruzzi MG *et al.* Unsaturated fatty acids promote bioaccessibility and basolateral secretion of carotenoids and α-tocopherol by Caco-2 cells. *Food Funct* 2014;**5**:1101–12.

Folch J, Lees M, Stanley GHS. A simple method for the isolation and purification of total lipids from animal tissues. *J Biol Chem* 1957;**226**:497–509.

Froehlich AC, Chen CH, Belden WJ *et al.* Genetic and molecular characterization of a cryptochrome from the filamentous fungus *Neurospora crassa*. *Eukaryot Cell* 2010;**9**:738–50.

Gong Z, Shen H, Zhou W *et al.* Efficient conversion of acetate into lipids by the oleaginous yeast *Cryptococcus curvatus*. *Biotechnol Biofuels* 2015;**8**:189.

He Q, Cheng P, Yang Y *et al.* White collar-1, a DNA binding transcription factor and a light sensor. *Sci (New York, NY)* 2002;**297**:840–3.

Hornero-Méndez D, Minguez-Mosquera MI. Rapid spectrophotometric determination of red and yellow isochromic carotenoid fractions in paprika and red pepper oleoresins. *J Agric Food Chem* 2001;**49**:3584–8.

Iigusa H, Yoshida Y, Hasunuma K. Oxygen and hydrogen peroxide enhance light-induced carotenoid synthesis in *Neurospora crassa*. *FEBS Lett* 2005;**579**:4012–6.

Khanafari A, Tayari K, Emami M. Light Requirement for the Carotenoids Production by *Mucor hiemalis*. *Iran J Basic Med Sci* 2008;**11**:25–32.

Koh CMJ, Liu Y, Moehninsi *et al.* Molecular characterization of *KU70* and *KU80* homologues and exploitation of a *KU70*-deficient mutant for improving gene deletion frequency in *Rhodosporidium toruloides*. *BMC Microbiol* 2014;**14**, DOI: 10.1186/1471-2180-14-50.

Kot AM, Błażejak S, Kurcz A *et al. Rhodotorula glutinis*—potential source of lipids, carotenoids, and enzymes for use in industries. *Appl Microbiol Biotechnol* 2016;**100**:6103–17.

Lichtenthler HK. Chlorophylls Carotenoids. *Methods in Enzymology*. Vol 148. 1987, 350–82.

Linden H, Ballario P, Macino G. Blue light regulation in *Neurospora crassa*. *Fungal Genet Biol* 1997;**22**:141–50.

Liu XY, Chi Z, Liu GL *et al.* Both Decrease in *ACL1* Gene Expression and Increase in *ICL1* Gene Expression in Marine-Derived Yeast *Yarrowia lipolytica* Expressing *INU1* Gene Enhance Citric Acid Production from Inulin. *Mar Biotechnol* 2013;**15**:26–36.

Lodato P, Alcaíno J, Barahona S *et al.* Expression of the carotenoid biosynthesis genes in *Xanthophyllomyces dendrorhous*. *Biol Res* 2007;**40**:73–84.

Mata-Gómez LC, Montañez JC, Méndez-Zavala A *et al.* Biotechnological production of carotenoids by yeasts: An overview. *Microb Cell Fact* 2014;**13**:1–11.

Palozza P, Luberto C, Bartoli GM. The effect of fatty acid unsaturation on the antioxidant acitivity of β-carotene and α-tocopherol in hexan solutions. *Free Radic Biol Med* 1995;**18**:943–8.

Sakaki H, Nakanishi T, Tada A *et al.* Activation of Torularhodin Production by *Rhodotorula glutinis* Using Weak White Light Irradiation. *J Biosci Bioeng* 2001;**92**:294–7.

Shi Q, Wang H, Du C *et al.* Tentative identification of torulene *Cis/trans* geometrical isomers isolated from *Sporidiobolus pararoseus* by high-performance liquid chromatography-diode array detection-mass spectrometry and preparation by column chromatography. *Anal Sci* 2013;**29**:997–1002.

Sieiro C, Poza M, De Miguel T *et al.* Genetic basis of microbial carotenogenesis. *Int Microbiol* 2003;**6**:11–6.

Takano H, Obitsu S, Beppu T *et al.* Light-induced carotenogenesis in *Streptomyces coelicolor* A3(2): Identification of an extracytoplasmic function sigma factor that directs photodependent transcription of the carotenoid biosynthesis gene cluster. *J Bacteriol* 2005;**187**:1825–32.

Vázquez M. Effect of the Light on Carotenoid Profiles of *Xanthophyllomyces dendrorhous* Strains (formerly *Phaffia rhodozyma*). *Food Technol Biotechnol* 2001;**39**:123–8.

Verdoes JC, Sandmann G, Visser H *et al.* Metabolic Engineering of the Carotenoid Biosynthetic Pathway in the Yeast *Xanthophyllomyces dendrorhous (Phaffia rhodozyma)*. *Appl Environ Microbiol* 2003;**69**:3728–38.

Verwaal R, Wang J, Meijnen JP *et al.* High-level production of beta-carotene in *Saccharomyces cerevisiae* by successive transformation with carotenogenic genes from *Xanthophyllomyces dendrorhous*. *Appl Environ Microbiol* 2007;**73**:4342–50.

Wang GY, Zhang Y, Chi Z *et al.* Role of pyruvate carboxylase in accumulation of intracellular lipid of the oleaginous yeast *Yarrowia lipolytica* ACA-DC 50109. *Appl Microbiol Biotechnol* 2014;**99**:1637–45.

Weber RWS, Anke H, Davoli P. Simple method for the extraction and reversed-phase high-performance liquid chromatographic analysis of carotenoid pigments from red yeasts (Basidiomycota, Fungi). *J Chromatogr A* 2007;**1145**:118–22.

Yang Z, Yang L, Liu Q *et al.* Photoactivation and inactivation of *Arabidopsis* cryptochrome 2. *Science (80-)* 2016;**354**:343–7.

Yen HW, Yang YC. The effects of irradiation and microfiltration on the cells growing and total lipids production in the cultivation of *Rhodotorula glutinis*. *Bioresour Technol* 2012;**107**:539–41.

Yu X, Liu H, Klejnot J *et al.* The Cryptochrome Blue Light Receptors. *Arab B* 2010;**8**, DOI: 10.1199/tab.0135.

Zhang J, Wang F, Yang Y *et al.* CmVVD is involved in fruiting body development and carotenoid production and the transcriptional linkage among three blue-light receptors in edible fungus Cordyceps militaris. *Environ Microbiol* 2020;**22**:466–82.

Zhang S, Skerker JM, Rutter CD *et al.* Engineering *Rhodosporidium toruloides* for increased lipid production. *Biotechnol Bioeng* 2016;**113**:1056–66.

Zhang Z, Zhang X, Tan T. Lipid and carotenoid production by *Rhodotorula glutinis* under irradiation/high-temperature and dark/low-temperature cultivation. *Bioresour Technol* 2014;**157**:149–53.

Zhu Z, Zhang S, Liu H *et al.* A multi-omic map of the lipid-producing yeast *Rhodosporidium toruloides*. *Nat Commun* 2012;**3**:1–11

Chapter 3: Target gene deletion in *R. toruloides* NBRC 10032 – *CRY1* disrupt establishing

3.1. Introduction

In our study, a two-step response not only in the main carotenogenic genes, geranylgeranyl diphosphate synthase, phytoene desaturase, and phytoene synthase/lycopene cyclase (encoding by *GGPSI*, *CAR1* and *CAR2*, respectively), but also in the *CRY1* (encoding putative Cryptochrome DASH, the blue-light receptor) was observed. The expression of *CRY1* in NBRC 10032 was expressed exponentially in the early light-exposure periods and increased again after 72 h after exposure to light. These results suggested a role for *CRY1* in carotenoid production.

Cryptochrome DASH which has been identified as a blue light receptor plays a role in promoting carotenoid production in *Arabidopsis Cordyceps, Fusarium* (Ahmad *et al.* 1998; Facella *et al.* 2006; Froehlich *et al.* 2010; Yu *et al.* 2010; Castrillo, García-Martínez and Avalos 2013; Castrillo and Avalos 2015). Therefore, the potential light regulator, Cryptochrome DASH (CRY1), has been suggested to contribute to light response mechanisms. *CRY1* therefore became the target gene to analyze its function in the light response mechanism. However, gene targeting has not been established in the NBRC 10032 strain. Hence, first, we established the recombined method in this strain, after which we analyzed the disrupted *CRY1* obtained.

3.2. Materials and methods

3.2.1 Yeast strain and culture conditions

The *R. toruloides* NBRC 10032 (a strain with high lipid production) was obtained from the Biological Resource Center of the National Institute of Technology and Evaluation (NITE, Chiba, Japan). *R. toruloides* was grown on YPD agar plates (1% yeast extract, 1% peptone, 2% D-Glucose, 2% agar (Nacalai Tesque, Tokyo, Japan)) at 30°C for four days and maintained at 4°C. YPD broth was used for pre-cultivation, and LS10 broth (0.805% powder yeast extract (Kyokuto Seiyaku Co.,), 15% D-Glucose, 0.047% NH_2CONH_2, 0.15% $MgSO_4 \cdot 7H_2O$, 0.04% KH_2PO_4, 1.9×10^{-6} mmol/L $ZnSO_4$, 1.22×10^{-4} mmol/L $MnCl_2$, 1×10^{-4} mmol/L $MnCl_2$, 1×10^{-4} mmol/L $CuSO_4$ and 1.5 mmol/L $CaCl_2$, (Nacalai Tesque, Tokyo, Japan)) was used as the main culture. Yeast cells were pre-cultivated for 24 h in YPD broth in L-shaped test tubes and

were then cultured in 200 mL Erlenmeyer flasks in 50 mL LS10 medium at an initial optical density (OD) of 660 nm = 0.1. Experiments were performed in the same dark room. In contrast, light conditions were established by employing a blue LED light irradiation Unit LC-LED 470B (Taitec, Saitama, Japan) with 80 µmol/m^2/s photon, whereas, the dark condition was set by wrapping the tubes in two layers of aluminum foil (24 µm thick in total). An orbital shaker set at 130 rpm was used for all cultures.

3.2.2. Construction of DNA fragments for yeast transformation

Table 3.1. Strains and plasmids used in this study.

Strains or plasmids	**Description**
Strains	
Rhodosporidium toruloides NBRC 10032	Parent strain
dURA3	*R. toruloides* NBRC 10032, deleted *URA3* by *hph* maker
dKU70	Deletion of *KU70* gene by using *URA3* recycling
dCRY1	Deletion of *CRY1* gene by using *URA3* recycling
Plasmids	
pUC-*URA3*	Amp-r; pUC118 with *URA3* containing its promoter and terminator.
pUC-*ΔURA3::hph*	Hyg-r, Amp-r; pUC118 with the hph maker driven by *URA3* promotor and *URA3* terminator.
pUC-*ΔKU70::URA3*	Amp-r, Ura+; pUC118 with DNA fragment composed of half of *KU70*-ORF, *URA3* maker, Direct Repeat sequence and *KU70* terminator
pUC-*ΔCRY1::URA3*	Amp-r, Ura+; pUC118 with DNA fragment composed of half of *CRY1*-ORF, *URA3* maker, Direct Repeat sequence and *CRY1* terminator

The construction of a *URA3* disruption cassette was carried out as follows: The DNA fragment containing *URA3* and its approximate 1.5 kbp of 5′- and 3′- flanking regions was amplified by PCR, with the primer sets URA3_all_Fw and URA3_all_Rv. The *R. toruloides* genome was used as a template. Next, the amplicon and linearized pUC118 vector at the EcoRI site was assembled to obtain pUC-*URA3* (**Figure 3.1a**). pUC-*URA3* was opened by inverse PCR using primer set pUCURA3_inV_Fw and pUCURA3_inV_Rv, which annealed just upstream of the start codon and just downstream of the stop codon of *URA3*, respectively. The

codon-optimized *hph* gene encoding hygromycin B phosphotransferase from *E. coli* was used and opened pUC-*URA3* was assembled to obtain pUC-Δ*URA3::hph* (**Figure 3.1b)**. A DNA fragment containing *URA3* at the upstream region, *hph*, and *URA3* at the downstream region was released by EcoRI treatment and used for transformation. In this fragment, *hph* was driven by the *URA3* promoter.

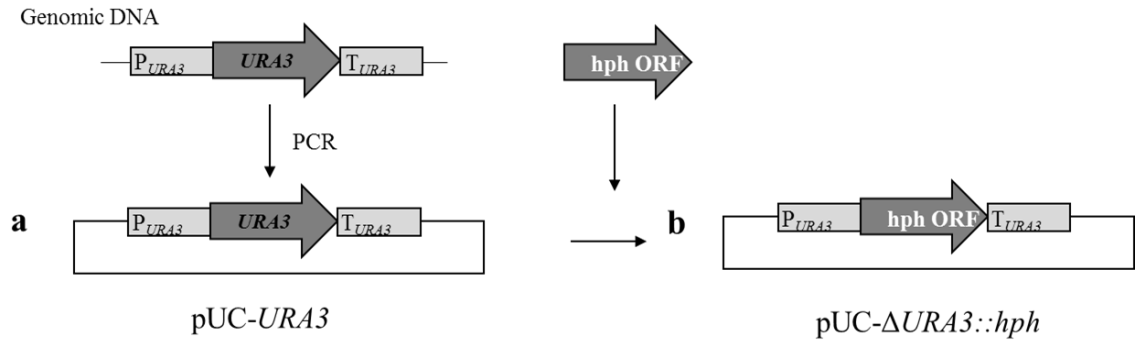

Figure 3.1. Structure of the constructed plasmid
a. pUC-*URA3* plasmid, b. pUC-Δ*URA3::hph* plasmid. ORF. Open reading frame, DR. Direct Repeat, P_{URA3}. *URA3* promoter, T_{URA3}. *URA3* terminator, Ter. terminator

The construction of a *KU70* disruption cassette was carried out as follows: A DNA fragment containing *URA3*, its 1.0 kbp upstream and 500 bp downstream regions were amplified by PCR with gene-specific primers by using *R. toruloides* genomic DNA as a template. DNA fragments of partial *KU70* (start codon to + 1.5 kbp), *KU70* upstream region (-500 bp to + 1 bp), and 1.5 kbp downstream region were also amplified by using fragment-specific primers. These amplicons were assembled into a HindIII site of pUC118 in the order of partial *KU70*, *URA3*, *KU70* upstream, and *KU70* downstream regions. From the resulting plasmid (**Figure 3.2a**), pUCΔ*KU70::URA3* was excised by BamHI and HindIII and the released *KU70* disruption cassette was used for transformation.

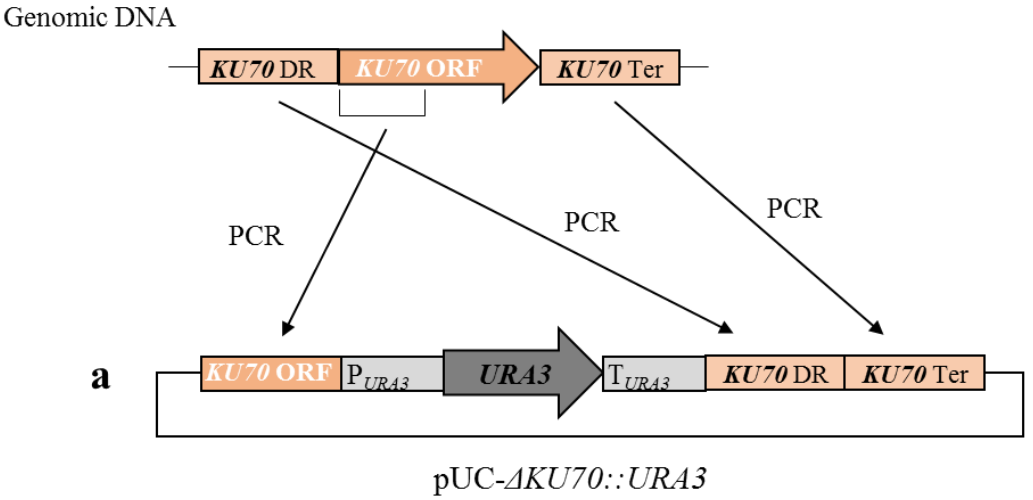

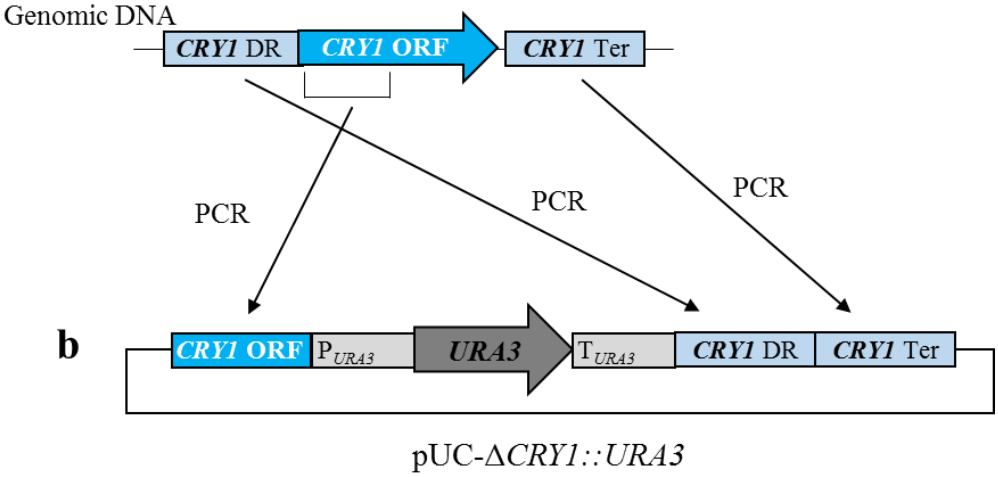

Figure 3.2. Structure of the constructed plasmid
a. pUC-*ΔKU70::URA3* plasmid, b. pUC-Δ*CRY1::URA3* plasmid. ORF. Open reading frame, DR. Direct Repeat, P_{URA3}. *URA3* promoter, T_{URA3}. *URA3* terminator, Ter. terminator

The construction of the *CRY1* disruption cassette was carried out similar to the *KU70* disruption cassette. *CRY1* partial *open reading frame* (ORF) (start codon to + 1.5 kbp), *URA3*, *CRY1* upstream region (- 500 bp to + 1 bp), and 1000 bp *CRY1* downstream region were amplified by PCR and assembled on a BamHI site of pUC118 to obtain pUCΔ*CRY1::URA3* (**Figure 3.2b)**. Then, the CRY1 disruption cassette was released by HindIII and AseI for transformation. The plasmids and strains that were used in this study are shown in **Table 3.1**. PCR primers used in the construction of each disruption cassette are listed in **Table 3.2**. As enzymes for assembly of DNA fragments, a Gibson assembly system or NEBuilder HiFi DNA assembly (New England Biolabs) was used in all experiments.

Table 3.2. PCR primers for constructing gene targets

Primer	Sequence (5'→ 3') *small character implies homologous sequence for DNA fragment assemble	Description
hph_Fw	cgctccgatttcgagATGAAGAAACCGGAGCTCACGG	For *URA3* disruption
hph_Rv	agaggattgcctcgtTCACTCCTTCGCGCGGG	
URA3_all_Fw	catgattacgaattcCGACGCGCTTCCTGCAG	
URA3_all_Rv	accgagctcgaattcACTGGGACCGCGTCGAGC	
pUCURA3_inV_Fw	ACGAGGCAATCCTCTCTAGACTT	
pUCURA3_inV_Rv	CTCGAAATCGGAGCGCGA	
URA3_for_KU70_Fw	AGAAAACGATCGCGTTCGAGTT	For *KU70* disruption
URA3_for_KU70_Rv	GCTGGAGTATGCGGACGAGAA	
KU70_ORF_Fw	gatcctctagagtCCATGTCGCGCTCGTTTGGAAG	
KU70_ORF_Rv	acgcgatcgttttctTCAGCGATCGAAGGAAGCG	
KU70_direct_repeat_Fw	tccgcatactccagcGCGGATGAGCCAGTCTTCCC	
KU70_direct_repeat_Rv	agtgaagacgaagacCTTTCAGCAGCGCACGAG	
KU70_terminator_Fw	GTCTTCGTCTTCACTGGCTCGT	
KU70_terminator_Rv	agcttgcatgcctgcagGTCGAATTCACCACACACTCCTCTCGTCC	
URA3_for_CRY1_Fw	ggatggtggaagcagAGAAAACGATCGCGTTCGAG	For *CRY1* disruption
URA3_for_CRY1_Rv	ctaccaccgcgtgatGCTGGAGTATGCGGACGAGA	
CRY1_ORF_Fw	agctcggtacccgggATGGGTCGCAAGGTCGTGCT	
CRY1_ORF_mid_Rv	acgcgatcgttttctCTGCTTCCACCATCCAGGCT	
CRY1_direct_repeat_Fw	tccgcatactccagcATCACGCGGTGGTAGACGC	
CRY1_direct_repeat_Rv	tctgccgtgtcgcgcCGTCTTGGCACCCTGCTGA	
CRY1_term_Fw	cagggtgccaagacgGCGCGACACGGCAGACTTT	
CRY1_termi_Rv	cgactctagaggatcTGTACGCTCGCAGGAGGG	

3.2.3. Yeast transformation

The NBRC 10032 strain was used for transformation using a previously reported electroporation method (Takaku *et al.* 2020) with little modification; 2 M LiAc and 1 M DTT were used, with 0.75 kV, 800 Ω, and 25 μF power conditions. After electroporation, restored cells were streaked on a YPD plate containing 100 mg/L Hygromycin B to screen for hygromycin resistance, YNB for uracil autotroph, or YNB containing 10 mM of 5-Fluoroorotic acid (5-FOA) and 10 mM uracil for *URA3* disruption.

3.2.4. Biochemical analysis

The DCW was quantified in lyophilized cells derived from 1 mL of broth. Carotenoids were extracted from dry cells in 100% acetone using a Multi-Beads Shocker (Yasui Kikai, Osaka, Japan) as described in Chapter 2, section 2.2.2. Carotenoid production was then calculated as the β-carotene equivalence (Wako Pure Chemical Industries Ltd., Osaka, Japan)

at an absorbance at 488 nm, which was measured using Infinite M200 Pro (Tecan, Kanagawa, Japan).

A Southern analysis was performed using Alkphos Direct™ Labeling and the CDP-star Detection System (GE Healthcare Life Science, Tokyo, Japan) following the manufacturer's instructions. Chromosomal DNA was digested by appropriate restriction enzymes and a gene-specific probe.

3.2.5. Quantitative reverse transcription polymerase chain reaction (qRT-PCR)

Total RNA extraction was performed using the hot phenol method, then purification of total RNA was carried out using Illustra RNAspin (GE Health Care Life Science, Tokyo, Japan) in accordance with the manufacturer's instructions. Quantitative real-time PCR was performed using Light Cycler 480 SYBR Green I Master Mix (Roche Applied Science, Bavaria, Germany) as described in Chapter 2, section 2.2.3. The relative expression level was calculated as a ΔCt power of 2, in which the ΔCt value was obtained by subtracting the Ct value of the housekeeping gene (*ACT1*, the gene encoding actin) from that of the target gene. The PCR primers for expression analysis are listed in **Table 2.1**.

3.3. Results

3.3.1. Establishment of gene targeting in NBRC 10032

To further evaluate the function of *CRY1* on carotenoid production, we constructed a *CRY1* deleted strain. Since gene targeting of NBRC 10032 had not been established until now, we first attempted to construct a host strain. Gene targeting frequency was extremely low in *Rhodosporidium* sp., because of the non-homologous end joining (NHEJ) system. Therefore, the *KU70* gene that was involved in NHEJ was deleted to increase the efficiency of the homologous recombination. To carry out multiple gene disruptions, we used *URA3* encoding orotidine 5'-phosphate decarboxylase as the selection marker for transforming NBRC 10032. Therefore, by using a *URA3* marker and carrying out positive selection in the presence of a uridine auxotroph and counter selection by 5-fluoroorotic acid resistance, we were able to obtain *CRY1* disruption following *KU70* disruption (**Figure 3.3**).

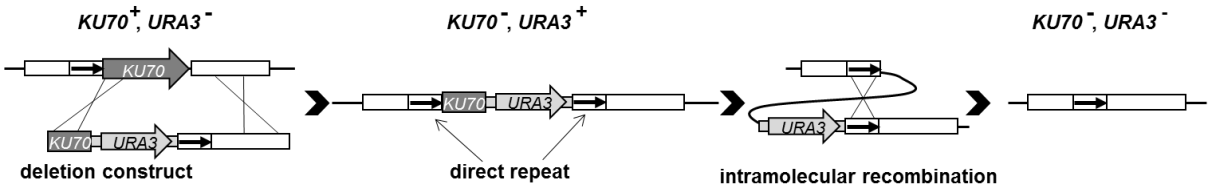

Figure 3.3. Schematic representation of *KU70* disruption
URA3 is the selection maker. The position of the homologous recombination is indicated.

In order to obtain a *URA3* disruption of NBRC 10032, first a DNA fragment containing the 5'-flanking region of *URA3*, the hygromycin resistance gene, and the 3'-flanking region of *URA3*, was introduced into NBRC 10032. From more than 800 hygromycin resistants, three 5'-FOA non-sensitive strains were obtained. Using Southern analysis, it was confirmed that one of the three strains was a homozygous *URA3* disruption (**Figure 3.4**), and this strain was named dURA3.

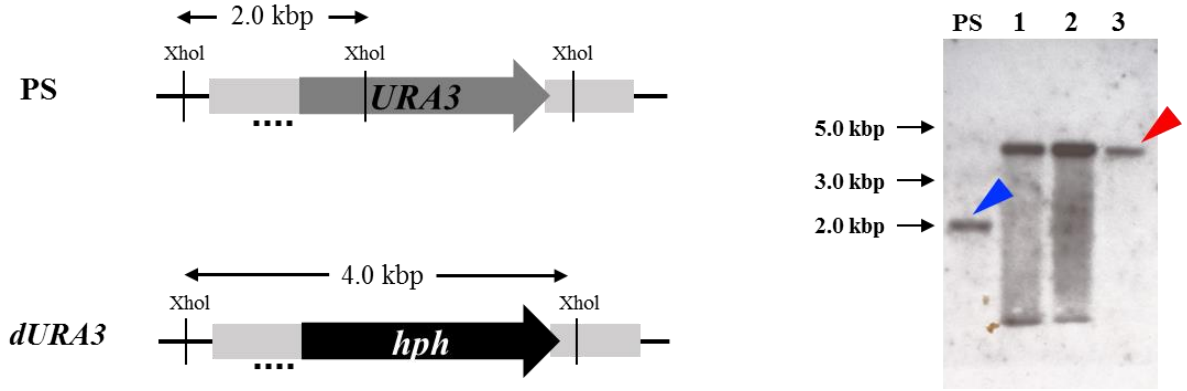

Figure 3.4. Southern analysis of *URA3* disruption
Genomic DNA was excised by XhoI. Dashed line shows hybridizing position of the probe. Blue and Red arrow-head represents hybridization signal of PS and transformants, respectively.

Next, we used dURA3 as the parental strain and *URA3* as the selection marker. The DNA fragment for transformation comprised a partial *KU70* ORF, *URA3*. The 3'-flanking region of *KU70* and the 5'-upstream region of *KU70* that was used as a direct repeat was inserted between *URA3* and the 3'-flanking region of *KU70*. In the transformation of dURA3 using this fragment, if homologous integration had taken place at the *KU70* locus, *URA3* would be looped out by intramolecular homologous recombination (**Figure 3.3** and **Figure 3.5b**).

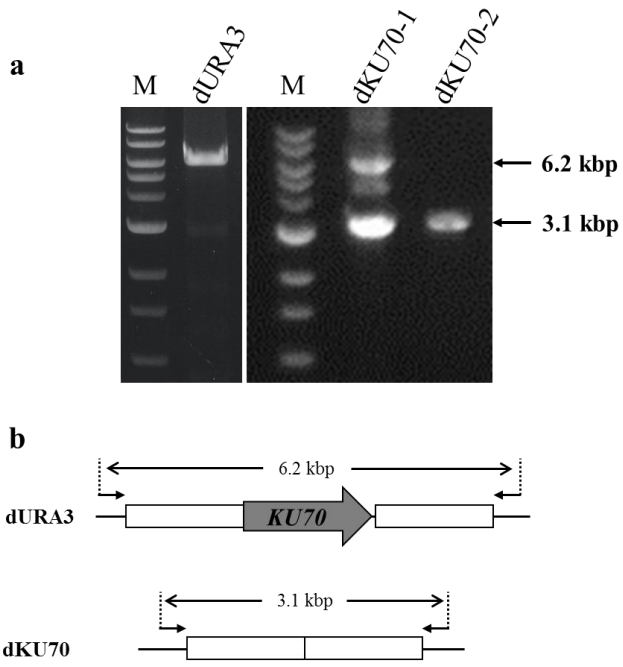

Figure 3.5. Results of *KU70* deletion. a. PCR analysis, b. The PCR amplification region

Therefore, only homologous recombinants could be obtained by selection of the 5-FOA. However, colony-PCR of 5-FOA resistant strains showed two amplicons that were 3.1 kbp and 6.2 kbp, which was expected following *KU70* deletion and native *KU70* bands, respectively (**Figure 3.5a**, dKU70-1). When dKU70-1 was transformed by the same DNA fragment, the 5-FOA resistant strain showed only one amplicon (**Figure 3.5a**, dKU70-2). These results led us to suspect that NBRC 10032 might be a diploid strain. The homozygosity of *KU70* disruption was confirmed by Southern analysis (**Figure 3.6**) and the *KU70* disruptant was named dKU70.

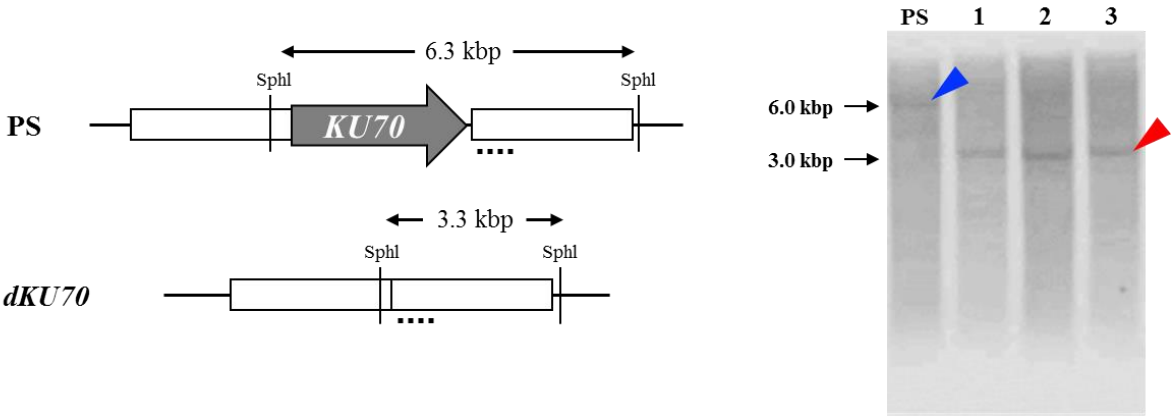

Figure 3.6 Southern analysis of *KU70* disruption. Genomic DNA was excised by SphI. Dashed line shows hybridizing position of the probe. Blue and Red arrow-head represents hybridization signal of PS and transformants, respectively.

Finally, *CRY1* was disrupted using dKU70 as the host strain. The DNA fragment for *CRY1* disruption was constructed in the same manner as for *KU70*. Similar to the *KU70* disruption experiment in which two transformation steps were necessary, the construction of *CRY1* disruptant involved two steps to obtain a homozygote of *CRY1* disruption. Finally, the homozygosity for *CRY1* disruption was confirmed by Southern analysis and the strain was named dCRY1 (**Figure 3.7**).). Regarding the acquisition of gene disruptions, the frequencies of obtaining a homologous recombinant was 4.5% and 85% for the *KU70*-disrupted strain and the *CRY1*-disrupted strain, respectively.

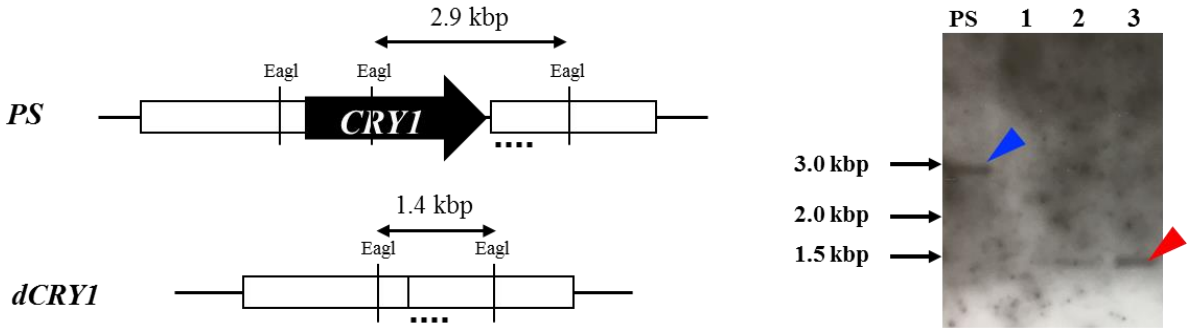

Figure 3.7. Southern analysis of *CRY1* disruption. Genomic DNA was excised by EagI. Dashed line shows hybridizing position of the probe. Blue and Red arrow-head represents hybridization signal of PS and transformants, respectively.

3.3.2. Effect of CRY1 disruption on carotenoid production

To analyze the effect of *CRY1* disruption on carotenoid production, we cultivated dCRY1 and parent strain (PS) NBRC 10032 under light and dark conditions and analyzed the carotenoid production. The dCRY1 strain had a lower growth rate than that of PS under both dark and light conditions. The carotenoid productivity of dCRY1 was higher than that of PS in the dark, but lower than that of PS in the light (**Figure 3.8**).

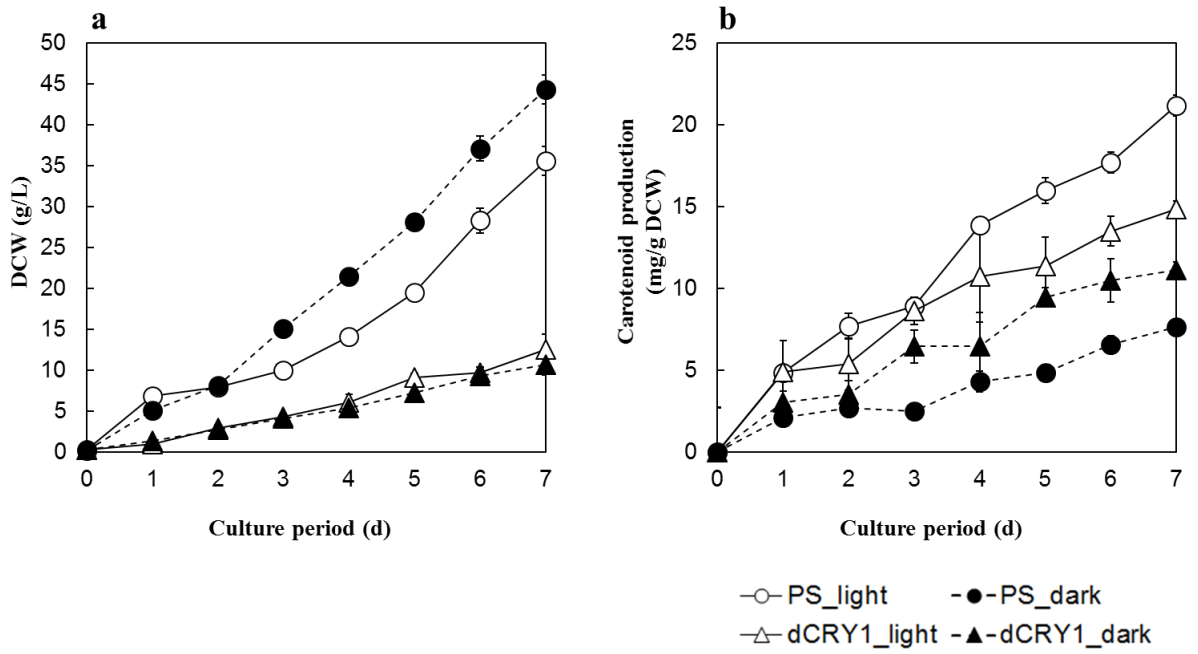

Figure 3.8. Growth rate (a) and carotenoid production (b) of *CRY1* deletion mutant dCRY1
Growth rate (a) and carotenoid production (b) were compared between the dCRY1 strain (triangles) and the PS strain (circles) under light (open) and dark (filled) conditions. Dry cell weight (DCW) was determined by g/L for the growth rate. Carotenoid production was determined by mg/g DCW depending on the β-carotene standard. Culture periods are represented in days (d). Error bars show SD derived from triplicate biological experiments.

For the gene expression analysis by qRT-PCR, genes in the carotenoid biosynthesis pathway, such as, *GGPSI* encoding geranylgeranyl diphosphate synthase, type III, *CAR2* encoding phytoene synthase/lycopene cyclase, and *CAR1* encoding phytoene desaturase responding to light were selected (**Figure 2.1**). In addition, white-collar complex (WCC) is known as the photoreceptor for blue light and plays a role in carotenoid production (Linden, Ballario and Macino 1997; C.Froehlich *et al.* 2002; Iigusa, Yoshida and Hasunuma 2005; Estrada and Avalos 2008). WCC might role in transcriptional activation in secondary metabolism (C.Froehlich *et al.* 2002; He *et al.* 2002). This protein was also reported in cooperative participation with Cryptochrome DASH into carotenoid biosynthesis in *Fusarium fujikuroi* (Castrillo and Avalos 2015) or in interdependent transcriptional relationships with Cryptochrome DASH in *Cordyceps militaris* (Zhang *et al.* 2020). Therefore, WC1 that is a white-collar in NBRC 10032 encoded by the *WC1* gene, was selected to analyze in the *CRY1*

deletion strain. Under the dark condition, reduced gene expression compared to PS was observed in *GGPSI* of dCRY1 from 0 h to 24 h experiment period (**Figure 3.9a**).

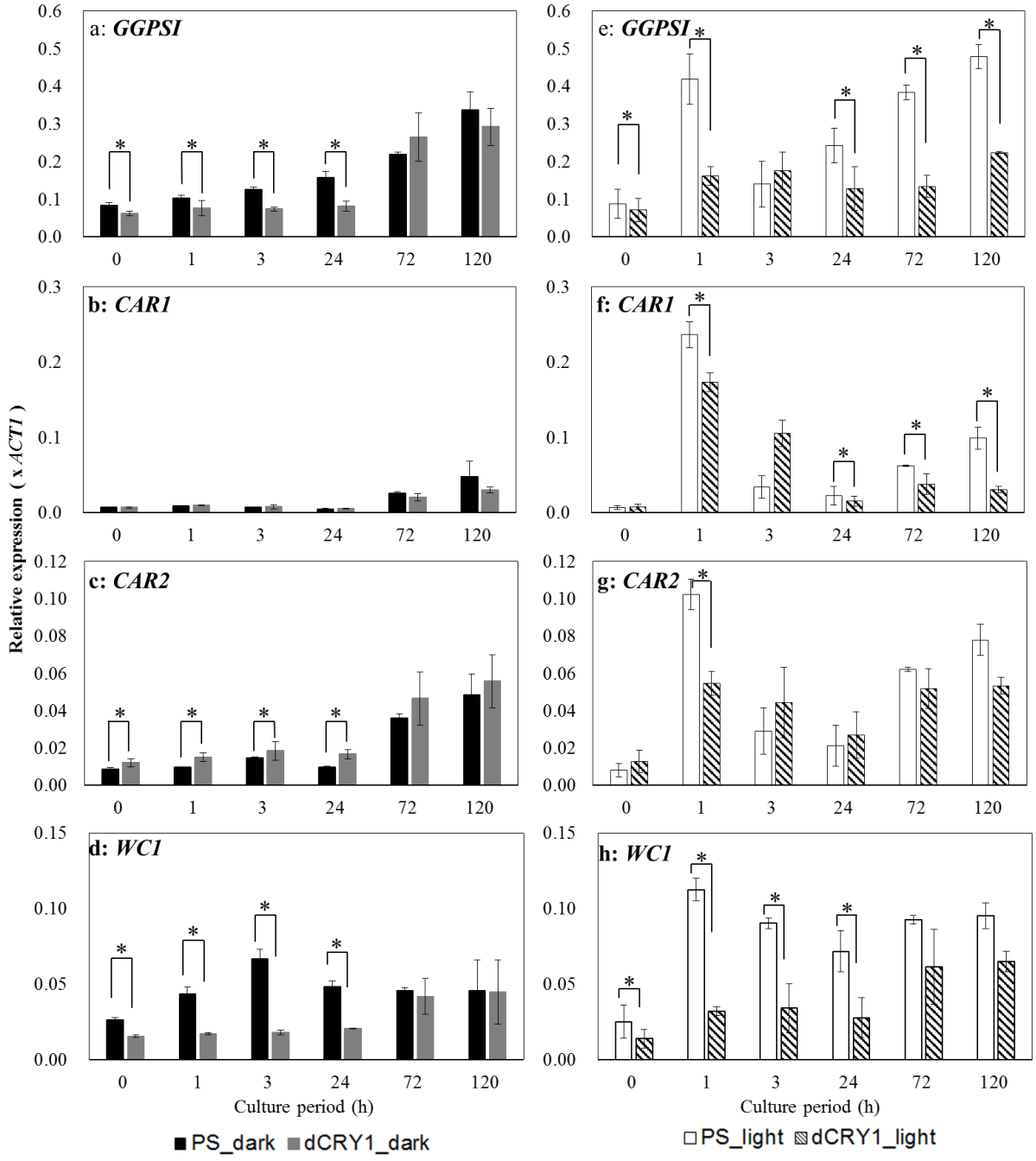

Figure 3.9. Gene expression of *GGPSI, CAR1, CAR2* and *WC1* of dCRY1

a. *GGPSI*, b. *CAR1*, c. *CAR2*, d. *WC1*. Left, gene expression of mutants under dark condition. Filled black and dark gray bars represent PS and dCRY1 respectively.

e. *GGPSI*, f. *CAR1*, g. *CAR2*, h. *WC1*. Right, gene expression of mutants under light condition. Unshaded and shaded bars represent PS and dCRY1 respectively.

Error bars show SD derived from triplicate biological experiments. Student's *t*-test was used to determine the statistically significant differences (*$P \leq .05$).

Although the significant difference was not observed in *CAR1* gene between dCRY1 and PS (**Figure 3.9b**), higher expression was detected in *CAR2* (**Figure 3.9c**). In the case of light condition, the expression of *GGPSI*, and *CAR1* genes in dCRY1 were lower than that in PS except 3 h cultivation (**Figure 3.9e**, **f**). Similarly, lower expression was also observed in the *CAR2* gene of dCRY1 at 1h light exposure than PS (**Figure 3.9g**). Also, the two-step light response was not observed in the *GGPSI* gene of the dCRY1 strain (**Figure 3.9e**). Although a two-step light response was observed in the *CAR1* and *CAR2* genes, that response was somewhat muted compared to that of PS (**Figure 3.9f, g**). *CAR1* and *CAR2* expression levels of dCRY1 increased at 1 h, but by less than that of PS, and then gradually decreased until the 24 h experiment period was concluded instead of the dramatic decrease seen in PS (**Figure 3.9h, g**). The expression of the *WC1* gene in dCRY1 was lower than that in PS under both light and dark conditions during the 24 h experiment period (**Figure 3.9d, h**). No peak of expression was observed in *WC1* by light, indicating that the light response was also disrupted in the *WC1* gene of the dCRY1 strain.

3.4. Discussion

In this study, we used two methods concurrently; gene targeting and mutagenesis to unravel carotenoid production as a response to light in *R. toruloides* NBRC 10032 strain. For gene targeting analysis, we established a gene recombination system in NBRC 10032. To avoid the NHEJ effect, we constructed a *KU70* disruptant of NBRC 10032 using a *URA3* marker recycling system based on the uracil autotroph and a 5'-FOA resistance. KU70 is one of the components of NHEJ and studies have reported *KU70* disruption leading to high-frequency homologous recombination in many fungi (Heidenreich *et al.* 2003; Choquer *et al.* 2008; Catalano *et al.* 2011; Feng *et al.* 2012; Verbeke, Beopoulos and Nicaud 2013; Huang *et al.* 2017; Dai *et al.* 2019). In the case of *R. toruloides*, high-frequency gene targeting was reported for the ATCC 10657 strain (Koh *et al.* 2014). Our results also showed high-frequency homologous recombination of the targeted gene in the homozygous *CRY1* disruptant.

Although *CRY1* disruption led to weakened carotenoid production under both light and dark conditions, light-stimulated carotenoid production was maintained. Additionally, *CRY1* deficiency affected carotenoid biosynthesis genes, which showed lower expression compared

to PS. However, the two-step activation of gene expression that is seen in *R. toruloides* NBRC 10032 was maintained. Moreover, *WC1* expression was also lower in the *CRY1* disruptant. In *Neurospora crassa*, the WCC, a protein complex formed by WC1 and WC2 proteins known as the primary photoreceptor system for blue light, promoted carotenoid biosynthesis by light irradiation (He *et al.* 2002; Iigusa, Yoshida and Hasunuma 2005; Belozerskaya *et al.* 2012). However, other reports mentioned Cryptochrome DASH (encoded by *CRY1*), which has been identified as a blue light receptor that plays the role of promoting carotenoid production (Ahmad *et al.* 1998; Facella *et al.* 2006; Froehlich *et al.* 2010; Yu *et al.* 2010; Castrillo and Avalos 2015). The WcoA, white-collar protein in *F. fujikuroi*, was also reported to play a role in carotenoid biosynthesis with light signaling acting in tandem with CryD (flavin photoreceptor, the DASH cryptochrome) (Castrillo and Avalos 2015). Thus, the lower expression level of *WC1* in the *CRY1* disruptant compared to PS under the same light or dark condition was proposed to be the result of repressed WC1 action by CRY1. Furthermore, the overall reduced expression of the carotenoid biosynthesis genes in the *CRY1* disruptant suggested that CRY1 might directly regulate *GGPSI, CAR1* and *CAR2* or might regulate carotenoid genes through the *WC1* gene. Cryptochrome was defined as a photolyase-like protein with no DNA repair activity but was known to have a blue light photoreceptor function (Chaves *et al.* 2011). In *N. crassa*, the expression of the *CryD* gene is strongly induced by light through WCC, which plays a central role in the control of circadian rhythmicity (Dunlap and Loros 2004; Chen and Loros 2009). The regulatory role of CryD also affects the synthesis of other metabolites as suggested by the differential pigmentation of Δ*CryD* strain cultivated in light (Castrillo, García-Martínez and Avalos 2013). Our data showed that CRY1 and WC1 are important for carotenoid production in NBRC 10032. However, since the light response still remained in the dCRY1 strain, the other factor(s) might control the two-step gene activation by light.

3.5. References

Ahmad M, Jarillo JA, Smirnova O *et al.* The CRY1 blue light photoreceptor of *Arabidopsis* interacts with phytochrome a in vitro. *Mol Cell* 1998;**1**:939–48.

Belozerskaya TA, Gessler NN, Isakova EP *et al. Neurospora crassa* Light Signal Transduction Is Affected by ROS. *J Signal Transduct* 2012;**2012**:1–13.

C.Froehlich A, Liu Y, J.Loros J *et al.* White Collar – 1 , a Circadian Blue Light Photoreceptor , Binding to the frequency Promoter. *Science (80-)* 2002;**297**:815–9.

Castrillo M, Avalos J. The flavoproteins CryD and VvdA cooperate with the white collar protein WcoA in the Control of photocarotenogenesis in *Fusarium fujikuroi*. *PLoS One* 2015;**10**:1–22.

Castrillo M, García-Martínez J, Avalos J. Light-dependent functions of the *Fusarium fujikuroi* CryD DASH cryptochrome in development and secondary metabolism. *Appl Environ Microbiol* 2013;**79**:2777–88.

Catalano V, Vergara M, Hauzenberger JR *et al.* Use of a non-homologous end-joining-deficient strain (delta-*ku70*) of the biocontrol fungus *Trichoderma virens* to investigate the function of the laccase gene lcc1 in sclerotia degradation. *Curr Genet* 2011;**57**:13–23.

Chaves I, Pokorny R, Byrdin M *et al.* The cryptochromes: Blue light photoreceptors in plants and animals. *Annu Rev Plant Biol* 2011;**62**:335–64.

Chen C, Loros JJ. *Neurospora* sees the light: Light signaling components in a model system. *Commun Integr Biol* 2009;**2**:448–51.

Choquer M, Robin G, Le Pêcheur P *et al. Ku70* or *Ku80* deficiencies in the fungus *Botrytis cinerea* facilitate targeting of genes that are hard to knock out in a wild-type context. *FEMS Microbiol Lett* 2008;**289**:225–32.

Dai Z, Pomraning KR, Deng S *et al.* Deletion of the *KU70* homologue facilitates gene targeting in *Lipomyces starkeyi* strain NRRL Y-11558. *Curr Genet* 2019;**65**:269–82.

Dunlap JC, Loros JJ. The *Neurospora* circadian system. *J Biol Rhythms* 2004;**19**:414–24.

Estrada AF, Avalos J. The White Collar protein WcoA of *Fusarium fujikuroi* is not essential for photocarotenogenesis, but is involved in the regulation of secondary metabolism and conidiation. *Fungal Genet Biol* 2008;**45**:705–18.

Facella P, Lopez L, Chiappetta A *et al. CRY-DASH* gene expression is under the control of the

circadian clock machinery in tomato. *FEBS Lett* 2006;**580**:4618–24.

Feng J, Li W, Hwang SF *et al.* Enhanced gene replacement frequency in *KU70* disruption strain of *Stagonospora nodorum*. *Microbiol Res* 2012;**167**:173–8.

Froehlich AC, Chen CH, Belden WJ *et al.* Genetic and molecular characterization of a cryptochrome from the filamentous fungus *Neurospora crassa*. *Eukaryot Cell* 2010;**9**:738–50.

He Q, Cheng P, Yang Y *et al.* White collar-1, a DNA binding transcription factor and a light sensor. *Sci (New York, NY)* 2002;**297**:840–3.

Heidenreich E, Novotny R, Kneidinger B *et al.* Non-homologous end joining as an important mutagenic process in cell cycle-arrested cells. *EMBO J* 2003;**22**:2274–83.

Huang Q, Cao Y, Liu Z *et al.* Efficient gene replacements in *ku70* disruption strain of *Aspergillus chevalieri* var. *intermedius*. *Biotechnol Biotechnol Equip* 2017;**31**:16–22.

Iigusa H, Yoshida Y, Hasunuma K. Oxygen and hydrogen peroxide enhance light-induced carotenoid synthesis in *Neurospora crassa*. *FEBS Lett* 2005;**579**:4012–6.

Koh CMJ, Liu Y, Moehninsi *et al.* Molecular characterization of *KU70* and *KU80* homologues and exploitation of a *KU70*-deficient mutant for improving gene deletion frequency in *Rhodosporidium toruloides*. *BMC Microbiol* 2014;**14**, DOI: 10.1186/1471-2180-14-50.

Linden H, Ballario P, Macino G. Blue light regulation in *Neurospora crassa*. *Fungal Genet Biol* 1997;**22**:141–50.

Takaku H, Miyajima A, Kazama H *et al.* A novel electroporation procedure for highly efficient transformation of *Lipomyces starkeyi*. *J Microbiol Methods* 2020;**169**, DOI: 10.1016/j.mimet.2019.105816.

Verbeke J, Beopoulos A, Nicaud JM. Efficient homologous recombination with short length flanking fragments in Ku70 deficient *Yarrowia lipolytica* strains. *Biotechnol Lett* 2013;**35**:571–6.

Yu X, Liu H, Klejnot J *et al.* The Cryptochrome Blue Light Receptors. *Arab B* 2010;**8**, DOI: 10.1199/tab.0135.

Zhang J, Wang F, Yang Y *et al.* CmVVD is involved in fruiting body development and carotenoid production and the transcriptional linkage among three blue-light receptors in edible fungus Cordyceps militaris. *Environ Microbiol* 2020;**22**:466–82.

Chapter 4: Analysis other light factors on carotenoid production through non-carotenoid producing and high carotenoid-producing mutants

4.1. Introduction

Rhodosporidium toruloides is a red yeast known for its ability to accumulate large amounts of lipids in cells and for its ability to produce carotenoids (Politino *et al.* 1997; Botes 1999; Zhu *et al.* 2012).Major advances have been made in identifying main carotenoid biosynthetic pathway genes in *R. toruloides* through biochemical and molecular approaches. However, the carotenoid biosynthesis mechanism, especially the regulatory mechanism of carotenogenic genes, is still unknown. Acetyl acid enters the carotenoid biosynthesis pathway through the MVA pathway (**Figure 2.1**); producing carotenoids final : β-carotene, γ- carotene, torulene, torulahordin as the main carotenoids (Frengova and Beshkova 2009; Kot *et al.* 2016). The light-absorbing features of colored carotenoids were due to the presence of a chromophore, consisting several conjugated double bonds generated by the activity of desaturase and cyclase enzymes. Different subsequent chemical changes, like the introduction of a cyclic end group on at least one of the ends of the molecule, and oxidative reactions, gives rise to the large diversity of known carotenoids. The improvement of an effective carotenoid producer in the red yeast, *R. toruloides* is therefore limited because of several tightly regulated genes. Carotenoid production could increase by improving the efficiency of carotenoid biosynthesis through the activity of carotenoid biosynthetic enzymes. In our previous section (Chapter 2) we observed a five-time higher carotenoid production in *R. toruloides* NBRC 10032 with exposure to light. In addition, we also deciphered a two-step response by light in which temporary gene activation occurred early in the cultivation period (1 h) and later (72 h) in the main carotenogenic genes, geranylgeranyl diphosphate synthase, phytoene desaturase, and phytoene synthase/lycopene cyclase (encoding by *GGPSI*, *CAR1* and *CAR2*, respectively) in the carotenoid biosynthesis pathway , and also in *CRY1*-photoreceptor genes. The carotenoid biosynthesis genes and light receptor genes suggested their relationship in the carotenoid production. Therefore, to deeply understand the carotenoid biosynthesis and light response mechanisms, the changed carotenoid producing mutants were created. Random mutagenesis was performed using mutagenic agents and ultraviolet (UV) light. Many studies have reported the overexpression of genes in the carotenoid biosynthesis pathway or light receptor genes to enhance carotenoid productivity. Also, a few studies have shown a deletion of the carotenoid biosynthesis pathway or no-carotenoid producing mutants. Thus, besides the high carotenoid-

producing mutants, non-carotenoid producing mutants are another way to study carotenoid biosynthesis mechanisms. Therefore, creation of non-carotenoid producing mutant was carried out. Light is known for its effect on carotenoid production via enhancing carotenoid productivity of *R. toruloides* (Chapter 1). Thus, to exclude a light effect on non-carotenoid mutants which do not produce carotenoid even if grown under light, light irradiation was applied into the screening step of the non-carotenoid producing created. Furthermore, we expect a repression of factor mutations in the high carotenoid-producing mutants, even if they grow under dark conditions. Therefore, the dark condition was applied into the screening step of the high carotenoid-producing mutants created.

4.2. Materials and methods

4.2.1. Ultraviolet (UV) irradiation mutagenesis and selection

To generate a random mutation in the genomic DNA of *R. toruloides*, cells in the exponential growth phase were mutagenized by UV light irradiation, using a UV Crosslinker CL-1000 (UVP, LLC, CA, US) under the following conditions: 254 nm, 100 V, 0.8 A, 8 W × 5 (UV discharge tube), × 100 μJ/cm. *R. toruloides* NBRC 10032 was cultivated in an L-shaped test tube with 5 mL YPD broth at 30°C. After cultivation for 24 h, cells were then collected, washed once and suspended in sterile 0.9% (w/v) NaCl solution. Next, 5 mL of 10^6 cells/mL on a 90 mm diameter petri plate (As One, Osaka, Japan) was irradiated by UV light for 30 s, which corresponded to approximately 0.1% of the survival ratio. Then, 0.2 mL × 10^3 living cells were placed on the YPD agar medium plates and incubated under light condition (for non-carotenoid producing mutant obtained) or dark condition (high carotenoid-producing mutant obtained) at 30°C for five days to check the color of the colonies.

4.2.2. Genome analysis of R. toruloides mutants

For preparing genomic DNA, yeast cells were inoculated in an L-shaped test tube containing 5 mL YPD medium and cultivated at 30°C for 24 h. Then, 1 mL of the culture solution was collected by centrifugation, after which the cells were frozen with liquid nitrogen. Cells were disrupted using a Multi-Beads Shocker (Yasui Kikai, Osaka, Japan) and suspended in an extraction buffer (50 mM Tris-HCl pH 7.5, 10 mM EDTA·2Na, 1% SDS). After adding 3 M potassium acetate, the mixture was centrifuged and the supernatant was purified through RNase treatment, phenol-chloroform treatment and ethanol precipitation. Finally, the

precipitated genomic DNA was dissolved in TE buffer (10 mM Tris-HCl (pH 8.0), 1 mM EDTA).

Genome sequences of mutants were sequenced by the Illumina MiSeq platform. Next, sequence reads of mutants, which were trimmed by trimmomatic 0.36 and mapped to the genome sequence of NBRC 10032 that was previously determined (Accession Nos. BJWK01000001 to BJWK01000039) using bwa 0.7.2. SNP call by samtools 2.8 and varscan 2.4.0. SNP annotation using snpEff 4.3q.

4.2.3. Biochemical analysis

The DCW was quantified in lyophilized cells derived from 1 mL of the broth. Carotenoids were extracted from dry cells in 100% acetone using a Multi-Beads Shocker (Yasui Kikai, Osaka, Japan), as previously described (Chapter 2, section 2.2.2). Carotenoid production was calculated as the equivalent of β-carotene (Wako Pure Chemical Industries Ltd., Osaka, Japan) with an absorbance at 488 nm, using Infinite M200 Pro (Tecan, Kanagawa, Japan).

4.2.4. Quantitative reverse transcription polymerase chain reaction (qRT-PCR)

Total RNA extraction was performed by hot phenol method and purification of total RNA was carried out using Illustra RNAspin (GE HealthCare Life Science, Tokyo, Japan) following the manufacturer's instructions. Quantitative real-time PCR was performed using Light Cycler 480 SYBR Green I Master Mix (Roche Applied Science, Bavaria, Germany) as described in the section 2.2.3. The relative expression level was calculated as the ΔCt power of 2, in which a ΔCt value was obtained by subtracting the Ct value of the housekeeping gene (*ACT1*, the gene encoding actin) from that of the target gene. The PCR primers used for the expression analysis are listed in **Table 2.1**.

4.3. Results

4.3.1. Isolated non-carotenoid producing mutants

In parallel with the *CRY1* disruption, we carried out mutation analysis to identify the other light-response factors. When *R. toruloides* NBRC 10032 was cultivated in continuous darkness, carotenoid production was much lower than that under continuous light irradiation. Also, by analyzing non-carotenoid producing mutants in the light, it was expected that the light

responsive factor(s) would be mutated. The non-carotenoid producing mutants (expectation) or low carotenoid producing mutants meant they could not produce the carotenoids in their cells or they produced a little carotenoid, which was depicted by plain color or white color in the colonies on the plates. And no affected by light was expected to these mutants. Thus, after UV irradiation, cells were incubated under white light fluorescence lamp to ensure low carotenoid contents even though under light exposure. After 5 d of light incubation, colonies appeared on plates, which showed a different color (**Figure 4.1a**). The colonies showed lighter color or white color comparing to the color showed by PS NBRC 10032, which suggests low or no carotenoid accumulating mutants. S1 mutant displayed specially the white colorations on the colony (**Figure 4.1b**), which significantly showed low carotenoid production (**Figure 4.2**). A clear coloration of the carotenoid product (**Figure 4.3**) was also observed. Therefore, it was suggested that S1 was the no carotenoid producing mutant. Thus, the S1 mutant was sub-cultured 5-6 times to stability.

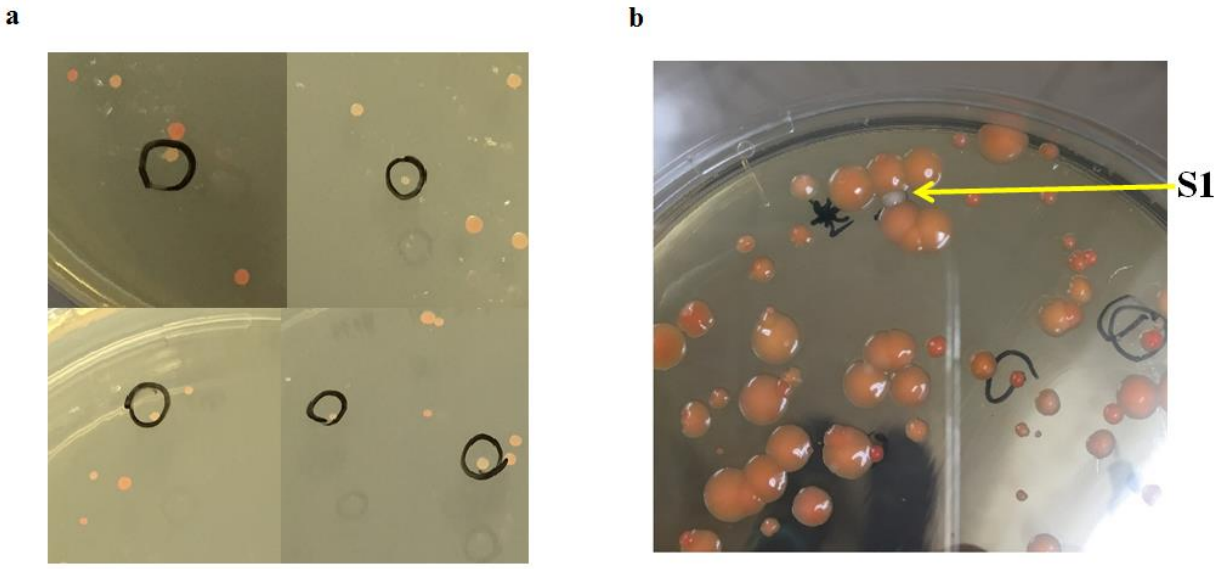

Figure 4.1. a. Colonies on the plates after 5 of incubation. b. The S1 colony under observation (white colony).

4.3.2. Growth rate and carotenoid production

Carotenoid production of the S1 mutant was extremely low (approaching 0.3 to 0.4) that was approximate rate of 30-fold drop than that of PS, which insignificantly changed its cultivation time. It was recorded that the carotenoid production of PS in the light stage is higher than that in the dark condition (Chapter 2 and **Figure 4.2**). However, carotenoid production of

S1 mutant at early cultivation (day 1 to day 5) was similar in the dark condition to the light condition and an only a little higher in the light condition at day-6 and day-7 of cultivation. Furthermore, the cell weight of the S1 mutant was higher than that of PS in both light and dark conditions, which shows similar patterns with PS during higher growth rates in the dark condition than in the light induction.

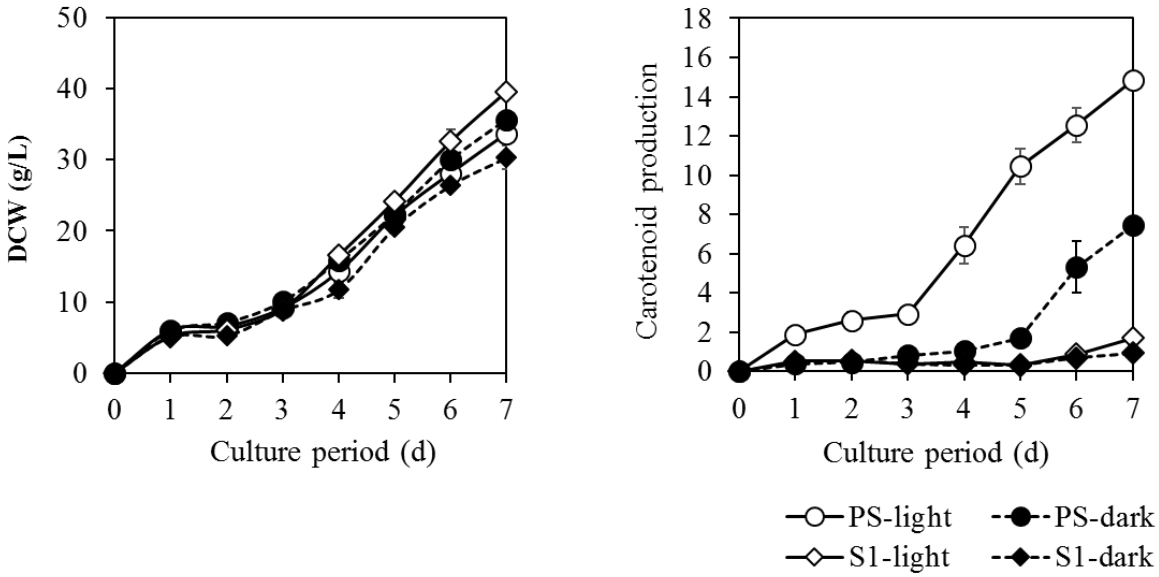

Figure 4.2. Growth rate and carotenoid production of the S1 mutant

Besides, a clear color was observed in the carotenoid product of the S1 mutant, instead of the orange-red color in the PS (**Figure 4.3**). Also, no carotenoid was suggested in the sample of the S1 mutant.

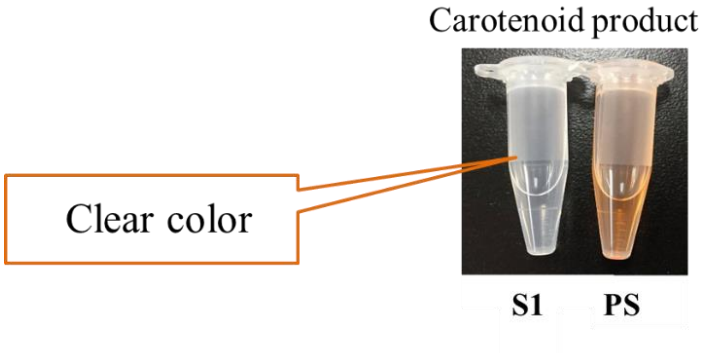

Figure 4.3. Color of the carotenoid product in the S1 mutant (left) and PS (right).

4.3.3. The expression of carotenoid genes

White mutant S1 was isolated from light to observe if light would affect the S1 mutant or not. The S1 mutant was also studied under dark and light conditions for more information on light affects. Furthermore, the experiment was conducted in the dark condition for 24 h, after which the cell number increased. The setup was then transferred into light illumination for the light condition or continued in the dark cultivation phase for the dark condition. Results are showed in **Figure 4.4**. Compared with the PS, levels of transcription of the *CAR1* and *CAR2* genes showed a similar pattern to that of PS that was specially increased at 1 h after light irradiation, then decreased after 3 h light induction. Finally, the transcription gene was changed again after 72 h. Results showed that the light effect on the white mutant was the same way as that of PS.

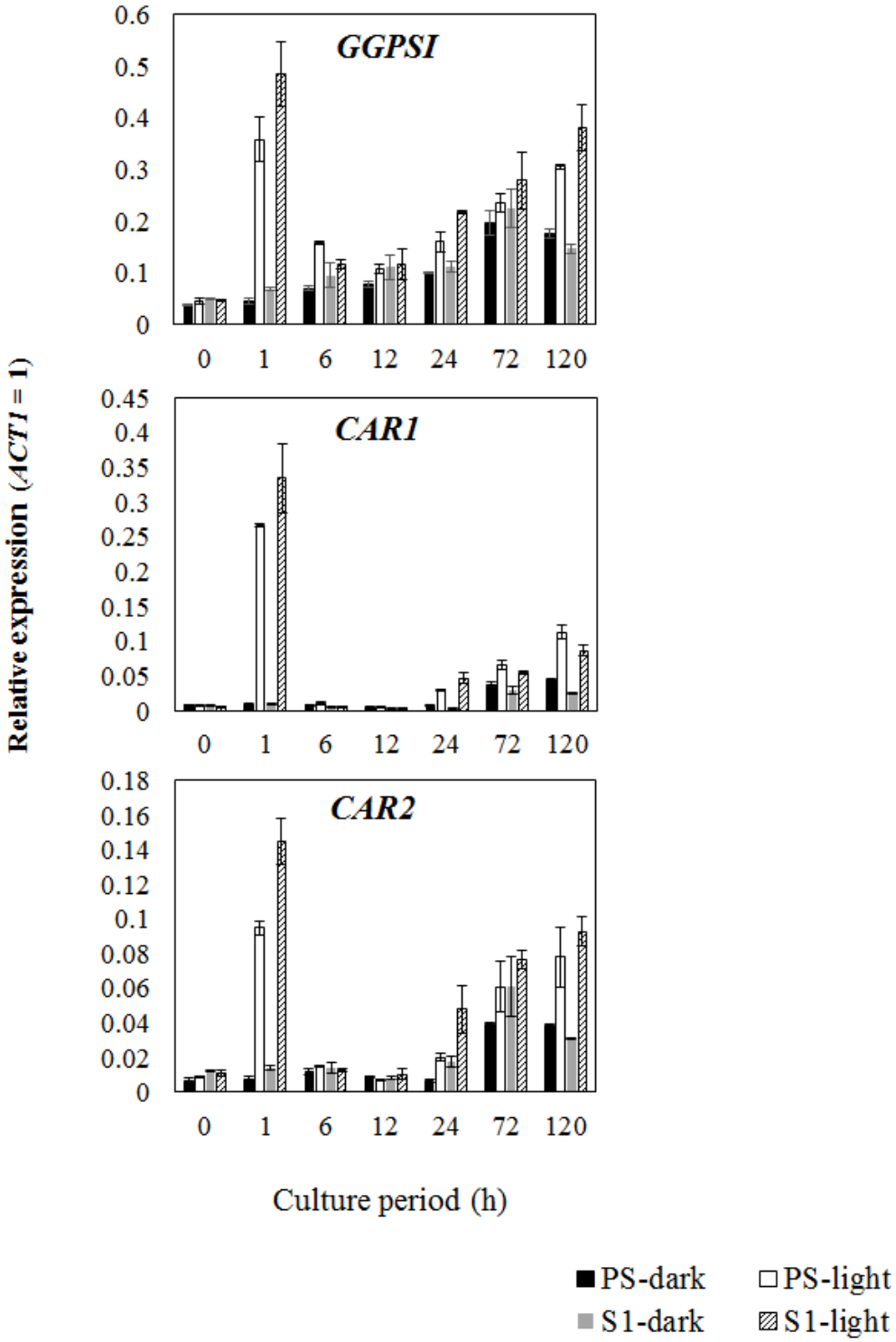

Figure 4.4. Gene expression of *GGPSI*, *CAR1* and *CAR2* of the S1 mutant

Filled black and dark gray bars represent PS and S1 under dark condition respectively. Unshaded and shaded bars represent PS and S1 under light condition respectively. Error bars show SD derived from triplicate biological experiments.

4.3.4. Comparative genomic analysis

To screen genetic mutations contributing to the phenotypes of S1 mutants, genome sequences of these mutants were sequenced using the MiSeq platform. Sequence reads of the mutants were then mapped to the genome sequence of NBRC 10032 that was determined previously (Accession No. BJWK01000001 to BJWK01000039). Some missense mutations were recognized, while others had duplication or deletion of some base pairs.

Alternatively, in the genome sequence of the white mutant S1, two mutations were detected in the carotenogenic genes: *CAR2* and *CAR1*. For the *CAR2* gene, the missense mutation occurred at the 245^{th} thymine position to cytosine, which resulted in a substitution of the 82^{th} phenylalanine position for serine. In the case of *CAR1*, deletion of the 1015^{th} cytosine occurred, thus resulting in a frame shift from the 339^{th} leucine position. As a result, a stop codon was generated at the 1630^{th} position. Therefore, we hypothesized that *CAR1* and *CAR2* encodes phytoene desaturase and phytoene synthase/lycopene cyclase, respectively, explained the non-carotenoid in this strain.

4.3.5. Isolated high carotenoid-producing mutants

To obtain high carotenoid-producing mutants in the dark condition, UV mutagenesis was carried out. After UV irradiation, about 3×10^4 isolated colonies were growing in the dark, some c of which showed intense colors compared to NBRC 10032, which showed a faint orange-red color. Mutant colonies showed a darker red color, suggesting that in the dark condition, were high carotenoid-accumulating mutants. After the first visual screening, the darker color colonies were sub-cultured on new plates. The 30 darkest red colonies were picked, after which carotenoid production was analyzed. Two mutants; R5 and R36, were chosen as the highest carotenoid-producing mutants, since the two mutants showed higher and faster carotenoid production than PS or other mutant strains (**Figure 4.5**) under the dark condition. The color of the mutant colonies is showed in the **Figure 4.6a**. Microscopic analysis did not show significant morphological differences between PS and the mutants (**Figure 4.6b)**. Mutant strains were sub-cultured several times to confirm their stability before investigating the growth rate, carotenoid productivity and gene expression.

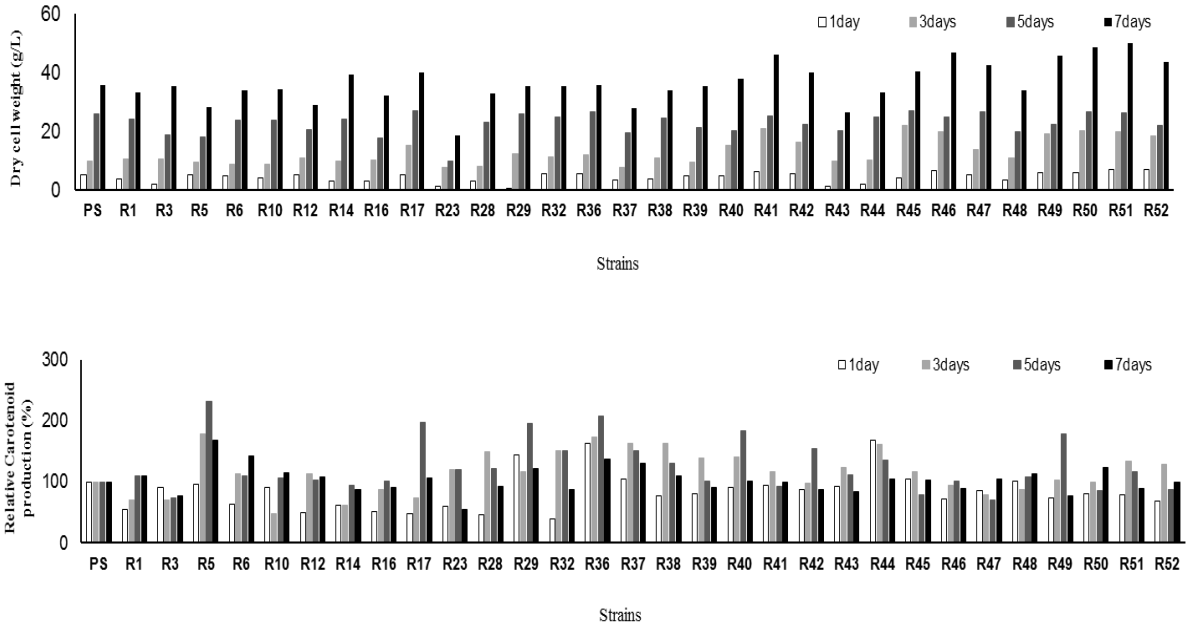

Figure 4.5. Screening high carotenoid-producing mutants in LS 10 broth medium. Carotenoid production of 30 best high carotenoid-producing mutants relative to that of PS. Unshaded, light gray, dark gray, and black bars represent 1, 3, 5, and 7 days of cultivation.

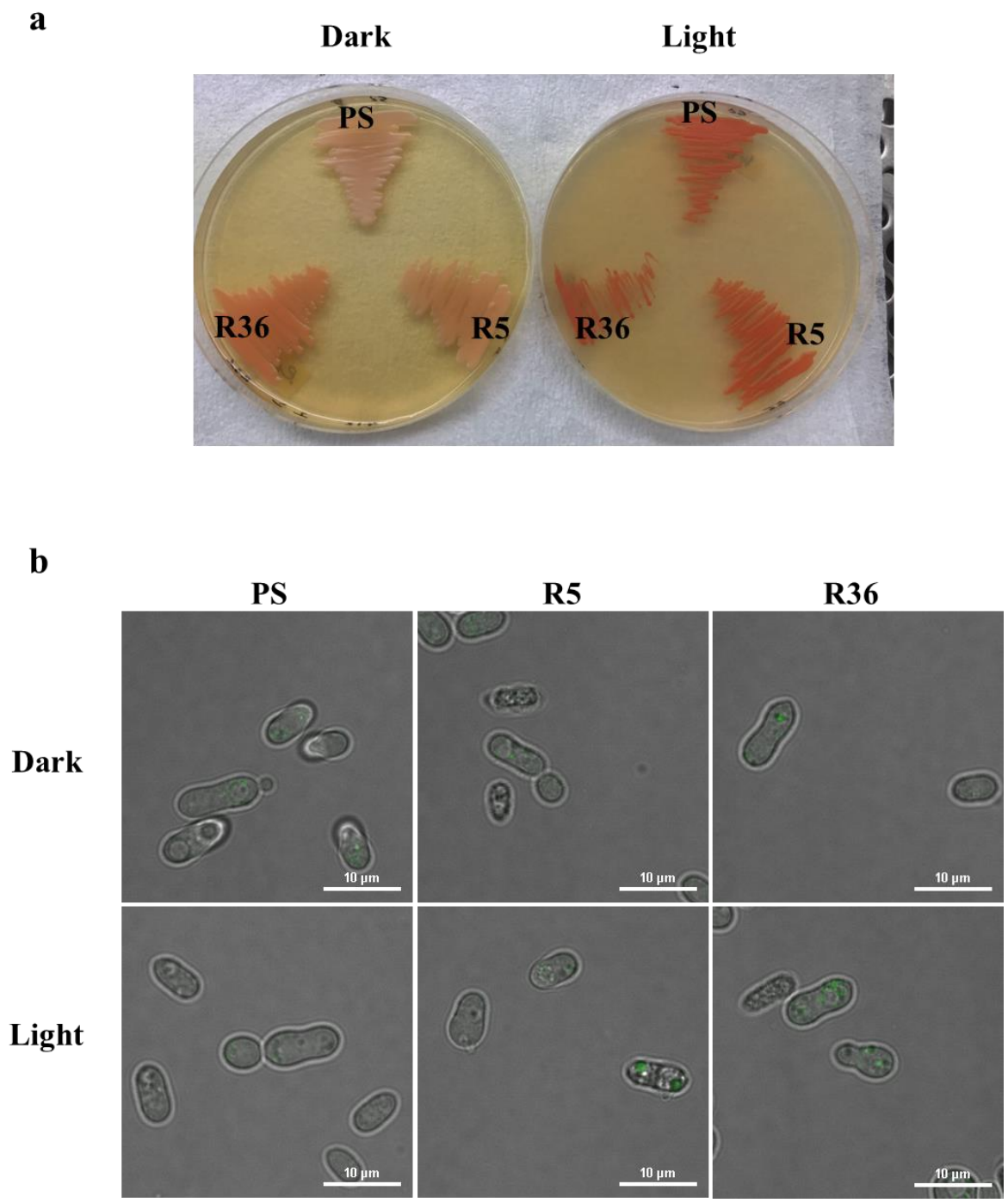

Figure 4.6. Morphology of PS (NBRC 10032) and high carotenoid-producing mutants R5, R36**.** a. Color of high carotenoid-producing mutants grown on the plate under dark (left) and light (right) conditions after 3 d of cultivation. b. Morphology image of PS and mutants under confocal microscopy 100 × (cells at 3 d cultivation). Green showed the lipid droplets in the cells after Nile Red staining.

4.3.6. Growth rate and carotenoid production of high carotenoid-producing mutants

Growth phenotypes of mutants were compared by culturing them under both dark and light conditions. The cell growth of R5 and R36 was lower than that of PS in both conditions. However, R5 and R36 showed higher carotenoid production than PS (**Figure 4.7**). Furthermore, under the dark condition, carotenoid production of R5 and R36, which was approximately twice as much and six times as much, respectively, as that of PS at one-day incubation. Thereafter, carotenoid production of R36 remained higher but was negligibly increased, with its highest production level at day six of incubation, and approximately 20 mg/ g DCW. In contrast, the R5 mutant increased its carotenoid productivity faster than PS and attained its highest carotenoid production after seven days of cultivation, with 20.3 mg/ g DCW, which was over twice as much as PS.

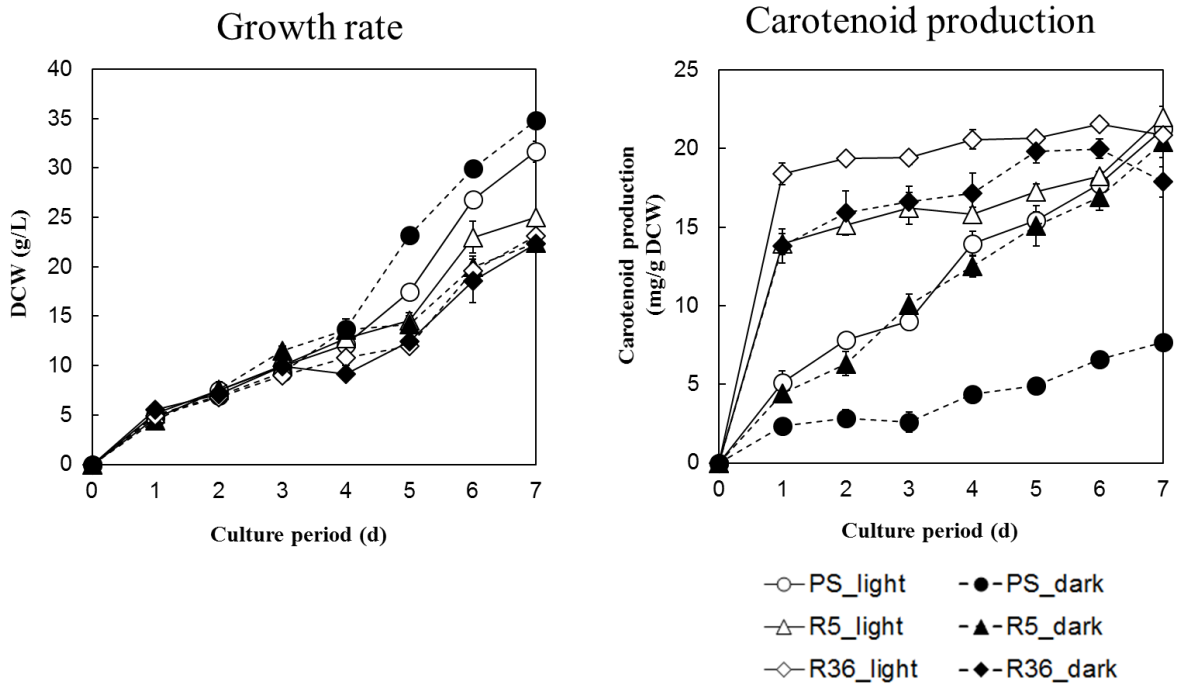

Figure 4.7. Growth rate (a) and carotenoid production (b) of high carotenoid-producing mutants. Growth rate (a) and carotenoid production (b) were compared between PS (circles) R5 (triangles) and R36 (diamonds) under light (open) and dark (filled) conditions. DCW was determined by g/L for the growth rate and carotenoid production was determined by mg/g DCW depending on the β-carotene standard. Culture periods are represented in days (d). Error bars show SD derived from triplicate biological experiments

Moreover, the higher carotenoid-producing phenotype of R5 and R36 was also detected in the light condition. However, both R5 and R36 produced high levels of carotenoids during the early culture period (after just one day of cultivation) (**Figure 4.7**). The R36 mutant attained a high carotenoid production, which was near the maximum carotenoid capacity yield, at just one day after cultivation in both dark and light conditions. The same result was found for the carotenoid productivity of R5 with only light cultivation. Altogether, carotenoid production of both mutants was enhanced not only in the dark but also in the light condition.

4.3.7. The gene expression in high carotenoid-producing mutants

As the carotenoid production of R5 and R36 was higher than that of PS, we analyzed the expression of genes encoding the carotenoid biosynthesis pathway in these two mutants. From the carotenoid biosynthesis pathway (**Figure 2.1)**, *GGPSI*, *CAR2* and *CAR1* were selected. *WC1* encoding white-collar and *CRY1* encoding Cryptochrome DASH, the putative photoreceptor, were also selected. Then, mutants and PS were pre-cultured for 24 h in the dark, after which the growing cells were transferred to a new medium and cultivated under continuous light or dark conditions. Results showed that light enhanced the gene expression of *GGPSI*, *CAR1* and *CAR2* of PS. Two-step activation was also detected, which dramatically increased the expression level at one hour, then, the second activation after 72 h as observed in PS (**Figure 4.8**).

In the R5 mutant, expression level of the *GGPSI*, *CAR1* and *CAR2* genes was higher than that in PS in the dark conditions in the first 24 h experiment period (**Figure 4.8a-c**). The expression level of *GGPSI*, *CAR1* and *CAR2* genes (especially *CAR1* and *CAR2*) dramatically increased at 1 h of light exposure (**Figure 4.8f-h**). Furthermore, the expression of the *CRY1* gene of R5 was substantially increased at 1 h of light exposure, surpassing that of PS at the same light exposure time that was two-fold higher in expression than PS (**Figure 4.8i**). Additionally, *CRY1* expression level at 1 h by light exposure was 15-fold compared to 0 h in R5, whereas, it was 5-fold in PS (**Figure 4.8i**). For *WC1* expression, significant differences were not observed between R5 and PS in the dark (**Figure 4.8e**). Gene activation by light at 1 h of cultivation was also observed in *WC1* expression in R5 (**Figure 4.8j**). However, the increase was not as remarkable as those of *CAR1*, *CAR2*, or *CRY1* genes in the light. Gene activation at a later cultivation time was also detected in these genes.

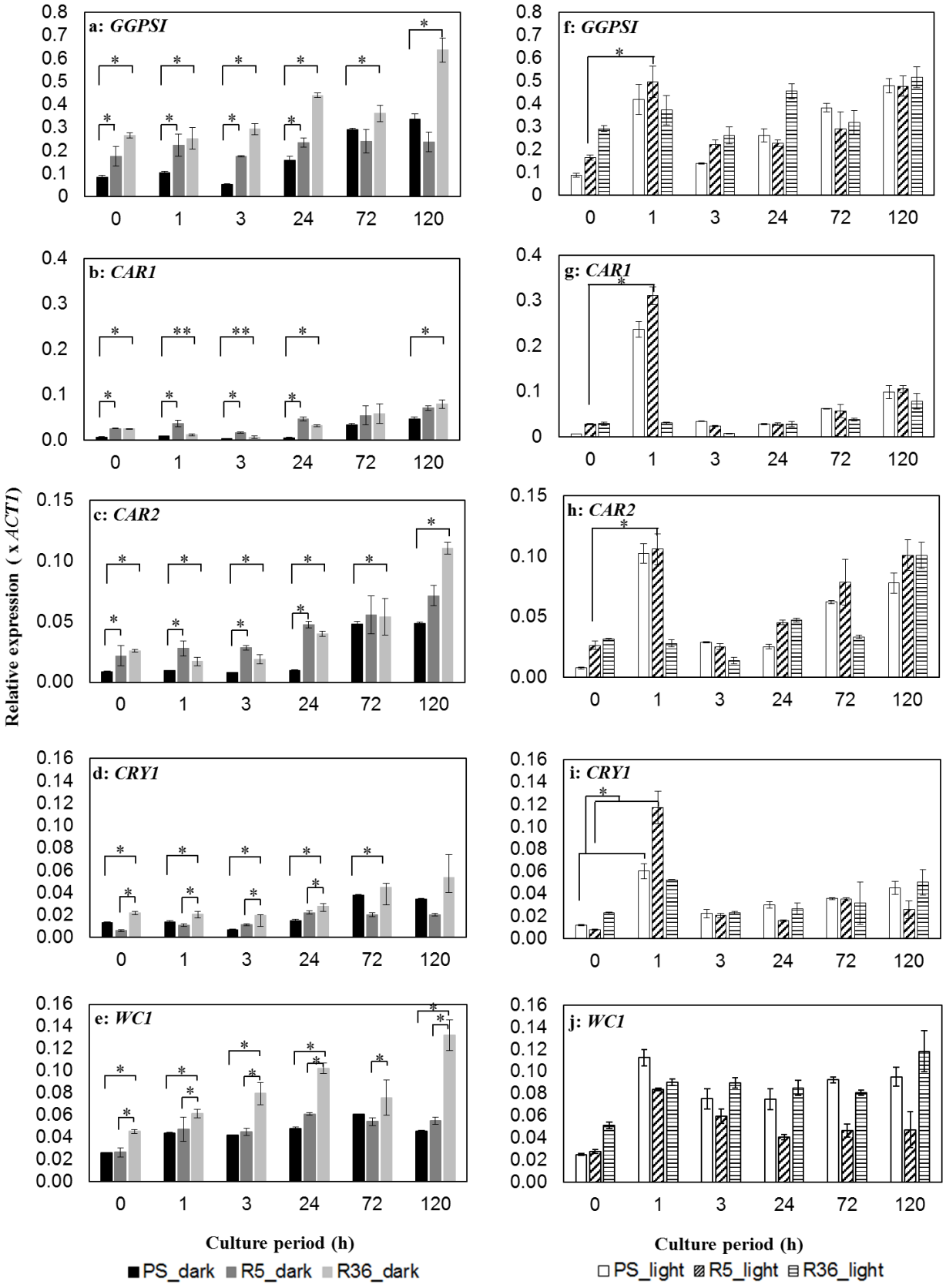

Figure 4.8. Effect of light irradiation on gene expression

a. *GGPSI*, b. *CAR1*, c. *CAR2*, d. *CRY1*, e. *WC1*. Left, gene expression of mutants under dark condition. Black, dark gray and light gray bars represent PS, R5 and R36, respectively.
f. *GGPSI*, g. *CAR1*, h. *CAR2*, i. *CRY1*, j. *WC1*. Right, gene expression of mutants under light condition. Unshaded, diagonally shaded and horizontally shaded bars represent PS, R5 and R36, respectively. Culture periods are represented in hours (h). Error bars show SD derived from triplicate biological experiments. Student's *t*-test was used to determine the statistically significant differences (*$P \leq .05$, ** $P \leq .1$).

In the case of the R36 mutant, increased expression compared to PS of all tested genes was evident in the dark condition (**Figure 4.8a-e**). However, in the light condition, the two-step light response remained in the *GGPSI* gene, which was absent in *CAR1* and *CAR2* genes (**Figure 4.8f-h**). For *CRY1*, gene expression of R36 was higher than that of PS in the dark (**Figure 4.8d**) but was almost at the same level as that of PS in the light (**Figure 4.8i**). Alternatively, *WC1* expression in the dark was higher than that of R5 and PS in the dark condition (**Figure 4.8e**). Additionally, the expression of *WC1* increased by light exposure (data at 1 h light exposure), and it was maintained until 120 h (**Figure 4.8j**).

4.3.8. Comparative genomic analysis

To screen genetic mutations contributing to the phenotypes of R5 and R36 mutants, genome sequences of these mutants were sequenced using the MiSeq platform. Sequence reads of mutants were mapped to the genome sequence of NBRC 10032 that was determined previously (Accession No. BJWK01000001 to BJWK01000039). Genomic analysis showed 118 and 34 SNPs for R5 and R36, respectively, in the coding region (**Table 4.1a-c**). Surprisingly, almost every mutated point observed was heterozygous, in which about half of the reads covering a mutation point supported the references, while the remaining reads supported mutations. Therefore, we suspected if the genome of the parental strain was contaminated, however, further analysis using Sanger sequencing confirmed mutant heterogeneity (data not shown). Along with the results of gene targeting experiments, these results also suggested that NBRC 10032 is a homozygous diploid, as the R36 mutant only had two mutated genes, with all reads supporting a mutation. One of the two genes was *FAS1* encoding a fatty acid synthase. Whereas, for r the R5 mutant, there was no mutation point in which all reads supported a mutation.

Table 4.1a. SNPs in the coding region and the resultant amino acid substitutions in high carotenoid-producing mutants. a. in strain R5 (heterozygous mutation)

gene ID[a]	product	position	NA mutation	AA mutation[b]
c09g3873	Bud emergence protein 1	895	C>T	Q299*
c14g5294	urease	740	T>G	L247*
c20g6340	cytoplasmic tRNA 2-thiolation protein 1	1081, 1082	T>A, A>T	*361K, *361L
c21g6526	MFS phosphate transporter	251	G>A	W84*
c01g0025	arginine-tRNA-protein transferase	125	A>C	K42T
c01g0093	zinc-binding oxidoreductase ToxD	875	C>T	S292L
c01g0128	major Facilitator Superfamily protein	1093, 1094	G>A, G>A	G365R, G365E
c01g0209	carbamoyl-phosphate synthase large subunit	686	T>C	F229S
c01g0249	major facilitator superfamily protein	1444	A>G	M482V
c01g0294	exocyst complex component sec5	1156	C>T	R386W
c01g0299	mitochondrial inner membrane protease subunit 2	526, 527	C>T, C>T	P176S, P176L
c01g0405	cAMP-dependent protein kinase catalytic subunit	6	G>T	M2I
c01g0420	DNA methyltransferase 1-associated protein 1	980	A>T	Y327F
c01g0548	TPR Domain containing protein	352	T>C	S118P
c02g0656	similar to RHTO_00054	226	A>G	N76D
c02g0684	capsular associated protein	126	T>A	D42E
c02g0731	armadillo-type fold domain containing protein	2939	G>A	G980E
c02g0962	CCR4-NOT transcriptional complex subunit CAF120	697	C>T	R233C
c02g1004	zinc finger, C2H2-type domain containing protein	1756	C>T	L586F
c02g1148	MFS transporter	1835	C>T	T612I
c02g1163	G1/S-specific cyclin Pcl5	158	C>T	S53L
c03g1356	-	327	T>A	D109E
c03g1378	WD repeat protein	536	C>T	S179L
c03g1446	C6 transcription factor	520	A>G	K174E
c03g1475	proteophosphoglycan ppg4	994	T>A	Y332N
c03g1505	histone H2B	392	C>T	S131L
c03g1531	glycoside hydrolase family 15 protein	754	C>T	H252Y
c03g1569	exosome complex exonuclease RRP6	755	C>T	S252F
c03g1581	serine-type endopeptidase	211	T>C	F71L
c03g1667	dnaJ family protein	95	T>C	L32S
c04g1797	ATP synthase oligomycin sensitivity conferral	284	C>T	P95L
c04g1818	late endosometo vacuole transport-related protein	2416	G>C	E806Q
c04g1853	GTP binding protein	727	A>G	N243D
c04g1866	argonaute	717	C>G	F239L
c04g1871	serine/threonine protein kinase ATG1	1946	C>T	S649L
c04g1876	-	182	A>G	Q61R
c04g1942	phenylalanyl-tRNA synthetase beta chain	2528	T>C	V843A
c04g1953	cell cycle regulatory protein	1453	C>T	R485C
c04g2004	ABC fatty acid transporter	290	G>A	G97E
c04g2014	proteophosphoglycan ppg4	256	A>G	N86D
c04g2018	arrestin/PY protein 1	703	T>C	S235P
c04g2072	SNF2 family helicase	566	C>T	S189L
c04g2076	serine/threonine protein phosphatase	911	T>C	F304S
c05g2183	sensor histidine kinase/response regulator	2911	C>G	H971D
c05g2186	ATP-dependent rnahelicase dbp7	2557	C>T	L853F
c05g2364	cytochrome oxidase complex assembly protein	322	T>C	F108L
c05g2425	arsenite-resistance protein 2	1706	A>C	K569T
c06g2663	STE/STE20/FRAY protein kinase	199	C>G	L67V
c06g2711	proteophosphoglycan ppg1	58	C>A	P20T
c06g2770	ferric-chelate reductase	145	A>G	I49V
c06g2802	ABC transporter	1718	A>G	E573G
c06g2904	proteophosphoglycan ppg1	907	A>C	I303L
c06g2940	sulfate transporter	473	T>A	I158K
c07g3016	raffinose synthase protein Sip1, glycoside hydrolase family 36 protein	1441	C>T	L481F
c07g3027	beta-catenin-like protein 1	587	A>G	E196G
c07g3106	proteophosphoglycan ppg4	241	G>A	G81S
c07g3118	proteophosphoglycan 5	1207	T>G	Y403D
c07g3123	DNA/RNA helicase, DEAD/DEAH boxtype	2237	A>C	N746T
c07g3134	MFS transporter	2380	C>T	L794F
c07g3344	-	38, 44	C>T, C>T	S13L, A15V
c08g3473	asparagine synthase	1132	C>T	H378Y
c08g3496	BRCT domain containing protein	785	C>T	S262F
c08g3522	6-phosphofructo-2-kinase / fructose-2,6-bisphosphatase	527	C>T	S176F
c08g3584	pre-mRNA branch site protein p14	338	C>T	P113L
c08g3630	transcription regulator HTH	3229	T>C	S1077P
c08g3714	inositolor phosphatidylinositol phosphatase	1427	G>A	R476Q
c09g3755	bZIP transcription factor	20	T>C	F7S
c09g3825	E3 ubiquitin-protein ligase synoviolin	224	T>A	I75N
c09g3974	ATP-dependent rnahelicase sub2	382	C>T	P128S

gene_ID[a]	product	position	NA_mutation	AA_mutation[b]
c10g4119	inositol hexakisphosphate kinase 1	1324	C>A	Q442K
c10g4175	aurora kinase	983	G>A	S328N
c10g4179	gamma-glutamyltranspeptidase	155	C>T	P52L
c10g4191	cysteinyl-trna synthetase	1156	G>A	E386K
c10g4372	HSP20-like chaperone domain protein	724	G>A	D242N
c11g4395	agmatinase	817	A>T	T273S
c11g4427	copper transporter	599	T>C	F200S
c11g4538	other/IRE protein kinase	2533	C>T	L845F
c11g4557	-	706	C>T	P236S
c11g4570	similar to RTG_02374	1079	G>A	S360N
c11g4602	bleomycin hydrolase	952	T>G	Y318D
c12g4736	transcription regulator	1289	G>A	S430N
c12g4807	RNase P subunit p30 family protein	283	C>G	P95A
c12g4852	similar to RHTO_01449	1055	C>T	S352L
c13g4960	V-type H+-transporting ATPase 54 kD subunit	775	C>T	R259C
c13g5110	similar to RTG_03196	505	G>A	E169K
c14g5333	endosomal peripheral membrane protein	2900	A>C	K967T
c15g5465	PAB-dependent poly(A)-specific ribonuclease subunit 3	1852	G>A	D618N
c16g5707	adrenodoxin-type ferredoxin	239	G>A	C80Y
c16g5733	transcription factor, FAR1-related domain-containing protein	203	C>T	S68L
c16g5742	-	142	G>A	D48N
c17g5869	tho2 protein	4528	G>A	D1510N
c17g5882	pyruvate dehydrogenase E1 component subunit alpha	38	C>T	P13L
c17g5886	MFS monocarboxylate transporter	1030	T>C	Y344H
c18g5964	proteophosphoglycan ppg4	2285	A>T	K762M
c18g6013	TRAF-like zinc finger	1007	C>T	P336L
c19g6143	eukaryotic translation initiation factor 3 subunit CLU1/TIF31	2342	A>T	Y781F
c19g6181	ralA-binding protein 1	308	T>C	I103T
c19g6234	G-patch and DUF1604 domain containing protein	436	T>A	Y146N
c19g6247	neutral amino acid permease	925	G>T	V309F
c20g6276	clathrin-coated vesicle protein	3847	A>G	K1283E
c20g6327	oxoglutarate/iron-dependent oxygenase	775	G>A	G259S
c20g6362	ribonuclease H-like protein	512	C>T	S171F
c20g6385	bifunctional dihydroflavonol 4-reductase/flavanone 4-reductase	899	C>A	P300Q
c20g6417	GATA-binding transcription factor	2870	A>G	Q957R
c22g6551	DNA/RNA helicase, DEAD/DEAH boxtype	2809	A>G	I937V
c22g6568	mitochondrial tricarboxylate transporter, citrate transporter	218	G>A	G73E
c22g6597	proteophosphoglycan 5	3314	T>C	L1105P
c23g6652	GTPase activatingrab protein	1567, 3046	T>C, A>T	S523P, T1016S
c23g6663	DNA polymerase lambda	731	T>C	L244S
c23g6670	gag-Pol polyprotein	1295	A>C	Y432S
c31g6880	vacuolar protein 8	263	T>C	L88P

[a]gene_ID corresponds to the locus tag of NBRC 10032 genome sequence (Accession No. BJWK01000001 to BJWK01000039). [b] Asterisk represents a stop codon

Table 4.1b, c. SNPs in the coding region and the resultant amino acid substitutions in high carotenoid producing mutants R36

b. in strain R36 (homozygous mutation)

gene_ID[a]	product	position	NA_mutation	AA_mutation
c06g2877	fatty acid synthase subunit alpha, fungi type	3536	C>T	S1179L
c06g2946	-	7047	G>C	E2349D

c. in strain R36 (heterozygous mutation)

gene_ID[a]	product	position	NA_mutation	AA_mutation[b]
c03g1620	tubulin-specific chaperone E	1549	G>T	G517*
c05g2309	uracil phosphoribosyltransferase	682	T>C	*228Q
c20g6282	DNA repairand recombination protein RAD54B	280	C>T	Q94*
c01g0374	heat shock 70kDa protein 1/8	638	C>T	S213L
c02g0724	chitin synthase, glycosyltransferase family 2 protein	266	C>T	S89L
c02g0990	peroxisomal biogenesis factor 19	43	G>A	D15N
c02g1121	blue (type 1) copper domain containing protein	635	C>T	S212L
c03g1552	-	8	C>T	S3L
c04g1774	E3 ubiquitin-protein ligase BRE1	634	T>C	S212P
c04g1821	methylthioribose-1-phosphate isomerase	1264	A>G	R422G
c05g2338	-	791	T>C	V264A
c05g2544	single-stranded DNA binding protein	623	C>T	S208L
c08g3577	ATP dependent helicase	1156	A>G	K386E
c09g3784	chromatin structure-remodeling complex subunit SFH1	806	T>C	F269S
c09g3977	midasin	12640	G>A	G4214S
c09g4034	craniofacial development protein 1	281	C>T	P94L
c11g4470	kinetochore protein spc25	877	G>T	G293W
c11g4620	-	208	T>A	Y70N
c12g4709	similar to RHTO_04096	419	G>A	S140N
c12g4775	similar to RHTO0S01e03224g1_1	2017	G>A	D673N
c14g5202	zinc finger, C2H2-type transcription factor	1559	C>T	S520L
c17g5816	proteophosphoglycan ppg4	2552	C>T	S851L
c17g5826	alcohol dehydrogenase	838	G>A	G280R
c17g5865	GATA transcription factor	1457	C>T	P486L
c18g6003	proteophosphoglycan ppg4	321	C>G	D107E
c18g6112	TBC domain protein, Rab GTPase activator	4154	C>T	S1385L
c19g6210	inorganic anion exchanger	1826	T>C	F609S
c20g6407	5-methyltetrahydropteroyltriglutamate-homocysteine S-methyltransferase	289	A>G	M97V
c21g6492	transcription factor	808	C>G	Q270E
c21g6498	multi-sensor hybrid histidine kinase	5050	C>A	Q1684K
c23g6679	-	1546	T>C	Y516H
c24g6727	copia-type polyprotein	550	T>G	Y184D

[a]gene_ID corresponds to the locus tag of NBRC 10032 genome sequence (Accession No. BJWK01000001 to BJWK01000039). [b] Asterisk represents a stop codon

NBRC 10032 was registered as mating type A at NITE, and it is expected to be a haploid strain. However, when an experiment to induce the formation of spores (basidiomycete spores) in the spore formation-inducing medium (ME medium: 2.0% Malt extract, 2.0% Agar) was performed, the formation of resting spores was not confirmed, and only the formation of pseudohyphae under nutrient starvation conditions was observed (**Figure 4.9**).

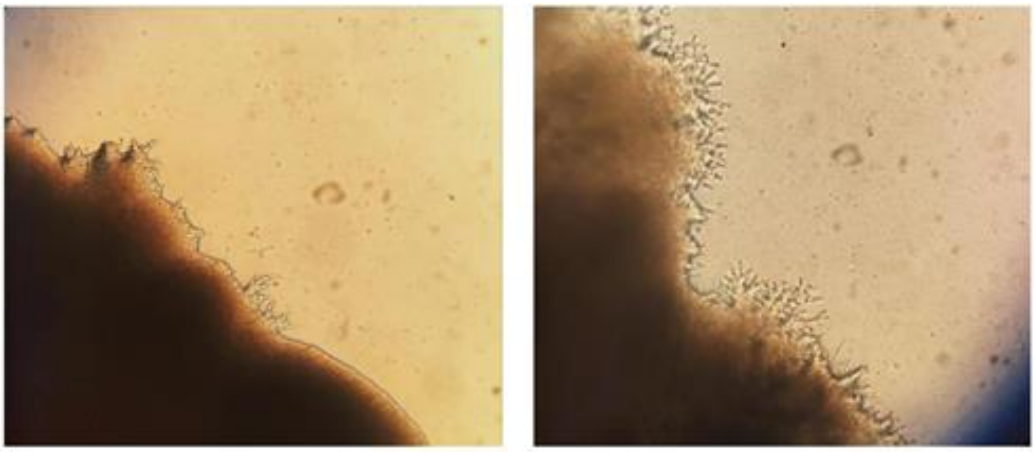

Figure 4.9. The colonies on the YPD agar medium were squeezed with a toothpick and transplanted to the YPD medium (left) and the ME medium (right) at 30°C

Furthermore, a mating test with the NBRC 0880 strain was conducted, and the mating type of the NBRC 10032 strain was investigated again. The NBRC 0880 strain was reported to be a conjugated haploid in NITE. Surprisingly, when NBRC 10032 strain and NBRC 0880 as a mating type were crossed, hyphal growth and teliospore formation was detected (**Figure 4.10**).

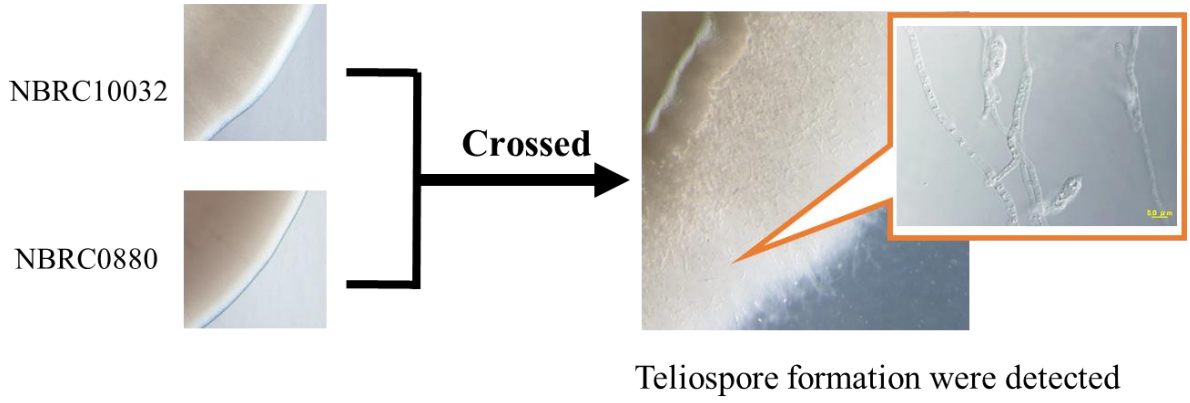

Figure 4.10. Cross testing of NBRC 10032 and NBRC 0880 strain.
Left. Colony edge of NBRC 10032 and NBRC 0880 strains when maintained on a sporulation medium. Right. NBRC 10032 crossed with NBRC 0880. Inset shows high magnification of the pseudohyphae

4.4. Discussion

Through the colony's color, carotenoid production and the isolated the non-carotenoid producing mutant was succeeded. The non-carotenoid producing mutant, S1, has low

carotenoid production approximate of zero, and carotenoid production of S1 was also low in both dark and light conditions, with no change in the cultivation time. The cell weight of the S1 mutant was higher than that of PS (both light and dark condition), it was also shown that the no carotenoid gene was expressed in S1 cells.

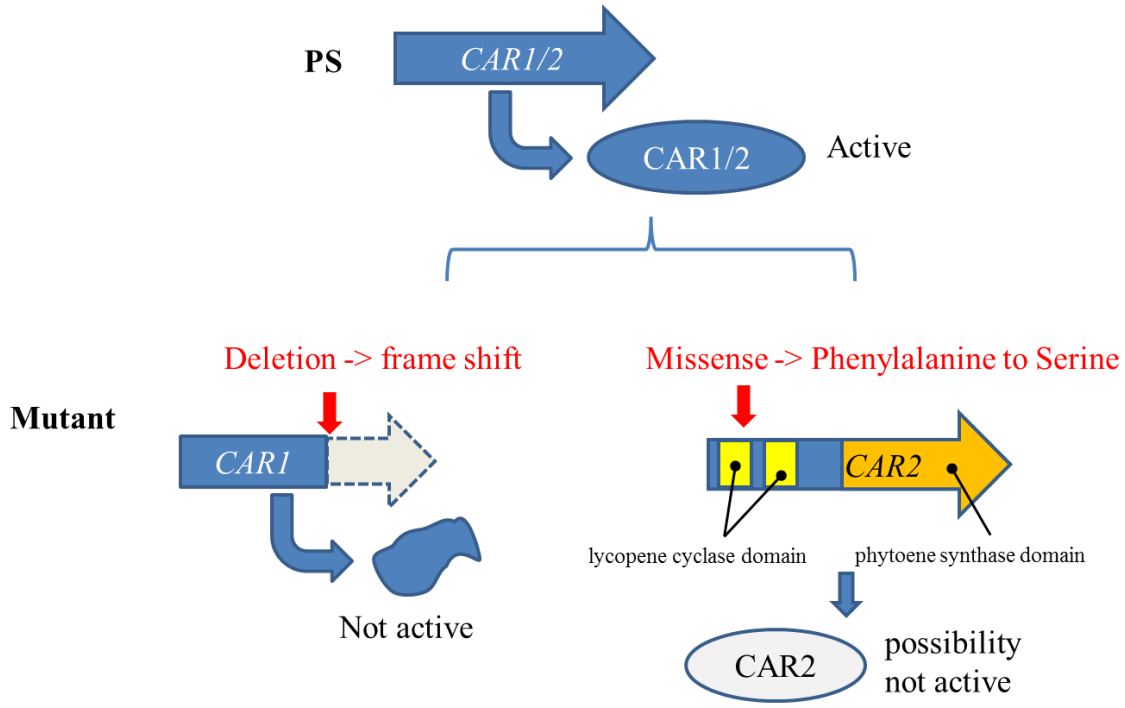

Figure 4.11. Hypothesis of the mutation point in *CAR1* and *CAR2* gene

After genomic analysis, the *CAR2* gene was identified to carry a missense mutation, which occurred when Phenylalanine changed to Serine. The mutation in the 82th position that included in the lycopene cyclase domain. Serine is known to be quite common in the protein's functional center and plays a role in the protein active sites. Therefore, it was hypothesized that the mutation in the *CAR2* gene occurred at the active site of the enzyme. And the lysopene cyclase action is high possible muted. Alternatively, in the *CAR1* gene, the INDELs mutation occurred at position 1015 with the deletion in this codon resulting in a frameshift mutation that affected the downstream codons, resulting in a loss-of-function mutation. Therefore, the mutation results in a gene that produce DNA but lacks gene activity, which happens when a gene lacks the functional domain of its product. Lycopene cyclase activation and encodes phytoene desaturase activation that are main enzymes for carotenoid components synthesis. Thus, there was a high possibility that loss of function of *CAR2* and *CAR1* genes contributed to the non-carotenoid production in this mutant.

High carotenoid production was obtained under a dark condition which enabled us decipher the production mechanism of carotenoids better because mutants that produced high carotenoids in the dark were expected to possess mutations that repressed the mechanism of carotenogenic genes. We obtained several high carotenoid-producing mutants. Among them, strains R5 and R36 showed the highest carotenoid production. However, their phenotypes exhibited a few differences. Carotenoid production was significantly increased on day 1 in R,5 then showed gradual increase in the light, whereas it increased gradually over time in the dark. In R36, carotenoid production reached close to maximum on day 1 under both light and dark conditions. This suggested that the effect of mutated genes affecting carotenoid production differed in each strain. The high carotenoid production under light condition, therefore, indicates that mutations in the genomes of both high carotenoid-producing strains happened in a repressing mechanism and this mechanism also in turn affected carotenoid production when subjected to light. Furthermore, enhancement of carotenoid production in R5 and R36 was supported at the transcriptional level as revealed by the higher expression amounts of *GGPSI*, *CAR1* and *CAR2* than those of PS in both strains. The important genes in carotenoid biosynthesis are phytoene synthase and carotene cyclase, which are encoded by two separate genes in bacteria and plants but are encoded by a single gene in fungi such as *crtYB* in the basidiomycete *Xanthophyllomyces dendrorhous*, *carRA* and *carRP* in the zygomycetes *Phycomyces blakesleeanus* and *Mucor circinelloides*, respectively, and *al-2* in the ascomycete *Neurospora crassa* (Schmidhauser *et al.* 1994; Velayos, Eslava and Iturriaga 2000; Lodato *et al.* 2007; Sanz *et al.* 2011). In *X. dendrorhous*, overexpression of *CrtYB* in the wild type showed enhanced production of carotenoids (Lodato *et al.* 2007). Although enzymatic characterization had not yet been carried out for *CAR2* from NBRC 10032, it had a high amino acid identity with these bifunctional enzymes. Previously, Jiao *et al.* reported that the *CAR2* disruptant of *R. toruloides* NP11 showed a phenotype with the white color colony (Jiao *et al.* 2019). Therefore, one reason for R5 and R36 to show high carotenoid production could be because of a higher expression of *CAR2*. On the other hand, the 15-fold higher expression of *CRY1* gene in R5 (1 h compared to 0 h) is proposed to contribute to high carotenoid yield at the short time of light exposure. This result was supported by the gene targeting analysis, which suggested that CRY1 activated carotenogenic genes. Also, the higher expression in all tested genes in the dark and light condition of R36 was higher than that of PS at 0 h, which resulted in the highest carotenoid production of R36 in both the dark and light conditions.

In the viewpoint of a two-step gene activation of carotenogenic genes, R5 showed a

similar gene expression profile to PS, but this phenomenon was only partially observed in R36 (*GGPSI*, *WC1* and *CRY1*). Therefore, the existence of other factor(s) regulating the two-step gene activation was proposed. Although comparative genome analysis was conducted to determine the SNPs in R5 and R36, genomes should lead to important insights for unraveling this mechanism. In this study, we encountered an unexpected barrier that NBRC 10032 was a diploid strain.

In the spore formation test, mating test between the NBRC 10032 and NBRC 0880 strains, the formation of spores was confirmed, suggesting that the NBRC 10032 strain can be mated with the type a NBRC 0880 strain. These results also suggested that the NBRC 10032 strain is diploid, but does not have the ability to form basidiomycetes, and has a monoploid life cycle. From the induction of teliospore formation and sexual crossing, it was also expected that NBRC 10032 was a diploid lacking sporulation ability, possessing a haploid life cycle.

4.5. References

Botes AL. Affinity purification and characterization of a yeast epoxide hydrolase. *Biotechnol Lett* 1999;**21**:511–7.

Frengova GI, Beshkova DM. Carotenoids from *Rhodotorula* and *Phaffia*: yeasts of biotechnological importance. *J Ind Microbiol Biotechnol* 2009;**36**:163–80.

Jiao X, Zhang Y, Liu X *et al.* Developing a CRISPR/Cas9 System for Genome Editing in the Basidiomycetous Yeast *Rhodosporidium toruloides*. *Biotechnol J* 2019;**14**:1–7.

Lodato P, Alcaíno J, Barahona S *et al.* Expression of the carotenoid biosynthesis genes in *Xanthophyllomyces dendrorhous*. *Biol Res* 2007;**40**:73–84.

Politino M, Tonzi SM, Burnett W V *et al.* Purification and characterization of a cephalosporin esterase from *Rhodosporidium toruloides*. *Appl Environ Microbiol* 1997;**63**:4807–11.

Sanz C, Velayos A, Álvarez MI *et al.* Functional analysis of the *Phycomyces carRA* gene encoding the enzymes phytoene synthase and lycopene cyclase. *PLoS One* 2011;**6**, DOI: 10.1371/journal.pone.0023102.

Schmidhauser TJ, Lauter FR, Schumacher M *et al.* Characterization of *al-2*, the phytoene synthase gene of *Neurospora crassa*. *J Biol Chem* 1994;**269**:12060–6.

Velayos A, Eslava AP, Iturriaga EA. A bifunctional enzyme with lycopene cydase and phytoene synthase activities is encoded by the *carRP* gene of *Mucor circinelloides*. *Eur J Biochem* 2000;**267**:5509–19.

Zhu Z, Zhang S, Liu H *et al.* A multi-omic map of the lipid-producing yeast *Rhodosporidium toruloides*. *Nat Commun* 2012;**3**:1–11.

Chapter 5: General conclusions and future perspectives

In this study, we investigated the effects of light on lipid and carotenoid production of *R. toruloides*. By comparing microbial growth and gene expression patterns, we demonstrated that carotenoid biosynthesis was controlled at the transcription level in response to light. Our results from phenotype and gene expression analysis showed that *R. toruloides* responded to light by producing darker pigmentation with an associated increase in carotenoid production. While there was no observable difference in lipid production, slight changes in the fatty acid composition were recorded. Furthermore, a two-step response was found in the three genes (*GGPSI*, *CAR1* and *CAR2*) under light conditions and the expression of the gene encoding the photoreceptor *CRY1* was similarly affected. It was clarified that carotenoid biosynthesis was promoted by activating the downstream pathways from the *GGPSI* gene encoding the geranylgeranyl diphosphate synthase of *R. toruloides* by light irradiation. It was as well clarified that the light response was triggered in two-step after 1 h and 72 h of light irradiation. From these, the carotenoid promotion of *R. toruloides* by light irradiation was clarified at the transcription level, and the molecular biological knowledge about them was obtained. Next, regarding the relationship between lipid production by light irradiation and carotenoid biosynthesis, it was clarified that light irradiation does not affect the amount of lipid production, although the growth of *R. toruloides* was reduced. Further, it was clarified that the fatty acid composition was changed by light irradiation and, in particular, the production of unsaturated fatty acid progressed. Also, the produced lipid contained fatty acids having excellent oxidative stability such as oleic acid. From these, we obtained a new finding that light promotes the production of carotenoids by *R. toruloides* and also produces fatty acids with excellent oxidative stability.

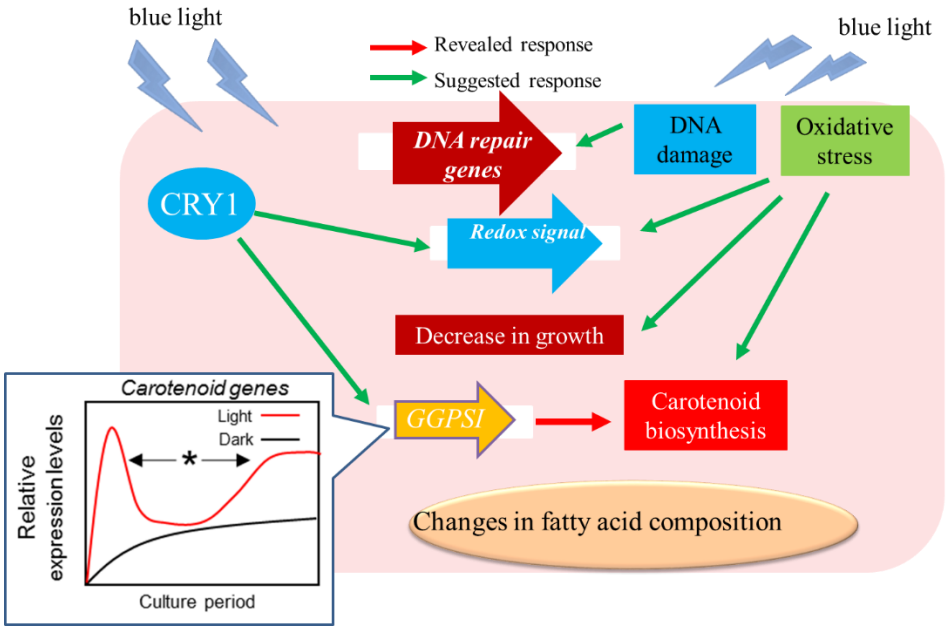

Figure 5.1. Light effect on carotenoid production at the transcription level in the two-step activation

To analyze the effects of the potential regulator *CRY1* in carotenoid production, we established a gene targeting system in this strain and analyzed the effect of *CRY1* on carotenoid production. Gene disruption using the URA3 marker recycling method and a high-frequency homologous recombination host was established. Although the homologous recombination efficiency of the NBRC 10032 was very low, we succeeded in a *KU70* disruptant strain through a two-step transformation and recycling maker. After that, the CRY1 disruptant was obtained. Our results using a *CRY1* disruptant suggested that *CRY1* might directly regulate *GGPSI*, *CAR1* and *CAR2* or might regulate carotenoid genes through the *WC1* gene or others. Through mutagenesis, we obtained two high carotenoid-producing mutants, which showed the contribution of CRY1 in carotenoid production, and the existence of other factors regulating the two-step light response of the carotenogenic genes. Therefore, these mutants are worth investigating further.

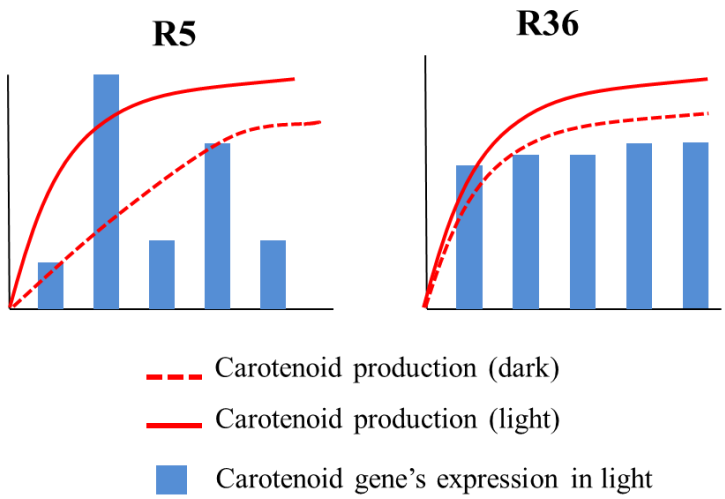

Figure 5.2. Two types of carotenoid production and carotenoid gene expression in high carotenoid-producing mutants

Through two types of high carotenoid-producing mutants, their genomic analysis suggested the existence of a control two-step gene activation. Additionally, we also found the strong possibility that NBRC 10032 was a diploid strain. Therefore, although analysis of the strain involves difficulties, the resulting mutants were valuable to investigate and better understand light-stimulated carotenoid production in this yeast.

Future perspectives involve regulation of the carotenoid biosynthesis mechanism in *R. toruloides*. In this study, we also unfolded the effect of light on carotenoid and lipid production. We developed a method for approaching the analysis of their function as well. Furthermore, many aspects of light regulation remain unknown. Concerning *WC1* expression, future studies should analyze the function of WC1 and the relationship between WC1 and CRY1 in the regulation of carotenoid production. Besides, whether the two-step activation remains in the dCRY1 or the disruption in one of the high carotenoid-producing mutants were unknown. More research is thus necessary to identify the two-step activation regulation factors. More analysis of the light regulatory mechanisms of *R. toruloides* helps to improve its ability in carotenoid production or lipid (such as unsaturated fatty acids omega 3) production, thereby leading to its potential application in industries.

Chapter 6: Publications

Journal Papers

1. Pham KD, Shida Y, Miyata A, Takamizawa T, Suzuki Y, Ara S, Yamazaki H, Masaki K, Mori K, Aburatani S, Hirakawa H, Tashiro K, Kuhara S, Takaku H and Ogasawara W. Effect of light on carotenoid and lipid production in the oleaginous yeast *Rhodosporidium toruloides*. *Biosci Biotechnol Biochem* 2020;**84**:1501–12.
2. Pham KD, Hakozaki Y, Takamizawa T, Yamazaki A, Yamazaki H, Mori K, Aburatani S, Tashiro K, Kuhara S, Takaku H, Shida Y and Ogasawara W. Analysis of the light regulatory mechanism in carotenoid production in *Rhodosporidium toruloides* NBRC 10032. *Biosci Biotechnol Biochem 2021* (in press)

Conferences

Pham KD, Miyata A, Shida Y, Yamazaki H, Masaki K, Mori K, Tashiro K, Kuhara S, Takaku H and Ogasawara W. 2016. Analysis of lipid production in the oleaginous yeast *Rhodosporidium toruloides. The 5th International Gigaku Conference in Nagaoka (IGCN2016).* Nagaoka University of Technology, Nagaoka.

Pham KD, Miyata A, Shida Y, Yamazaki H, Masaki K, Mori K, Tashiro K, Kuhara S, Takaku H and Ogasawara W. 2016. Analysis of light response mechanisms in carotenoid synthesis of the yeast *Rhodosporidium toruloides. The 68th Society of Biotechnology of Japan (SBJ) Annual Meeting,* Toyama.

Pham KD, Miyata A, Shida Y, Yamazaki H, Masaki K, Mori K, Tashiro K, Kuhara S, Takaku H and Ogasawara W. *2017.* Analysis of light response mechanism in carotenoid synthesis of the yeast *Rhodosporidium toruloides. The 69th Society of Biotechnology of Japan (SBJ) Annual Meeting,* Waseda University, Tokyo.

Pham KD, Miyata A, Shida Y, Yamazaki H, Masaki K, Mori K, Tashiro K, Kuhara S and Ogasawara W. 2017. Analysis carotenoid production in the yeast *Rhodosporidium toruloides* by light response. *2017 2nd STI-Gigaku*, Nagaoka University of Technology, Nagaoka.

Pham KD, Shida Y, Yamazaki H, Mori H, Aburatani S, Tashiro K, Kuhara S, Takaku H Ogasawara W. 2018. Study of the expression of carotenoid biosynthesis genes in wild type and hyper carotenoid strains of the yeast *Rhodosporidium toruloides*. *SGMJ Annual Conference 12th (12 回日本ゲノム微生物学会年会)*. Kyoto University, Kyoto.

ACKNOWLEDGMENT

First of all, I would like to express my heartfelt gratitude to my advisor, Prof. Wataru Ogasawara, for accepting me as his PhD student, offering me the great opportunity to conduct this remarkable research topic, and supporting me with his kind guidance, intelligence and strong experiences. I would like to especially thank Dr. Yosuke Shida for his suggestions on this research, and his enthusiasm to come up with new research ideas. They encouraged and supported me a lot through my work, and I am extremely grateful to them for their valuable suggestions.

Also, I would like to extend my thanks to Prof. Kazuki Mori, in the Cell Innovator Co., Ltd. Fukuoka and Prof. Takaku, in Niigata University of Pharmacy and Applied Life Sciences, Niigata, Japan for their advice on various analytical skills.

Further, I would like to thank my research group members, Mr. Atsushi Miyata, for patiently taking me through the experiment step by step, Mr. Takeru Takamizawa, Mr. Iwamoto and Mr. Yuuki Hakozaki for helping me a lot in research and life as well.

I specially thank other students and staff members at the Ogasawara's laboratory for their unconditional friendship and support over the years.

Lastly, I want to thank my family and parents for their huge love in supporting me continuously through the research period.